1985

A stochastic model to predict radio interference caused by corona on high voltage transmission systems

Yun-Ok Cho
Iowa State University

Cho, Yun-Ok

A STOCHASTIC MODEL TO PREDICT RADIO INTERFERENCE CAUSED BY CORONA ON HIGH VOLTAGE TRANSMISSION SYSTEMS

Iowa State University PH.D. 1985

A stochastic model to predict radio interference caused by corona on high voltage transmission systems

by

Yun-Ok Cho

A Dissertation Submitted to the
Graduate Faculty in Partial Fulfillment of the
Requirements for the Degree of
DOCTOR OF PHILOSOPHY

Department: Electrical Engineering and Computer Engineering
Major: Electrical Engineering (Electric Power)

Approved:

Signature was redacted for privacy.

In Charge of Major Work

Signature was redacted for privacy.

For the Major Department

Signature was redacted for privacy.

For the Graduate College

Iowa State University
Ames, Iowa

1985

TABLE OF CONTENTS

PAGE

I. INTRODUCTION 1

A. Introductory Background 1

B. Problem Formulation 4

C. Research Objectives 6

D. Research Outline 6

II. STATISTICAL CONSIDERATIONS 12

A. Fourier Transformations 12

B. Power Spectral Density 15

C. Spectra and Autocorrelation Function 17

III. STOCHASTIC CORONA MODELING 19

A. Properties of Corona - Literature Review 19
1. Onset pulses 20
2. Streamers 20
3. Pulsative corona discharges under alternating fields . . 22

B. Stochastic Corona Current Modeling 23

C. Power Spectral Density of Pulse Trains 26

D. Stationarity of Pulse Trains 30

IV. RADIO INTERFERENCE CAUSED BY CORONA ON THE SINGLE CONDUCTOR LINE 33

A. Introduction 33

B. Transmission Line Equations 33

C. The Solution of Transmission Line Equations 37

D. Power Spectral Density of Noise Voltage 41

E. Electric Field Calculation 46

F. Radio Interference Field 49

V. RADIO INTERFERENCE IN THREE PHASE TRANSMISSION LINES 52

A. Introduction 52

B. Transmission Line Equations 53

C. Modal Analysis 55

D. Solution of Transmission Line Equations 57

E. Power Spectral Voltage of Component Voltage 60

F. Electric Field Intensity Calculation 61

VI. DETERMINATION OF RANDOM PARAMETERS FROM THE EMPIRICAL RI MEASUREMENT 65

A. Introduction 65

B. Generation Function 66

C. Determination of Random Parameters From Generation Functions 68

D. Determination of the Mean Square Spectrum of Corona Pulse 70

E. Summary and Conclusions 72

VII. NUMERICAL CALCULATIONS AND DISCUSSIONS 74

A. Introduction 74

B. Base Case Line Characteristics 74

C. Random Parameters 76

D. Calculated Results 78
1. Effect of the terminating impedances of the line 78
2. Effect of the mean number of corona events 79
3. RI frequency spectrum 84
4. Lateral RI field profile 94
5. Axial RI field profile 94
6. Design parameters 97

VIII. CONCLUSIONS 104

IX. BIBLIOGRAPHY 106

X. ACKNOWLEDGMENT 111

XI. APPENDIX I. STATISTICAL PRELIMINARIES 113

A. Elements of Probability Theory 113
1. Events and probability 113
2. Random variables 115
3. Expectation of random variable 117
4. Independence 118

B. Stochastic Processes 118
1. Definition and preliminary considerations 118
2. Moments of stochastic processes 120
3. Stationary and wide-sense stationary processes 122
4. Ergodicity 122
5. Independent-increment processes 123

XII. APPENDIX II. FORTRAN PROGRAM FOR R.I. FIELD CALCULATION . . 125

LIST OF TABLES

PAGE

TABLE 1. The Effect of Line Terminations on the RI Field 79

TABLE 2. The Effect of λ on the RI field and Corona Current, Case 1 81

TABLE 3. The Effect of λ on the RI field and Corona Current, Case 2 82

TABLE 4. The RI Fields by Different Methods during Foul-Weather 83

TABLE 5. RI Field Spectrum for Different Line Length, λ = 1 87

TABLE 6. RI Field Spectrum for Different Line Length, λ = 5 90

LIST OF FIGURES

PAGE

FIGURE 1. Equivalent circuit of transmission line subject to corona 35

FIGURE 2. Cross-sectional view of a single-phase line with ground return 47

FIGURE 3. Single-circuit Horizontal Line Configuration, 345 kv . . . 75

FIGURE 4. The Effect of λ on the RI Field 80

FIGURE 5. RI Field Spectrum for Different Line Length, λ = 1 85

FIGURE 6. RI Field Spectrum for Different Line Length, λ = 5 86

FIGURE 7. Lateral RI Field Profile 95

FIGURE 8. Typical Lateral Profile Attenuation Curves [26] 96

FIGURE 9. Axial RI Field Profile 98

FIGURE 10. Effect of Variation of Conductor Diameter 99

FIGURE 11. Effect of Variation of Voltage 100

FIGURE 12. Effect of Variation of Conductor Height 101

FIGURE 13. Effect of Variation of Phase Spacing 102

I. INTRODUCTION

A. Introductory Background

The history of the electric power industry has been one of rapid growth throughout the years of existence. As power system loads have increased and need for transfer of large blocks of power has developed, there has been a continuing increase in transmission voltage levels from about 60 kv at turn of century to 765 kv in 1965 [1]. Even now, research and development work is well under way for the next higher voltage level which is expected to be in the 1000-1500 kv range [1,2]. The motivation for the trend to higher transmission voltage is the need to supply low cost, reliable electric services to a growing population having a vigorous growing in per-capita use of electric energy. These and other reasons for higher transmission voltage are discussed in detail in the literature [1,2,3]. Increasing the voltage of power network is associated with a large number of design criteria for a transmission system [4]. One of most important requirement is to meet the acceptable audible and radio noise level. In fact, conductor size and arrangement are determined based on the radio and audible interference level calculation, and this may result in selecting a larger conductor area than is dictated by loss economics.

Since the days of Townsend, corona has been investigated in many of its theoretical aspects [5-10]. Because of the extreme complexity of the phenomenon, however, progress attained in a small step, each dealing

with a particular problem. In a nonuniform field, various visual manifestation of locally confined ionization and excitation processes can be viewed and measured long before the complete voltage breakdown between the electrodes. These manifestation have long been called "coronas". A more precise, physical definition is [10]: A corona is a self-sustained electrical gas discharge where the Laplacian (geometrically determined) electrical field confines the primary ionization process to regions close to high field electrodes or insulators. Electrical energy in the corona discharge is transformed into other forms of energy: light, sound, electromagnetic energy, etc. The fast current variation produced by streamers induces waves which cause disturbances in electronic devices and audible noise. These phenomena such as power loss and radio noise caused by corona discharges are the main reasons to attract the attention of electric utility industry for many years.

The term radio interference or RI is normally used as a general designation for communication system interference originating from a variety of electrical causes [11,12]. It is used throughout this work in reference to radio noise caused by corona discharges on high voltage transmission systems in the AM (amplitude-modulated) broadcast band from 10 KHz to 10 MHz.

In the connection with the trend to higher voltages and the great influence of this high voltage on the radio interference, a considerable amount of research of the radio interference caused by corona has been

carried out in the past half-century. RI measurements made on short full-scale single- and three-phase test lines as well as on operating lines have resulted in several empirical and semi-empirical methods of radio interference calculation. However, the method can be divided into two separate groups which will be referred to as analytical and comparative [13].

The analytical method was initially undertaken by G. E. Adams [14], and has been presented in various papers [14-19]. This method is based on characteristic quantity called generation function which is determined by measurements made in test cages of short lines for different conductor arrangements and under known conductor surface conditions. The generation functions so determined are used to calculate electric intensity of the interference field near the line. An empirical formula [2] for generation functions, based on the results of cage and line tests on a large number of line configurations, was established.

In the comparative methods, a well-defined RI field intensity measurement, which includes the combined effects of RI generation and propagation is used as reference value. All comparative method representation of the interference field intensity are expressed as the sum of the RI reference value and correction factors for gradient, diameter, bundle, distance, frequency, and foul weather. Comparative method can be found in numerous literature [20-25].

The basic advantage of the analytical method is the flexibility. It can be used for any line configuration even unusual ones. Two particular advantages for the comparative method of analysis is: (1) The coefficients and constants appearing in the several correction terms may be determined using operational or test transmission lines rather than specialized laboratory facilities, and (2) the physical processes contributory to radio interference generation and propagation are individually identified.

However, the RI analysis methods, either analytical method or comparative method, do not entirely explain the difference between the measured RI fields of lines, nor the substantial fluctuation in level which have been obtained from a given line in the course of time [26].

B. Problem Formulation

Radio interference, generated by corona discharges, is caused by the movement of the space charges in the electric field in the vicinity of conductor surfaces of high voltage transmission lines. The corona discharges are due to a high electric field in the vicinity of the conductor [14,18].

Corona sources are known to be random both in magnitude and repetition time [7,9,10,13,14,19,27]. In most of cases, the corona currents injected into the conductor surface of a transmission line have been represented by the spectral density to deal with the randomness of the corona generation. To simplify the analysis, corona generation has

also been assumed to be uniform along the line and represented by a constant value [14,15,17,18,19].

However, spectral density of corona generation has meaning only when the corona generation has the property of at least wide-sense stationarity. Therefore, without developing the statistical model for corona generation, the power spectral representation for corona current would be incomplete and probably inaccurate. In this connection, physical and analytical models of these corona processes appear necessary.

In 1956, it was discovered [28] that it was not the imperfection of ACSR conductors but the airborne substances which produce the noise level of EHV lines during fair weather. Tseng-Wu Liao and N. A. Hoglund concluded [29] that the radio noise level during fair weather depends primarily on the sources of plumes not on the metal protrusions of the conductor material which will give only glow-type corona at the system operating voltage. While in the glow condition even with many sources the radio noise produced is generally very low. It has also been found [29,30] that each positive streamer repels other streamers to form the distinctive plume shape. Consequently, the assumption of uniform distribution of corona generation along the line appears inaccurate in the RI analysis. Therefore, discrete random distribution of corona generation would be more suitable in the RI analysis rather than uniform distribution.

C. Research Objectives

The purpose of this study is to determine the statistical nature of RI generation, propagation, and reception. The specific objectives of this research may be summarized as follows:

1. Determination or postulation of the statistical properties of radio interference generation such as frequency, mean peak-amplitude, and waveform.
2. Solution of the transmission line equations with random sources in time and space based on stochastic methods.
3. Determination of the received radio interference field based on random corona sources in time and space.
4. Determination of the relationship between the theoretical random parameters and RI levels obtained from empirical formulas, specially generation function.

D. Research Outline

To achieve the above objectives of this work, the primary focus is the establishment of a stochastic model to predict radio interference field caused by corona discharges on high voltage transmission systems. This requires the application of modern statistical methods to random phenomenon, corona discharge, which influence the design and operation of high voltage transmission systems.

Corona discharges are basically random both in time and space. Phenomena, or processes, of this kind are characterized by the

unpredictable changes in time and space: they exhibit variations from observation to observation which no amount of effort or control in the course of a run or trial can remove. However, if they show regularities or stabilized properties as the number of such observations is increased under similar conditions, these regularities are called statistical properties and it is for these that a mathematical theory can be constructed. Physical processes in the natural world which possess wholly or in part a random mechanism in their structure and therefore exhibit this sort of behavior are called stochastic processes. Since corona generations in the high voltage transmission lines in part exhibit some regularities with regard to radio interference field, they may be represented by mathematical description as stochastic processes. The necessity of statistical approach stems, of course, from the fact not only that it is impossible to exactly specify the characteristics of corona generation but also that the very laws of nature are themselves idealization, which ignore all but the principal characteristics of the model and of necessity omit the perturbations. Even then, a detailed application is often unworkable because of the inherent complexity of the system, so that a statistical treatment is productive.

This work is divided into seven Chapters and two Appendices. The first chapter starts with an introduction to the importance and prediction methods of radio interference analysis in power transmission engineering. Corona discharges on high voltage line are responsible for the power loss and radio interference. In the published literature

[2,3,14-26], two formulations to predict RI level are found: analytical and comparative methods. Brief discussion of these RI analysis methods is presented. However, these RI prediction methods, either analytical or comparative method, do not entirely explain the difference between the measured RI fields of lines, nor the substantial fluctuations in level which have been obtained from a given line in the course of time. This may be caused by inaccurate corona generation model made in each method. Thus, it appears necessary to develop a rigorous statistical model to predict the RI fields caused by corona discharges on high voltage transmission systems.

Chapter 2 presents the first and second moments, specially the concept of power spectral density of a stochastic process. Since the most of the contents in this chapter are well-presented in the Chapters 3 and 4 of [31] and in [32,33,34], only results and simple descriptions will be presented. For many applications, Fourier transform turns out to be the appropriate device for treating the steady-state conditions. It is shown that any aperiodic random disturbance such as corona does not possess Fourier transform in the usual sense. The concept of spectrum is broadened in order to deal with corona discharges from the frequency point of view in the steady-state. Based on this broadened concept of spectrum or Fourier transform the average power density of any random process is represented by the power spectral density.

Chapter 3 starts with the reviews of the basic characteristics of corona discharges required in the stochastic current modeling. It is

presented that only pulsative forms of corona discharges are responsible for the RI fields of concern. Thus, the discussion of corona is confined to pulsative forms of corona. The rest of this chapter is devoted to a stochastic corona current modelling which determines or postulates the statistical properties of radio interference generation. A rigorous statistical model for corona current is proposed. Based on the proposed corona current model, the power spectral density of single corona current source has been evaluated. Upon some assumptions, it is proven that corona current is a at least wide-sense stationary process.

Chapter 4 deals with stochastic analysis of RI propagation and reception for single-conductor transmission line terminated with arbitrary impedances at two ends. For any transmission line, the phase currents and line to ground voltages are related at any points of line. A rigorous stochastic analysis is presented to obtain transmission line equations of single-conductor line subject to random corona. Solution of transmission line equations yields a specific member (sample function) of ensemble interference voltage process. The ensemble property of this radio interference voltage is represented by the power spectral density of process. At an observation point in the vicinity of line, the interference field strength is then computed from the electrostatic gradient of the total interference voltage. With the help of Wiener-Khintchine theorem mean (ensemble average) square radio interference field is derived.

Chapter 5 is basically a application of the stochastic RI analysis developed for single-conductor line to actual three phase line. Similar analysis as in the case of single conductor is applied to develop transmission line equations. Transmission line equations are usually composed of three sets of coupled differential equations. The solution of transmission line equations is carried out using the theory of natural modes in which the voltage and current are expressed in terms of modal components by means of modal transformation matrices. The main advantage of this modal method is to decouple the coupled transmission line equations. In this chapter only a special type of line which terminates both ends in networks producing no or negligible intermode coupling is considered in order to avoid extreme difficulty in the RI propagation analysis. In this case, the propagation of each mode is analyzed as in the case of singe-conductor line having same characteristic impedance, propagation constant and terminal impedance for each mode.

Chapter 6 connects the random parameters generated from the stochastic RI analysis to the RI levels obtained from the empirical/semi-empirical formulas, specially generation function. To predict RI level with the developed stochastic RI analysis method, the random parameters generated by this method must be determined by a set of experiments. Since considerable amounts of RI measurements have been made on short full-scale single- and three-phase lines as well as on operating lines, however, the best way to determine random parameters is

to utilize the considerable amount of existing RI measurements, instead of a new set of experiments. In this connection, the power spectral density of corona generation is related to the generation function.

Chapter 7 includes results of RI field calculations using a developed digital algorithm (listed in Appendix II) based on the stochastic RI analysis for different parameters which affects the RI levels. In order to demonstrate practical applications of newly developed stochastic RI analysis, radio interference field is calculated for a single-circuit three-phase horizontal 345 kv transmission line. The effects of different parameters on the radio interference level are compared.

Chapter 8 is devoted to conclusions. The principal contributions which the stochastic RI analysis makes are presented.

Appendix I reviews some of probability theory and basic concepts of random variables and stochastic processes required in Chapters 2,3,4,and 5.

II. STATISTICAL CONSIDERATIONS

The purpose of this chapter is to present the background materials required in subsequent chapters, specially the concept of the power spectral density of a stochastic process. Most contents in this chapter are well-presented in Chapters 3 and 4 of [31]. Therefore, only basic definitions and results of the Fourier transformation and the power spectral density of a stochastic process which are needed in the subsequent chapters are presented. The statistical preliminaries which are needed in this chapter and the following chapters are reviewed in Appendix I.

A. Fourier Transformations

Let $g(t)$ be a real function defined over $(-\infty < t < \infty)$, and absolutely integrable, then the Fourier-transform pair of $g(t)$ is defined as

$$F(g(t)) = \int_{-\infty}^{\infty} e^{-j\omega t} g(t)\, dt = g(\omega) \tag{2.1}$$

with

$$F^{-1}(g(\omega)) = g(t) = \int_{-\infty}^{\infty} e^{j\omega t} g(\omega)\, df.$$

Suppose $g(t) = y^{(j)}(t)$, some suitably bounded member of an ensemble, in the observation interval $(0,T)$, so that $g(t) = y^{(j)}(t) = y^{(j)}_T(t)$ in $(-\infty,\infty)$, with zero outside the region $(0,T)$. Then, Eq. (2.1) can be applied to get

$$f_T(\omega) = F(y_T^{(j)}(t)) = \int_0^T e^{-j\omega t} y^{(j)}(t)\, dt$$

and as long as T is finite, this transform exists in the usual sense.

However, when random variables are dealt with, it should be observed that $F(y^{(j)}(t)) = \lim_{T\to\infty} F(y_T^{(j)}(t))$ does not exist since $y^{(j)}$ does not die down to zero as $t \to \pm\infty$ with sufficient rapidity to ensure convergence, nor does $y^{(j)}$ possess a definite periodic structure which could be interpreted as a line spectrum in terms of δ functions.

Strictly, then, it is observed that the Fourier transform of any steady-state aperiodic disturbance does not converge to a finite limit for all frequencies. Therefore, it is needed to extend the usual notions of the Fourier transform to include random function where the familiar treatment fails.

Consider a member $y^{(j)}(t)$ of an ensemble $y(t)$ such that $y^{(j)}(\omega)$ converges. This means that $\lim_{T\to\pm\infty} y^{(j)}(t) \to 0$ sufficiently rapidly so that

$$\int_{-\infty}^{\infty} |y^{(j)}(t)|\, dt < \infty$$

then, by Plancherel's theorem, we have

$$\int_{-\infty}^{\infty} y^{(j)}(t)^2\, dt = \int_{-\infty}^{\infty} |y^{(j)}(\omega)|^2\, df < \infty . \qquad (2.2)$$

When the disturbance $y^{(j)}(t)$ vanishes outside some interval $(-T/2,T/2)$, an <u>average power</u>, or <u>average intensity</u>, over the interval in question, can be defined according to

$$P_y^{(j)}(T) = 1/T \int_{-T/2}^{T/2} y^{(j)}(t_0)^2\, dt_0 = 1/T \int_{-\infty}^{\infty} y_T^{(j)}(t_0)^2\, dt_0$$

where $y_T^{(j)} = y^{(j)}(t)$ $(-T/2 \le t \le T/2)$ and is zero outside this interval. From Eq. (2.2), this can be written in still another form,

$$P_y^{(j)}(T) = \int_{-\infty}^{\infty} |y_T^{(j)}(\omega)|^2/T \, df,$$

where $y_T^{(j)}(\omega) = \int_{-\infty}^{\infty} y_T^{(j)}(t) \, e^{-j\omega t} \, dt.$

Defining,

$$W_y^{(j)}(\omega)_T = 2|y^{(j)}(\omega)_T|^2/T \ ,$$

we have

$$P_y^{(j)}(T) = \int_0^{\infty} W_y^{(j)}(\omega)_T \, df$$

so that $W_y^{(j)}(\omega)_T$ may be called the average power density of $y_T^{(j)}(t)$.

If $y^{(j)}(t)$ is a member of an ensemble $y(t)$ so that $y^{(j)}(t)$ does not die down properly to zero as $t \to \pm \infty$, average power $P_y^{(j)}$ can still be defined as the limit $T \to \infty$ of $P_y^{(j)}(T)$, i.e.,

$$P_y^{(j)} = \lim_{T \to \infty} \int_0^{\infty} W_y^{(j)}(\omega)_T \ . \qquad (2.3)$$

It is shown (page 140 of [31]) that, although $\lim_{T \to \infty} P_y^{(j)}(T)$ exists, it is not true $\lim_{T \to \infty} W_y^{(j)}(\omega)_T$ approaches a definite limit. In fact, $\lim_{T \to \infty} W_y^{(j)}(\omega)_T = W_y^{(j)}(\omega)_{\infty}$ is usually bounded but oscillates indefinitely as $T \to \infty$.

An immediate consequence is that the order of the limit and integration in Eq. (2.3) cannot be exchanged. More important, this result indicates that the power spectral density W_{∞}, in order to be

suitably defined in the limit $T \to \infty$, must be expressed as a property of the ensemble as a whole.

Consider, accordingly, an ensemble $y_T(t)$ which is obtained from the ensemble y ($-\infty < t < \infty$), with $E(y^2) < \infty$ for every finite interval (t), by truncation, so that y_T vanishes everywhere outside (-T/2,T/2).

Fourier-transform pair of ensemble $y_T(t)$ is defined in the mean square as follows:

$$y_T(\omega) = F(y_T(t)) = \int_{-T/2}^{T/2} y(t)\, e^{-j\omega t}\, dt$$

$$= \int_{-\infty}^{\infty} y_T(t)\, e^{-j\omega t}\, dt \ , \ \omega = 2\pi f \qquad (2.4)$$

with the usual inverse relation

$$y_T(t) = F^{-1}(y_T(\omega)) = \int_{-\infty}^{\infty} y_T(\omega)\, e^{j\omega t}\, df \ .$$

B. Power Spectral Density

Define

$$W_y(\omega)_T = E(2/T\ y_T(\omega)\ y_T(\omega)^*) = 2/T\ \overline{|F(y_T)|^2} \ . \qquad (2.5)$$

Definition of Fourier transform in the mean square guarantees the existence of $W_y(\omega)_T$. Substituting Eq. (2.4) into Eq. (2.5), we have

$$W_y(\omega)_T = 2/T \int_{-T/2}^{T/2} \int \overline{y(t_1)y(t_2)}\ e^{-j\omega(t_1 - t_2)}\, dt_1 dt_2$$

$$= 2/T \int_{-T/2}^{T/2} \int M_y(t_1,t_2)\, e^{-j\omega(t_1 - t_2)}\, dt_1 dt_2 \ , \qquad (2.6)$$

where, $M_y(t_1,t_2) = a_{11}(t_1,t_2) = \overline{y(t_1)\ y(t_2)}$.

The Fourier-transform of the power density $W_y(\omega)_T$, as defined over the ensemble, is

$$\int_{-\infty}^{\infty} W_y(\omega)_T \, e^{j\omega t} \, df = 2/T \int_{-T/2}^{T/2} \int M_y(t_1,t_2) dt_1 dt_2 \int_{-\infty}^{\infty} e^{-j\omega(t_1-t_2-t)} df$$

$$= 2/T \int_{-T/2}^{T/2} M_y(t_1, t_1-t) \, dt_1$$

since $\int_{-\infty}^{\infty} e^{j\omega(t_2-t_1+t)} \, df = \delta(t_2-t_1+t)$.

At this point, it is assumed that y(t) be a wide-sense stationary process so that $M_y(t_1,t_2) = M_y(t_1 - t_2)$. Then, Eq. (2.6) becomes

$$W_y(\omega)_T = 2/T \int_{-T/2}^{T/2} \int M_y(t_1 - t_2) \, e^{-j\omega(t_1 - t_2)} dt_1 dt_2$$

$$= 2 \int_{-T}^{T} M_y(x)_T \, e^{-j\omega x} dx \geq 0$$

where, $M_y(x)_T = M_y(x) \, (1 - |x|/T)$. Now if $M_y(x)$ is continuous,

$$\lim_{T\to\infty} W_y(\omega)_T = 2 \int_{-\infty}^{\infty} M_y(x) e^{-j\omega x} \, dx = 2 \, F(M_y(x))$$

$$= W_y(\omega)_\infty \quad .$$

The power spectral density $W_y(\omega)$ of a random process y(t) is defined by

$$W_y(\omega) = \lim_{T\to\infty} W_y(\omega)_T = \lim_{T\to\infty} E(W_y^{(j)}(\omega))$$

$$= \lim_{T\to\infty} 2/T \, \overline{|y^{(j)}(\omega)|^2}$$

where, this average must be carried out before the limit is taken.

In summary, the power spectral density and the autovariance function of y(t) are each other's Fourier transforms, i.e.,

$$W_y(\omega) = 2\,F(M_y)\ ,\ \omega = 2\pi f \tag{2.7}$$

$$M_y(t) = 1/2\,F(W_y)\ . \tag{2.8}$$

Eqs. (2.7) and (2.8) are known as the Wiener-Khintchine theorem. This theorem is easily extended to complex process y if we define

$$M_y(t) = E(y(t_1)\,y^*(t_2))\ .$$

C. Spectra and Autocorrelation Function

In the physical world, a single member alone of the ensemble y(t) is normally available. But if the process is ergodic, the Wiener-Khintchine theorem can be used to determine the ensemble spectral density of the process from the appropriate time average on this single member function.

To show this, define the autocorrelation function $R_y^{(j)}(t)$ of a member $y^{(j)}(t)$ of the ensemble y(t) as follows:

$$R_y^{(j)}(t) = \lim_{T\to\infty} 1/T \int_{-T/2}^{T/2} y^{(j)}(t_0)y^{(j)}(t_0 + t)\,dt_0,$$

where, $t = t_2 - t_1$. From the definition of the Fourier transform, we have

$$R_y^{(j)}(t) = \lim_{T\to\infty} 1/T \int_{-\infty}^{\infty} y_T^{(j)}(t_0)y_T^{(j)}(t_0 + t)\,dt_0$$

$$= \lim_{T\to\infty} 1/2 \int_{-\infty}^{\infty} W_y^{(j)}(f)\, e^{j\omega t}\, df \quad . \tag{2.9}$$

Next, take the ensemble average of both sides of Eq. (2.9) to get

$$\overline{R_y^{(j)}(t)} = 1/2 \int_{-\infty}^{\infty} \lim_{T\to\infty} \overline{W_y^{(j)}(\omega)_T}\, e^{j\omega t}\, df$$

$$= \int_0^{\infty} W_y(\omega) \cos(\omega t)\, df \quad .$$

If y is wide-sense stationary,

$$\overline{R_y^{(j)}(t)} = \lim_{T\to\infty} 1/T \int_{-T/2}^{T/2} \overline{y_T^{(j)}(t_0) y_T^{(j)}(t_0 + t)}\, dt_0$$

$$= M_y(t) \lim_{T\to\infty} 1/T \int_{-T/2}^{T/2} dt_0 = M_y(t) \quad .$$

Now if y(t) is ergodic,

$$R_y^{(j)}(t) = M_y(t) \qquad \text{with probability one} \quad .$$

so that the Wiener-khintchine theorem becomes finally

$$R_y^{(j)}(t) = 1/2\, F^{-1}(W_y)$$

$$W_y(\omega) = 2\, F(R_y^{(j)}(t)) \qquad \text{with probability one.}$$

III. STOCHASTIC CORONA MODELING

A. Properties of Corona - Literature Review

In the nonuniform field various visual manifestations of locally confined ionisation and excitation process can be viewed and measured long before the complete voltage breakdown between electrodes occurs. These manifestation have long been called " coronas ".

A precise, physical definition of corona discharge is [10] : A corona is a self-sustained electrical gas discharge where the Laplacian (geometrically determined) electrical field confines the primary ionization processes to regions close to high-field electrodes. A DC corona is called positive, negative or bipolar according to the polarity of the active electrodes [10]. AC coronas are power frequency fed in high voltage power lines. Sometimes corona are quite noisy both acoustically and on a wide range of radio and television broadcast bands. For example, high voltage power lines may exhibit corona discharges that cause considerable radio interference and acoustic noise.

The modes of positive corona in air are onset pulses, Hermstein glow, and steamers. The negative corona modes are Trichel pulses, pulseless glow, and negative streamers [8,9,10].

It has been known that only pulsative forms of corona can produce significant radio interference on the high voltage transmission systems [8,11]. In long gap, the highest noise level is produced by positive

streamers under AC excitation. The positive streamers under DC voltage give a slightly lower level, Trichel pulses a much lower one.

Therefore, it seems reasonable to confine the discussion of corona discharges to the positive pulsative forms of corona as far as the radio interference analysis is concerned.

1. Onset pulses

The sudden appearance of corona pulses at the threshold having magnitudes much higher than the ground current marks the formation of streamer (or burst pulses) discharges. The pulses occur randomly and intermittently.

The current pulse of these streamers has a rise time of the order of 20 to 40 nanoseconds. They decay to a half-peak value in about 100 nanoseconds [8,9]. The amplitudes of onset streamers range from a few tenths milliamperes in high divergent fields up to a few hundred milliamperes at large electrodes [8]. The repetition rate of onset streamers increases with the voltage up to a certain critical value at which the negative charge developed chokes off this form of discharge. Rough estimates have indicated that the frequency increases with voltage from zero to a peak of 3000 to 4000 pulses per second, after which the pulse frequency declines but its duration increases [7].

2. Streamers

This intermittent mode develops from the glow when the field is adequately nonuniform. Given a certain anode, the gap spacing must be large enough so that these streamers can materialize.

The frequency of occurrence of streamers ranges from 1000 pulses per second near their onset to 10000 pulses per second just before spark occurs [9].

Their amplitude is of same order as the amplitude of the onset streamers. The length, amplitude, and repetition rate of pulses grow with the voltage.

The observed form of streamer current pulse is the function of streamer length, amplitude, and field configurations. The rise times of streamer discharges observed on transmission lines and apparatus are usually in the nanosecond ranges (below 100 nanoseconds) [8].

The shape of the positive pulse in the high voltage transmission lines is of the following double exponential form [35,36]:

$$i(t) = A(e^{-at} - e^{-bt}) \quad . \tag{3.1}$$

In the relation (3.1), the parameters A, a, and b depend upon the high voltage line geometry, and voltage as well as the atmospheric conditions.

Perel'man and Chernobrodov [37] satisfactorily approximated the shape of positive pulse by the formula

$$i(t) = A \chi t e^{(1 - \chi t)} \quad . \tag{3.2}$$

where χ is the amplitude of the pulse, and $\chi = (1.0 - 1.4)\times 10^7$

Formula (3.2), which is a special case of expression (3.1), provides a simpler expression for the frequency spectrum of the impulse than formula (3.1).

3. Pulsative corona discharges under alternating fields

When alternating potential is applied to the electrodes, several differences will be observed in comparison with the corona in the DC field.

There are two primary sources of these differences [8,9]:

1. Oscillation of the voltage.
2. Oscillatory movement of the space charge developed by corona.

The first phenomenon results in continuous changes of corona generation conditions. Thus, several modes may appear in one voltage cycle. The second phenomenon exists only in gaps longer than the distance of the crossing during the period from corona extinction to the voltage decrease to zero. The critical distance in uniform field, at power frequency, is about 1.2 m. When the critical distance is exceeded, the negative-ion space charge will suppress the development of onset pulses. If, under the alternating field, the negative ions do not have ample time to escape to the electrodes, they will accumulate and force the steady glow to materialize.

The effect of the negative ions on the development of the breakdown streamers during the positive half-cycle is not very clear. In fields of moderate gradient (spherical and cylindrical electrodes), the onset of the breakdown streamer is lowered, whereas in highly divergent fields, the reverse seems to be the case.

B. Stochastic Corona Current Modeling

In practice, corona sources are distributed randomly along the length of the line. At a given point on the line, the corona current induced in a transmission line by corona discharge varies randomly with time, and it may be considered as pulse trains with random shapes. Such currents are generally best described in terms of stochastic processes in time and space. In this section, a stochastic model is thus proposed for the corona currents. Since only positive pulsative forms of corona can produce significant radio interference on the high voltage transmission systems [8,11], it is sufficient to consider only pulsative positive corona as far as the radio interference analysis is concerned.

Let $J(x,t)$, $o \leq x \leq L$, $-\infty < t < \infty$, be the corona current injection at time t and a point x along the transmission line. At a specific location (x,t), $J(x,t)$ denotes the random current with the value in $R = (-\infty, \infty)$, and can be called a random variable mapping from Ω to R, where Ω is the sample space consisting of all possible corona generations.

A stochastic process $J(x,t)$ may be seen as an indexed family of random variables. The collective outcome of all the experiments comprising random process $J(x,t)$ is denoted by $J^{(j)}(x,t)$, the realization of the stochastic process $J(x,t)$. The outcome of the random variable associated with any location (x,t) is referred to as the state of the stochastic process at that location.

At a given time t_0, $J(x,t_0)$ can be modeled by the Poisson process. If it is assumed that the corona current is so localized to one point on

the transmission line that it can be represented by a point current source, the corona currents will inject into the conductor only at discrete points, for example, x_1, x_2,..., x_N. Here, x_j's, j = 1,2,...,N, may be called the arriving points. The number of corona sources N is of course random process mapping from Ω to (1, 2, ...). Let $N(z_1,z_2)$ be the process denoting the number of the corona sources on the line section (z_1,z_2), where z_1, z_2 ϵ [0, L]. Since $N(z_1,z_2)$ can be assumed to be independent of the number of corona in an interval prior to the interval (z_1,z_2), and the probability that a certain corona occurs in a certain interval can be thought of independent of where the interval situated, N may be modeled as a Poisson process. It is noted that N depends only on the length of line, so that $N(z_1,z_2)$ can be replaced by $N(z_1-z_2)$.

At a given point x_0, $J(x_0,t)$, $-\infty < t < \infty$, may be considered as a stochastic process in time with a value in $R^+ = [0, +\infty)$, and denotes pulse trains. The shape and repetition rate of corona pulses comprise of random parameters which allow us to treat a variety of corona sources that may be operating concurrently but may arise from different mechanisms.

Assumptions:

1. Corona pulse trains are almost periodic in the sense that only one pulse can exist in each period interval.
2. The peak-value of each pulse varies randomly from pulse to pulse.

3. The pulse shape can be represented by a function of some random parameters.
4. The duration of each pulse is so short as to prevent overlapping between period intervals.
5. Pulses vary in position within the period interval, i.e., pulses have leading edges such that the period interval is not exceeded.
6. Corona current is so localized to one point on the transmission line that it can be represented by a point current source.

Let $J(x,t)$ be the corona current density defined on $[0, L] \times (-\infty, \infty)$, where L is the length of transmission line. A representation $J_T^{(j)}$ of corona current density $J(x,t)$ truncated in the interval $[-T/2, T/2]$, which consists of exactly 2N periods, each B seconds long may be represented by

$$J^{(j)}(x,t)_T = \sum_{n=1}^{N(L)} \sum_{m=1}^{M} y_m^{(j)} u_m(t - mB - \varepsilon_m^{(j)}) \delta(x - x_n)$$

$$\text{for } x \in [0,L],\ t \in [-T/2,T/2], \qquad (3.3)$$

where:

$u_m(t-mB-\varepsilon_m) = u_m(t)$ for $mB + \varepsilon_m \le t \le (m+1)B$

$N(L)$: the point process denoting the number of corona sources on the transmission line $[0,L]$.

y_m : the stochastic process denoting the peak amplitude of the m th pulse in time.

τ_m : the stochastic process denoting the leading edge of the m th pulse in time.

x_n : the stochastic point process denoting the position on the transmission line where the corona occurs.

$\delta(x)$: distribution function satisfying

$$\int_{-\infty}^{\infty} \delta(x-x_j)\, f(x)\, dx = f(x_j)$$

for any continuously differentiable f(x) which dies down quickly as x goes to $\pm \infty$.

In equation (3.3), it should be noted that N(L) and x_n's, n = 1, 2,..., are actually the functions of time, and τ_n's are the functions of x. In the followings, however, the statistical independence between time parameters and space parameters will be assumed to make the spectral analysis of J(x,t) more feasible.

Under certain assumptions, $J(x_0,t)$ can be easily shown to be a wide-sense stationary process (section D). $J(x_0,t)$ is thus assumed to be a stationary process in the following section.

C. Power Spectral Density of Pulse Trains

At a given point x_0 on the line, a realization of stochastic process $J^{(j)}(t)$ on time $(-\infty, \infty)$ is the summation of the pulses which has the properties assumed in the preceding section, and can be represented by

$$J^{(j)}(t) = \sum_{n=-\infty}^{\infty} y_n^{(j)} u_n(t - nB - \varepsilon_n^{(j)}). \tag{3.4}$$

In this section, it is attempted to derive the power spectral density of $J(x_0,t)$ which will be useful in the following chapters.

To obtain the power spectral density $W_J(\omega)$ of $J(t)$, start with a member of the truncated ensemble

$$J^{(j)}(t)_T = \sum_{n=-N}^{N} y_n^{(j)} u_n(t - nB - \varepsilon_n^{(j)}) \tag{3.5}$$

where $u_n(t)_{max}$ is unity, $u_n(t)$ vanishes outside an interval $\tau < B$ and τ is the maximum duration of a typical pulse. Similarly ε is also bounded, so that ε is less than $B - \tau$ to prevent overlapping between period intervals. The tighter restriction of strict stationarity will be imposed on the process ε.

If it is assumed that $J^{(j)}(t)_T$ is absolutely integrable, i.e.,

$$\int_{-\infty}^{\infty} |J^{(j)}(t)_T| \, dt = \int_{-T/2}^{T/2} |J^{(j)}(t)| \, dt < \infty ,$$

Fourier transform can be defined in the mean square as follows:

$$F\{J^{(j)}(t)_T\} = J^{(j)}(\omega)_T = F\{\sum_{n=-N}^{N} y_n^{(j)} (t - nB - \varepsilon_n^{(j)})\}$$

$$= \sum_{n=-N}^{N} y_n^{(j)} u_n(\omega) \exp\{-j\omega(nB + \varepsilon_n^{(j)})\}.$$

where, $u_n(\omega) = F\{u_n(t)\}$ and $\omega = 2\pi f$.

From the definition in Chapter 2, the power spectral density of process $J(t)$, $-\infty < t < \infty$, can be written as

$$W_J(\omega) = \lim_{T\to\infty} E(2|J^{(j)}(\omega)_T|^2/T) \quad . \tag{3.6}$$

In the above equation, it must be noted that average must be carried out before the limit is taken. The squared absolute value $|J^{(j)}(\omega)_T|^2$ in the Eq. (3.6) is

$$|J^{(j)}(\omega)_T|^2 = \sum_{n=-N}^{N} y_n^{(j)^2} |u_n(\omega)|^2 + \sum_{\substack{n,m=-N \\ n\neq m}}^{N} y_n^{(j)} y_m^{(j)} u_n(\omega)\, u_m^*(\omega)$$

$$\times \exp(-j\omega(nB-mB+\varepsilon_n^{(j)}-\varepsilon_m^{(j)})). \tag{3.7}$$

Substituting Eq. (3.7) into Eq. (3.6) and noting that $T = (2N+1)B$, we have

$$W_J(\omega) = \lim_{N\to\infty} \frac{2}{(2N+1)B} E\Big\{ \sum_{n=-N}^{N} y_n^{(j)^2} |u_n(\omega)|^2 + \sum_{\substack{n,m=-N \\ n\neq m}}^{N} y_n^{(j)} y_m^{(j)}$$

$$\times u_n(\omega)\, u_m^*(\omega) \exp(-j\omega B(n-m) - j\omega(\varepsilon_n^{(j)}-\varepsilon_m^{(j)}))\Big\}. \tag{3.8}$$

The first term in the bracket can be computed easily provided that y_n are independent of random parameters of $u_n(t)$ as follows:

$$\begin{aligned} &\lim_{N\to\infty} \frac{2}{(2N+1)B} E\Big\{ \sum_{n=-N}^{N} y_n^{(j)^2} |u_n(\omega)|^2 \Big\} \\ &= \lim_{N\to\infty} \frac{2}{(2N+1)B} \sum_{n=-N}^{N} \overline{y_n^{(j)^2}}\, \overline{|u_n(\omega)|^2} \\ &= \lim_{N\to\infty} \overline{y_n^{(j)^2}}\, \overline{|u_n(\omega)|^2} \frac{2}{(2N+1)B} \sum_{n=-N}^{N} 1 \\ &= \frac{2}{B} \overline{y^2}\, \overline{|u(\omega)|^2} \quad . \end{aligned} \tag{3.9}$$

In the derivation of Eq. (3.9), it is assumed that y and u are stationary stochastic processes.

To reduce the second term in the bracket of Eq. (3.8), it will be further assumed that random parameters of $u_n(t)$ are independent of those of $u_m(t)$ when $n \neq m$, and y and ε are mutually independent. Then, it can be reduced as follows:

$$\lim_{N\to\infty}\frac{2}{(2N+1)B}E\Big[\sum_{n,m=-N}^{N} y_n^{(j)}y_m^{(j)}u_n(\omega)\,u_m^{*}(\omega) \times \exp(-j\omega B(n-m) - j\omega(\varepsilon_n^{(j)}-\varepsilon_m^{(j)}))\Big]$$

$$= \frac{2}{B}\overline{y_n^{(j)}}\,\overline{y_m^{(j)}}\,\overline{u_n(\omega)}\;\overline{u_m^{*}(\omega)}\lim_{N\to\infty}\frac{1}{(2N+1)B}\sum_{\substack{n,m=-N\\ n\neq m}}^{N} e^{-j\omega B(n-m)} \times E\{e^{-j\omega(\varepsilon_n^{(j)} - \varepsilon_m^{(j)})}\}$$

$$= \frac{2}{B}(\bar{y})^2|\overline{u(\omega)}|^2\sum_{\substack{k=-\infty\\ k\neq 0}}^{\infty} e^{j\omega kB}\lim_{N\to\infty}\frac{1}{(2N+1)B} \times \sum_{m=-N}^{N} E\{e^{-j\omega(\varepsilon_{m+k}^{(j)}-\varepsilon_m^{(j)})}\}$$

$$= \frac{2}{B}(\bar{y})^2|\overline{u(\omega)}|^2\sum_{\substack{k=-\infty\\ k\neq 0}}^{\infty} E\{e^{j\omega(\varepsilon_2-\varepsilon_1)}\}_{kB}e^{j\omega kB} \quad . \tag{3.10}$$

Substituting Eqs. (3.9) and (3.10) into Eq. (3.8), we get

$$W_J(\omega) = \frac{2}{B}\left[\overline{y^2|u(\omega)|^2} + (\bar{y})^2|\overline{u(\omega)}|^2\sum_{\substack{k=-\infty\\ k\neq 0}}^{\infty} e^{j\omega kB}e^{j\omega(\bar{\varepsilon}_2-\bar{\varepsilon}_1)}\right] .$$

Now it can be shown that $E\{ e^{j\omega(\varepsilon_2-\varepsilon_1)} \}_{kB}$ is negligible at high frequency which is the main interest in the RI analysis. Let us assume that the epochs ε_n are uniformly distributed in the interval $(B/2-\tau)$ so that

$$f_1(\varepsilon) = 1/\tau_0 \qquad \text{for} \quad 0 \le \varepsilon \le B/2-\tau$$

where $f_1(\varepsilon)$ is the probability density function of ε.

Then, the expected value of $e^{j\omega(\varepsilon_2 - \varepsilon_1)}$ is

$$\begin{aligned} E\{ e^{j\omega(\varepsilon_2 - \varepsilon_1)} \} &= |E(e^{-j\omega\varepsilon})|^2 \\ &= \left| \int_0^{\tau_0} 1/\tau_0 \, e^{-j\omega\varepsilon} \, d\varepsilon \right|^2 \\ &= 2 \sin^2\omega\tau_0/(\omega\tau_0)^2 \\ &\le 2/(\omega\tau_0)^2 \ . \end{aligned}$$

The power spectral density $W_J(\omega)$ can be, therefore, approximated practically by

$$W_J(\omega) = 2/B \; E(y^2) \; E\{|u(\omega)|^2\) \ . \qquad (3.11)$$

D. Stationarity of Pulse Trains

Consider pulse trains J(t) represented by Eq. (3.4). It can be shown that pulse trains J(t) is a wide-sense stationary process if the followings are satisfied:

1. y, ε, and u are identically distributed stochastic processes which are mutually independent.
2. $u_n(t - \tau)$ are essentially zero except for small $t-\tau$.

Under above assumptions, it can be shown that the mean value is constant and the variance of J is the function of t-τ in a following way:

$$E(J(t)) = E\Big(\sum_{n=-\infty}^{\infty} y_n u_n(t-nB-\varepsilon_n)\Big) = \sum \overline{y_n u_n(t-nB-\varepsilon_n)}$$

$$= \bar{y} \sum \int_{-\infty}^{\infty}\int_{0}^{B} u_n(t-nB-\varepsilon_n)\, f(\varepsilon_n)\, f(u_n)\, d\varepsilon_n du_n$$

$$= \frac{\bar{y}}{B} \sum \int_{-\infty}^{\infty}\Big(\int_{t-(n+1)B}^{t-nB} u_n(q_n)\, dq_n\Big)\, f(u_n)\, du_n$$

$$= \frac{\bar{y}}{B} \int_{-\infty}^{\infty}\Big(\int_{-\infty}^{\infty} u(q)\, dq\Big)\, f(u)\, du$$

$$= \frac{\bar{y}}{B} \int_{-\infty}^{\infty} Q(u)\, f(u)\, du$$

$$= \frac{\bar{y}}{B}\, \bar{Q} \quad . \tag{3.12}$$

$$E(J(t)\, J(t-\tau)) = E\Big(\sum_{n,m=-\infty}^{\infty} y_n y_m u_n(t-nB-\varepsilon_n)\, u_m(t-mB-\varepsilon_m-\tau)\Big)$$

$$= \frac{\overline{y^2}}{B} \sum_{n=-\infty}^{\infty} \int_{-\infty}^{\infty}\int_{0}^{B} u_n(t-nB-\varepsilon_n)\, u_n(t-nB-\varepsilon_n-\tau)\, f(u_n)\, d\varepsilon_n du_n$$

$$+ \frac{\bar{y}^2}{B} \sum_{\substack{n,m=-\infty \\ n\neq m}}^{\infty} \int\int\int\int u_n(t-nB-\varepsilon_n)\, u_m(t-\tau-mB-\varepsilon_m)\, f(u_n,u_m)$$

$$\times\, d\varepsilon_n d\varepsilon_m du_n du_m$$

$$= \frac{\overline{y^2}}{B} \sum_{n=-\infty}^{\infty} \int_{-\infty}^{\infty}\Big(\int_{t-(n+1)B}^{t-nB} u_n(q_n)\, u_n(q_n-\tau)\Big)\, f(u_n)\, du_n$$

$$+ \frac{\bar{y}^2}{B} \int\int\int_{-\infty}^{\infty} \int_{t-(n+1)B}^{t-nB}\int_{t-\tau-(m+1)B}^{t-\tau-mB} u_n(q_n)\, u_m(q_m)\, f^2(u)$$

$$\times\, dq_n dq_m du_n du_m$$

$$= \frac{\overline{y^2}}{B} \int_{-\infty}^{\infty}\int u(q)\, u(q-\tau)\, dq\, f(u)\, du$$

$$+ \frac{\bar{y}^2}{B} \int_{-\infty}^{\infty}\int\int\int u(q)\, u(q')\, f^2(u)\, dq\, dq'\, du\, du'$$

$$= \Gamma(\tau) \quad . \tag{3.13}$$

where

$$Q = \int_{-\infty}^{\infty} u(q)\, dq$$

$$f(\varepsilon) = \frac{1}{B} \qquad \text{when } 0 \leq \varepsilon \leq B.$$

Thus, it is shown that $J(t)$ is a wide-sense stationary process under above assumptions.

IV. RADIO INTERFERENCE CAUSED BY CORONA ON THE SINGLE CONDUCTOR LINE

A. Introduction

The RI level of transmission line depends on two principal calculations: the generation of RI near the conductor and the propagation of the interference along the line [19].

The RI generation is generally characterized in Chapter 3. The RI propagation depends on the electrical characteristics of the line, the line length and the impedance characteristics of the line terminations. The solution of transmission line equations with suitable boundary conditions is presented for the RI propagation calculation.

The case of the single-conductor line is treated in this chapter for the sake of simplicity and completeness. Detailed analytical expressions presented in this case, however, are not to be found in published literature and are therefore to be believed to be very original and useful. Single-conductor RI analysis not only provides the general principles of RI analysis, but also is directly usable in the multiconductor analysis.

Application of the proposed analysis to some practical line configurations will be followed in later chapters.

B. Transmission Line Equations

Consider a single-conductor transmission line which has a resistance per unit length R, inductance per unit length L and shunt

admittance per unit length C. A short length of line Δx, is shown in Fig. 1. $J(x,t)$ is the corona current per unit length injecting into the conductor, which is the random field in space and time.

With polarity marks and current directions as shown in Fig. 1, Kirchhoff's voltage law and current law give

$$\Delta V = -R\,dx\,I - L\,dx\,\partial I/\partial t$$
$$\Delta I = -C\,dx\,\partial V/\partial t - J\,dx \quad . \tag{4.1}$$

In the limit as $\Delta x \to 0$, Eq. (4.1) becomes

$$\partial V/\partial x = -R\,I - L\,\partial I/\partial t$$
$$\partial I/\partial x = -C\,\partial V/\partial t - J(x,t) \quad . \tag{4.2}$$

Let us consider next an ensemble $J(x,t)_T$ which is obtained from the ensemble $J(x,t)$, $-\infty < t < \infty$, with $E(J^2) < \infty$ for every finite interval (t), by truncation so that J_T vanishes everywhere outside $(-T/2,T/2)$. Then, the transmission line equation (4.2) can be written as follows:

$$\partial V_T/\partial x = -R\,I_T - L\,\partial I_T/\partial t$$
$$\partial I_T/\partial x = -C\,\partial V_T/\partial t - J_T \quad . \tag{4.3}$$

where V_T and I_T are the voltage and current induced from J_T when we consider only the corona events in $-T/2 \le t \le T/2$.

In the next step, J_T, V_T, and I_T are assumed to be absolutely integrable in terms of t for $-T/2 \le t \le T/2$, i.e.,

$$\int_{-T/2}^{T/2} |f_T|\,dt < \infty \quad , \quad f_T = J_T,\ V_T,\ \text{or}\ I_T \tag{4.4}$$

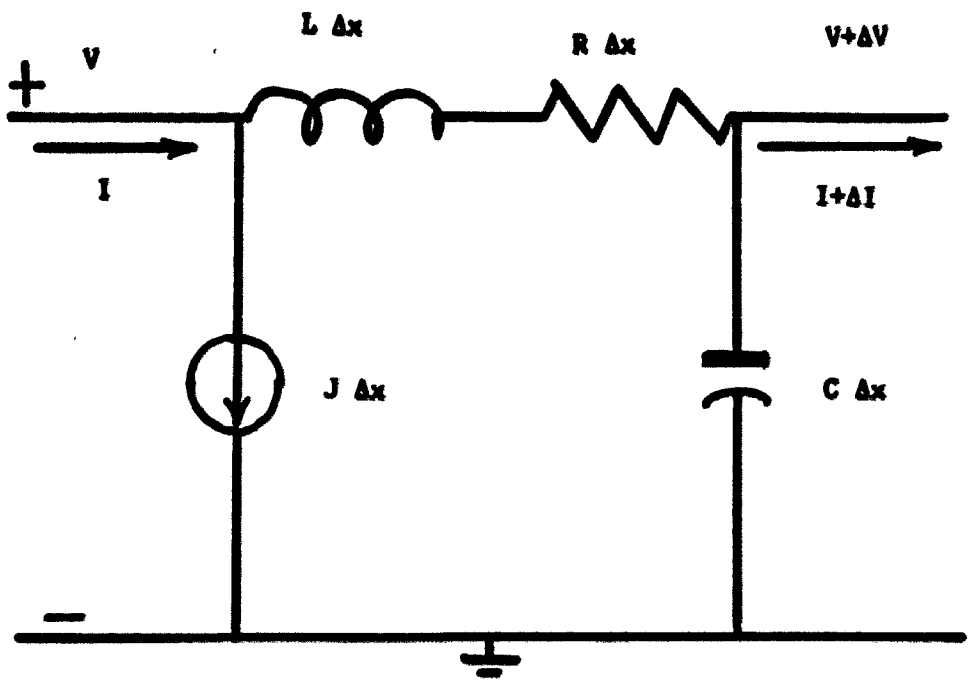

FIGURE 1. Equivalent circuit of transmission line subject to corona

then there exist Fourier transformations of V_T, I_T, and J_T in the mean square.

Taking the Fourier transforms in terms of t on both sides of Eq. (4.3), we have

$$\partial V(x,\omega)_T/\partial x = - Z\ I(x,\omega)_T \tag{4.5}$$

$$\partial I(x,\omega)_T/\partial x = - Y\ V(x,\omega)_T - J(x,\omega)_T \tag{4.6}$$

where $f_T(x,\omega)$, $f = V$, I, or J, is the Fourier transform of $f(x,t)_T$. Z and Y are line parameters defined by

$$Z = R + j\omega L$$

$$Y = j\omega C \quad . \tag{4.7}$$

In the derivation of Eqs. (4.5) and (4.6) the system is initially to be at rest, i.e.,

$$V(x,-\infty) = I(x, -\infty) = 0.0 \quad . \tag{4.8}$$

Equations (4.5) and (4.6) are the transmission line equations for the single-conductor line subject to corona in $-T/2 \leq t \leq T/2$. It should be noted that $J(x,\omega)_\infty$, $V(x,\omega)_\infty$, and $I(x,\omega)_\infty$ are not defined in the usual sense because they are not integrable in $-\infty < t < \infty$. Hence, the Fourier transforms of $V(x,t)$ and $I(x,t)$ are not defined in the usual sense. However, the definition of Fourier transform in the mean square sense guarantees the existence of

$$W_y(\omega)_T = E\{2/T\ y(\omega)_T\ y^*_T(\omega)\}, \text{ for } y_T = V_T(x,\omega),\ I_T(x,\omega),$$

and in the limit as $T \to \infty$, $W_y(\omega)_\infty$ is defined well.

In the following section, therefore, it is attempted to solve Eqs. (4.5) and (4.6) for specific boundary conditions, and to find the power spectral density $W_V(\omega)$ which can be related to the radio interference field.

C. The Solution of Transmission Line Equations

Let us consider a single-conductor line AB of length L subject to corona discharges. Let it be terminated in arbitrary impedances Z_1 and Z_2 at two extremities of the line. The line is assumed to have following characteristics:

Z : series impedance per unit length, Ω/m .

Y : shunt admittance per unit length, mhos/m.

$Z_c = \sqrt{Z/Y}$: characteristic impedance, Ω.

$\gamma = \sqrt{ZY} = \alpha + j\beta$: propagation constant.

α : attenuation constant, nepers/m.

β : phase constant, radians/m.

Combining Eqs. (4.5) and (4.6), we have

$$d^2V(x,\omega)_T/dx^2 - \gamma^2 V(x,\omega)_T = Z J(x,\omega)_T \quad . \tag{4.9}$$

If a specific member $J^{(j)}(x,\omega)_T$ of the ensemble $J(x,\omega)_T$ is considered, Eq. (4.9) can be written as:

$$d^2V^{(j)}(x,\omega)_T/dx^2 - \gamma^2 V^{(j)}(x,\omega)_T = Z J^{(j)}(x,\omega)_T \quad . \tag{4.10}$$

For a single source at $x = x_j$, $J^{(j)}(x,\omega)_T$ is

$$J^{(j)}(x,\omega)_T = \delta(x - x_j) F\{ \sum_{n=-N}^{N} y_n^{(j)} u_n(t - n\Delta - \varepsilon_n^{(j)}) \} \quad . \tag{4.11}$$

If we let

$$f^{(j)}(t)_T = \sum_{n=-N}^{N} y_n^{(j)} u_n(t - nB - \varepsilon_n^{(j)}),$$

then

$$J^{(j)}(x,\omega)_T = \delta(x - x_j)\, F\,(f^{(j)}(t)_T) = \delta(x - x_j)\, f^{(j)}(\omega)_T \quad . \quad (4.12)$$

Substituting Eq. (4.12) into Eq. (4.10), we have a second order differential equation

$$d^2V^{(j)}(x,\omega)_T/dx^2 - \gamma^2\, V^{(j)}(x,\omega)_T = Z\, f^{(j)}(\omega)_T\, \delta(x - x_j) \quad . \quad (4.13)$$

In order to solve Eq. (4.13), divide the line into region - I, to the left of the point $x_j = \xi$ and II, to the right of the point ξ - and apply the source conditions to join the solution for region I with the region II.

Both region I and II are then source free. The solutions for both regions have therefore the forms as follows:

$$V^{(j)}(x,\xi)_T = \begin{cases} A\, e^{-\gamma x} + B\, e^{\gamma x} & \text{for } 0 \le x < \xi \\ C\, e^{-\gamma x} + D\, e^{\gamma x} & \text{for } \xi < x \le L \end{cases} \quad (4.14)$$

and

$$I^{(j)}(x,\xi)_T = \begin{cases} (A\, e^{-\gamma x} - B\, e^{\gamma x})/Z_0 & \text{for } 0 \le x < \xi \\ (C\, e^{-\gamma x} - D\, e^{\gamma x})/Z_0 & \text{for } \xi < x \le L \end{cases} \quad (4.15)$$

where $V^{(j)}(x,\xi)_T$ is the voltage at x when a point source is located at x = ξ.

At the point x = 0, we have conditions

$$Z_1 = - V^{(j)}(0,\xi)_T / I^{(j)}(0,\xi)_T = Z_0 \, (1 + \rho_1)/(1 - \rho_2) \qquad (4.16)$$

where the symbol

$$\rho_1 = A/B = (Z_1 - Z_0)/(Z_1 + Z_0) \quad . \qquad (4.17)$$

The solution for region I can therefore be written in the form

$$V^{(j)}(x,\xi)_T = B \, e^{\gamma x} \, (1 + \rho_1 \, e^{-2\gamma x}) \qquad (4.18)$$

$$I^{(j)}(x,\xi)_T = B \, e^{\gamma x} \, (\rho_1 \, e^{-2\gamma x} - 1)/Z_0 \quad . \qquad (4.19)$$

In a similar fashion, the condition at x = L is

$$Z_2 = V^{(j)}(L,\xi)_T / I^{(j)}(L,\xi)_T = Z_0 \, (1 + \rho_2)/(1 - \rho_2) \qquad (4.20).$$

where, $\rho_2 = D \, e^{2\gamma L}/C = (Z_2 - Z_0)/(Z_2 + Z_0)$. (4.21)

The solution for region II can therefore be written in the form

$$V^{(j)}(x,\xi)_T = C \, e^{-\gamma x} \, (1 + \rho_2 \, e^{2\gamma(x - L)}) \qquad (4.22)$$

$$I^{(j)}(x,\xi)_T = C \, e^{-\gamma x} \, (1 - \rho_2 \, e^{2\gamma(x - L)})/Z_0 \quad . \qquad (4.23)$$

Now apply the source conditions at x = ξ, i.e.,

$$I^{(j)}(\xi + 0,\xi)_T - I^{(j)}(\xi - 0,\xi)_T = - \mathcal{E}^{(j)}(\omega)_T \qquad (4.24)$$

$$V^{(j)}(\xi + 0,\xi)_T - V^{(j)}(\xi - 0,\xi)_T = 0 \, . \qquad (4.25)$$

The solutions for the four unknown constants are, therefore,

$$A = \rho_1 B$$

$$B = - Z_0 f^{(j)}(\omega)_T e^{-\gamma\xi} (1 + \rho_2 e^{2\gamma(\xi - L)})/\Delta$$

$$C = - Z_0 f^{(j)}(\omega)_T e^{\gamma x} (1 + \rho_1 e^{-2\gamma\xi}) /\Delta$$

$$D = C \rho_2 e^{-2\gamma L} \tag{4.26}$$

where

$$\Delta = 2 (1 - \rho_1 \rho_2 e^{-2\gamma L}) \quad . \tag{4.27}$$

The constants substituted into the general forms for the solution in region I and II, give the complete solution. Thus, from Eqs. (4.18), (4.19), (4.22), (4.23), and (4.26), the noise voltage at x when a point source is located at $x = \xi$ can be written by:

$$V^{(j)}(x,\xi;\omega)_T = \begin{cases} - Z_0/\Delta f^{(j)}(\omega)_T (1 + \rho_2 e^{2\gamma(\xi - L)}) \\ \quad \times (e^{\gamma(x - \xi)} + \rho_1 e^{-\gamma(x + \xi)}), \ 0 \le x < \xi \\ - Z_0/\Delta f^{(j)}(\omega)_T (1 + \rho_1 e^{-2\gamma\xi}) \\ \quad \times (e^{-\gamma(x - \xi)} + \rho_2 e^{\gamma(x + \xi - 2\Omega)}), \ \xi < x \le L. \end{cases} \tag{4.28}$$

Equation (4.28) is the general solution with arbitrary terminations Z_1 and Z_2. Having obtained the voltage $V^{(j)}(x,\xi;\omega)_T$ for the problem of single corona source, the problem with a general source distribution can be obtained with a superposition. The solution for the multiple source can therefore be written as follows:

$$V^{(j)}(x,\omega)_T = \Sigma\, V^{(j)}(x,\xi;\omega)_T$$

$$= -\, Z_0/\Delta\, f^{(j)}(\omega)_T \sum_{n=1}^{N} \left(e^{-\gamma|x-x_n|} + \rho_1 e^{-\gamma(x+x_n)}\right.$$

$$\left. + \rho_2\, e^{-\gamma(2L-\, x_n-x)} + \rho_1\, \rho_2\, e^{-\gamma(2L\, -\, |x-x_n|)}\right) . \qquad (4.29)$$

It is noted that N in Eq. (4.29) is the stochastic process denoting the number of corona on the transmission line, and $f^{(j)}(\omega)_T$ is the Fourier transform of corona current at a given point x.

The Fourier transform of $V^{(j)}(x,t)_T$ is therefore the product of the Fourier transform of corona current at a given point and the factor which can be determined from the distribution of corona along the transmission line, the line parameters, and the terminations of line.

D. Power Spectral Density of Noise Voltage

In the present section, such an ensemble property as the power spectral density which is most important in practical engineering applications is considered. The power spectral density $W_V(x,\omega)$ of V(x,t) will be used to find the average mean square value of the radio interference field caused by V(x,t) in the following section.

The power spectral density $W_V(x,\omega)$ of V(x,t) at a given point x is defined as

$$W_V(x,\omega) = \lim_{T\to\infty} 2/T\; E\{V^{(j)}(x,\omega)_T\; V^{(j)\,*}(x,\omega)_T\} \quad . \qquad (4.30)$$

Substituting Eq. (4.29) into Eq. (4.30), we get

$$W_V(x,\omega) = \left|\frac{Z_0}{\Delta}\right|^2 \left\{ \lim_{N\to\infty} \frac{2}{T}\, \overline{|f(\omega)_T|^2}\right\}$$

$$
\begin{aligned}
&\times E \sum_{n,m=-N}^{N} \Big[\exp(-\gamma|x-x_n| - \gamma^*|x-x_m|) \\
&\quad + |\rho_1|^2 \exp(-\gamma(x+x_n) - \gamma^*(x+x_m)) \\
&\quad + |\rho_2|^2 \exp(-\gamma(2L-x-x_n) - \gamma^*(2L-x-x_m)) \\
&\quad + |\rho_1\rho_2|^2 \exp(-\gamma(2L-|x-x_n|) - \gamma^*(2L-|x-x_m|)) \\
&\quad + 2\,\mathrm{Re}\Big\{ \rho_1 \exp(-\gamma^*|x-x_n| - \gamma(x+x_m)) \\
&\qquad + \rho_2 \exp(-\gamma^*|x-x_n| - \gamma(2L-x-x_m)) \\
&\qquad + \rho_1^* \rho_2 \exp(-\gamma^*(x-x_n) - \gamma(2L-x-x_m)) \\
&\qquad + \rho_1\rho_2 \exp(-\gamma^*|x-x_n| - \gamma(2L-|x-x_m|)) \\
&\qquad + |\rho_1|^2\rho_2 \exp(-\gamma^*(x-x_n) - \gamma(2L-|x-x_m|)) \Big\} \\
&\quad + |\rho_2|^2\rho_1 \exp(-\gamma^*(2L-x-x_n) - \gamma(2L-|x-x_m|)) \Big] \Big\}. \qquad (4.31)
\end{aligned}
$$

Note that the term in the brace is the spectral density of f(t), and was evaluated in Chapter 3 (see Eq. (3.11)).

The first term in the bracket can be evaluated in a following way:

$$
\begin{aligned}
&E \sum_{n,m=1}^{N(L)} \exp(-\gamma|x-x_n| - \gamma^*|x-x_m|) \\
&= \int_{-\infty}^{\infty} \int_0^L \cdots \int_0^L \sum_{n,m=1}^{N(L)} \exp(-\gamma|x-x_n| - \gamma^*|x-x_m|) \\
&\qquad \times f(x_1)\, f(x_2) \cdots f(x_N)\, dx_1 \cdots dx_N\, dN \\
&= \int_{-\infty}^{\infty} f(N) \Big[\int_0^L \cdots \int_0^L \sum_{n,m=1}^{N(L)} \exp(-\gamma|x-x_n| - \gamma^*|x-x_m|)\, L^{-N} \\
&\qquad \times dx_1 dx_2 \cdots dx_N \Big]\, dN
\end{aligned}
$$

$$= \int_{-\infty}^{\infty} f(N) \left(\int_0^L \cdots \int_0^L \sum_{n=1}^{N} \exp(-\gamma|x-x_n| - \gamma^*|x-x_m|)\, dx_1 \cdots dx_N \right.$$

$$\left. + \int_0^L \cdots \int_0^L \sum_{\substack{n,m=1 \\ n \neq m}}^{N(L)} \exp(-\gamma|x-x_n| - \gamma^*|x-x_m|)\, dx_1 dx_2 \cdots dx_N \right) dN$$

$$= \int_{-\infty}^{\infty} f(N) \left(\frac{N}{L} \int_0^L \exp(-\gamma|x-x_n| - \gamma^*|x-x_m|)\, dx_n \right.$$

$$\left. \frac{N^2-N}{L^2} \int_0^L \int_0^L \exp(-\gamma|x-x_n| - \gamma^*|x-x_m|)\, dx_n dx_m \right) dN$$

$$= \int_{-\infty}^{\infty} f(N) \left[\frac{N}{2\alpha L} \left(2 - e^{-2\alpha x} - e^{-2\alpha(L-x)}\right) \right.$$

$$\left. + \frac{N^2-N}{L^2|\gamma|^2} \left|2 - e^{-\gamma x} - e^{-\gamma(L-x)}\right|^2 \right] dN$$

$$= \frac{\lambda}{2\alpha} \left(2 - e^{-2\alpha x} - e^{-2\alpha(L-x)}\right) + \lambda^2 \left| \frac{1}{\gamma} \left(2 - e^{-\gamma x} - e^{-\gamma(L-x)}\right) \right|^2 \Big]. \quad (4.32)$$

The other terms in the bracket can be easily evaluated in a similar method. The power spectral density of V(x,t) is thus as follows:

$$W_V(x,\omega) = \left|\frac{Z_0}{\Delta}\right|^2 W_f(\omega) \left[\frac{\lambda}{2\alpha} \left(2 - e^{-2\alpha x}(1-|\rho_1|^2)\right.\right.$$

$$- |\rho_1|^2(1-|\rho_2|^2)\, e^{-2\alpha(L+x)} - (1-|\rho_2|^2)\, e^{-2\alpha(L-x)}$$

$$- |\rho_2|^2(1-|\rho_1|^2)\, e^{-2\alpha(2L-x)} - |\rho_1\rho_2|^2\, e^{-4\alpha L}$$

$$+ 2\,\mathrm{Re}\left(\rho_1 e^{-2\alpha x} - \rho_1 e^{-2(\alpha L + j\beta x)} + \rho_2 e^{-2\alpha(L-x)}\right.$$

$$+ \rho_2(1-|\rho_1|^2) e^{-2(\gamma L - j\beta x)} - \rho_2|\rho_1|^2 e^{-2(\gamma L + \gamma^* x)}$$

$$\left.\left. + \rho_1|\rho_2|^2 e^{-2(\alpha L + 2j\beta x)} - \rho_1|\rho_2|^2 e^{-2(2\alpha L - \gamma^* x)} \right)\right]$$

$$+ \frac{\lambda}{\beta}\, \mathrm{Im}\left[\rho_1 (e^{-2\alpha x} - e^{-2\gamma x}) + \rho_2 (e^{-2\alpha(L-x)} - e^{-2\gamma(L-x)}\right]$$

$$+ \rho_1\rho_2\{e^{-2(\gamma L-j\beta x)} + e^{-2(\alpha L+j\beta x)} - 2\, e^{-2\alpha L}\}$$

$$+ \rho_1^*\rho_2\{e^{-2(\alpha L-j\beta x)} - e^{-2(\gamma L-j\beta x)}\}$$

$$+ \rho_2|\rho_1|^2\{e^{-2\alpha(L+x)} - e^{-2(\gamma^* x+\gamma L)}\}$$

$$+ \rho_1|\rho_2|^2\{e^{-2\alpha(2L-x)} - e^{-2(2\alpha L-\gamma^* x)}\}]$$

$$+ \frac{\lambda^2}{|\gamma|^2}\,|2 - e^{-\gamma x} - e^{-\gamma(L-x)}|^2$$

$$+ |\rho_2|^2\,|e^{-\gamma(2L-x)} - e^{-\gamma(L-x)}|^2$$

$$+ |\rho_1|^2\,|e^{-\gamma x} - e^{-\gamma(L+x)}|^2$$

$$+ |\rho_1\rho_2|^2\,|e^{-\gamma(2L-x)} + e^{-\gamma(L+x)} - 2e^{-2\alpha L}|^2]$$

$$+ \frac{\lambda^2}{|\gamma|^2}\,\mathrm{Re}[(2 - e^{-\gamma^* x} - e^{-\gamma^*(L-x)})\,\{\rho_1 e^{-\gamma x}$$

$$- \rho_1(1-\rho_2)\,e^{-\gamma(L+x)} - \rho_2(1-\rho_1)\,e^{-\gamma(2L-x)}$$

$$+ \rho_2\,e^{-\gamma(L-x)} - 2\rho_1\rho_2\,e^{-2\gamma L}\}$$

$$+ \rho_1^*\rho_2\{e^{-\gamma^* x} - e^{-\gamma^*(x+L)}\}\,\{e^{-\gamma(L-x)}$$

$$- (1-\rho_1^*)\,e^{-\gamma(2L-x)} + \rho_1^*\,e^{-\gamma(L+x)}$$

$$- 2\rho_1^* e^{-2\gamma L}\} + \rho_1|\rho_2|^2 e^{-4\alpha L}\,\{e^{\gamma x} + e^{\gamma(L-x)}$$

$$- 2)\,\{e^{\gamma^*(x+L)} - e^{\gamma^* x}\}]]_j. \qquad (4.33)$$

where

$$W_f(\omega) = \frac{2}{B}\,\overline{\gamma^2}\;\overline{|u(\omega)|^2}. \qquad (4.34)$$

Let the product of $|1/\Delta|^2$ and the expression in the outermost bracket be $\Gamma(\lambda;x,L,\omega,\gamma,\rho_1,\rho_2)$, then the power spectral density of voltage can be written by

$$W_V(x,\omega) = 2|Z_0|^2/B\ Ey^2\ E|u(\omega)|^2\ \Gamma(\lambda;x,L,\omega,\gamma,\rho_1,\rho_2)\ . \qquad (4.35)$$

Thus, the spectral density $W_V(x,\omega)$ at a given point x due to corona discharges on a single-conductor transmission line of length L is the product of the following three factors:

1. $|Z_0|^2$ which can be determined from line parameters.
2. $W_f(\omega)$ which can be determined from the pulse shape, peak value, and repetition rate of basic corona streamer.
3. $\Gamma(\lambda;x,L,\omega,\gamma,\rho_1,\rho_2)$ which can determined from the line length, the reflection coefficients at the extremities of line, the number of corona events per unit length, and the propagation constant of the line.

In a matched line which is an interesting special case, the reflection coefficients ρ_1 and ρ_2 are both zero, so that the expression $W_V(x,\omega)$ simplifies as follows:

$$W_V(x,\omega) = \frac{|Z_0|^2}{2B}\ \overline{y^2}\ \overline{|u(\omega)|^2}\ \left[\frac{\lambda}{2\alpha}(2 - e^{-2\alpha x} - e^{-2\alpha(L-x)})\right.$$
$$\left. + \frac{\lambda^2}{|\gamma|^2}\ |2 - e^{-\gamma x} - e^{-\gamma(L-x)}|^2\right]\ . \qquad (4.36)$$

E. Electric Field Calculation

The analysis, so far, has led to the derivation of the noise voltage in the power spectral form. This interference voltage can be connected to the electric field intensity around conductor which causes the radio interference to the radio placed near the transmission line.

At the present time, the quasi-static method is widely used to determine the electric field from corona voltage. The electric field analysis in this section is also based on static electric fields. It should be, however, noted that for frequency higher than 10 MHz the field intensity must be determined by an exact solution of the Maxwell's equations.

The cross-sectional view of a single-phase line with ground return is shown in Fig. 2, when the conducting earth is replaced by the image of the conductor.

Let the electric field intensities be defined as

$$E_c = e_c \, e^{j\theta_c}$$

$$E_i = e_c \, e^{j\theta_c} \quad . \tag{4.37}$$

where E_c and E_i are the field intensities due to conductor and the image of conductor, respectively. The electric field intensity E at a point P(x,y) is then,

$$E = E_c + E_i$$

$$= (e_c x/d_i + e_i x/d_i) + j(e_c(y - h)/d_c + e_i(y + h)/d_i) \quad . \tag{4.38}$$

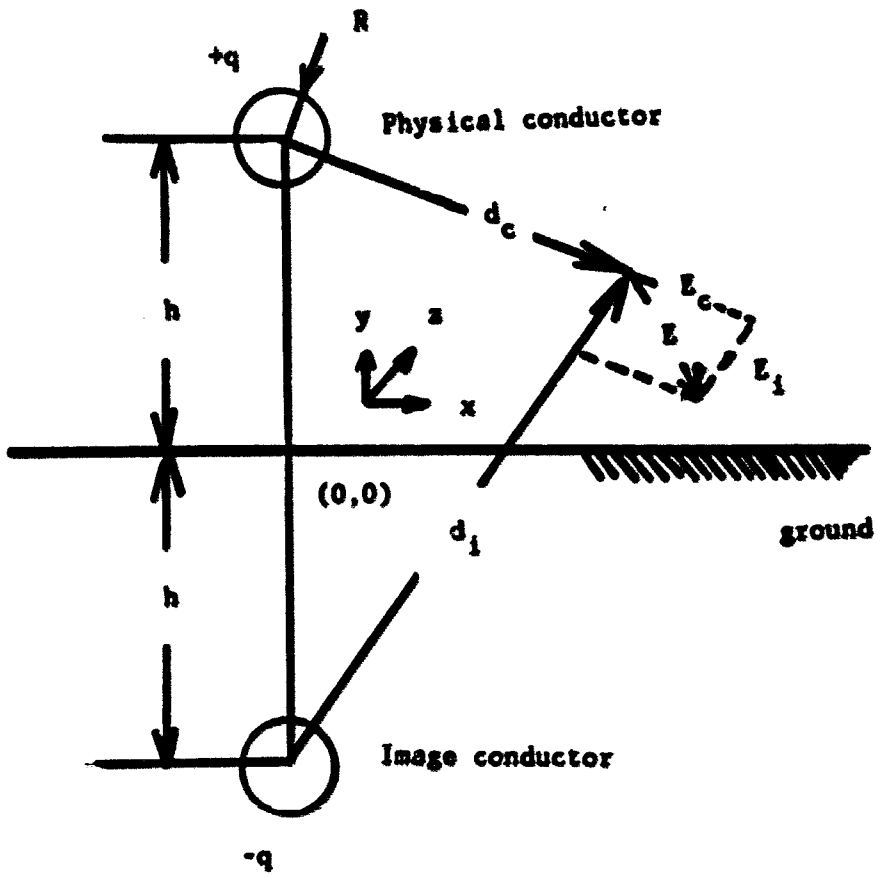

FIGURE 2. Cross-sectional view of a single-phase line with ground return

The electric fields e_c and e_i are given by

$$e_c = q/(2\pi\varepsilon_0 d_c)$$

$$e_i = -q/(2\pi\varepsilon_0 d_i) \quad , \tag{4.39}$$

where q is the electric charge due to corona on the transmission line.

In the derivation of Eq. (4.39), it was assumed that the field structure is almost TEM, i.e., the electric and magnetic field vectors lie in a plane (xy) perpendicular to the axis (z) of the line. In this sense, electric field intensities e_c and e_i are only an approximation (usually a reasonable one for good conductors and for frequencies concerned in the RI analysis).

The phase voltage V(x,t) and the charge are related as

$$q = 2\pi\varepsilon V/\ln_e(2h/R) \quad . \tag{4.40}$$

Substituting Eq. (4.40) into (4.48), we have

$$e_c = V/\{d_c \ln_e(2h/R)\}$$

$$e_i = -V/\{d_i \ln_e(2h/R)\} \quad . \tag{4.41}$$

The substitution of Eq. (4.41) into (4.48) yields

$$E = V\, x/\{\ln_e(2h/R)\}\ (1/d_c^2 - 1/d_i^2)$$

$$+ jV/\ln_e(2h/R)\ ((y-h)/d_c^2 - (y+h)/d_i^2)$$

$$= e_x + je_y \quad . \tag{4.42}$$

Equation (4.42) connects the noise voltage on the conductor to the electric field intensity at a point P(x,y). The power spectral density of E may be defined by

$$W_E(x,y,z,\omega) = (W_{e_x}(x,y,z,\omega)^2 + W_{e_y}(x,y,z,\omega)^2)^{\frac{1}{2}}. \tag{4.43}$$

where

$$W_{e_x}(x,y,z;\omega) = W_V(z,\omega)\ (x(1/d_c^2 - 1/d_i^2)/\ln_e(2h/R))^2$$

$$W_{e_y}(x,y,z;\omega) = W_V(z,\omega)\ [((y - h)/d_c^2 - (y + h)/d_i^2))/\ln_e(2h/R)]. \tag{4.44}$$

The power spectral density $W_E(x,y,z;\omega)$ at ground level $y = 0$, specially, is given by

$$W_E(x,y=0,z;\omega) = 4\ h^2\ W_V(z,\omega)/((x^2 + h^2)(\ln\ 2h/R))^2\ . \tag{4.45}$$

F. Radio Interference Field

In the preceding section, it was shown that the power spectral density of the electric field around transmission line could be determined from the spectral density of interference voltage.

The electric field intensity in the region immediately adjacent to the antenna of a radio receiver induces a voltage in the antenna circuit. This is an interference voltage or noise signal. After passing through the mixer and the intermediate frequency (i-f) section of the receiver, the noise signal is detected, amplified, and then

converted to sound by the speaker. The overall characteristics of the mixer and of i-f sections are bandpass in nature, i.e., only small range of frequencies from f_a to f_b and centered f_0 is transmitted without appreciable attenuation.

Let $Y(j\omega)$ be the overall transfer function of the mixer and i-f sections of the receiver. Let $W_e(x,y,z,\omega)$ be the power spectral density of the output of the receiver. Then, W_e can be written in terms of input W_E and the transfer function by (see pp 173-174 of [31] for detailed discussion)

$$W_e(x,y,z,\omega) = |Y[j(\omega - \omega_0)]|^2 \, W_E(x,y,z,\omega) \tag{4.46}$$

where it is assumed that the receiver is a narrowband filter and the input noise signal is broadband. ω_0 is the frequency to which the receiver is tuned.

For the total average intensity, we have alternatively (by the Wiener-Khintchine theorem)

$$\begin{aligned} M_e(x,y,z,t) &= E\{e(x,y,z,t_0)\, e(x,y,z,t_0 - t)\} \\ &= 1/2\, F(W_e(x,y,z,\omega)) \\ &= 1/2 \int_{-\infty}^{\infty} W_e(x,y,z,\omega)\, e^{-j\omega t}\, df \quad . \end{aligned} \tag{4.47}$$

Thus,

$$\begin{aligned} M_e(x,y,z,0) &= E\{e(x,y,z,t)^2\} \\ &= \int_{-\omega_0}^{\infty} |Y(j\omega')|^2 \, W_E(x,y,z,\omega_0 + \omega')\, df' \end{aligned}$$

$$= \int_{-\infty}^{\infty} |Y(j\omega')|^2 \, W_E(x,y,z,\omega_0 + \omega') \, df' \qquad (4.48)$$

since $\omega_0 >> 2\pi \, \Delta f_{filter}$. Δf_{filter} is the bandwidth of the receiver.

If the spectral density of the noise signal does not vary strongly with the frequency over the passband of the receiver, the mean square value of output can be approximated by

$$E(e(x,y,z,t)^2) = |Y(j\omega')|^2 \, W_E(x,y,z,\omega_0 + \omega') \, \Delta f_{filter}. \qquad (4.49)$$

If it is further assumed that the output noise signal is ergodic, the mean square value of output is same as the time average of the square of any member of output ensemble e(x,y,z,t), i.e.,

$$\langle e^{(j)}(x,y,z,t)^2 \rangle = E(e(x,y,z,t)^2) \quad . \qquad (4.50)$$

Thus, in the extension of the familiar nonstatistical treatment of deterministic noise signal in the time and frequency domains, analogous relations in the case of the ensemble and its representative members can be now constructed. Thus, if the output noise signal is ergodic, the time average of the square of the noise measurement represents the mean square value of output noise.

V. RADIO INTERFERENCE IN THREE PHASE TRANSMISSION LINES

A. Introduction

The analysis of RI on short multiconductor line involves two important elements: firstly, a modal propagation analysis of RI and secondly an analysis of the short line effects, taking into account the effect of the terminating impedances.

In the case of short lines, the propagation analysis is complicated by the reflection of the voltage and current waves which might be produced at the two ends of line, depending on the impedance networks terminating two ends. In the general case, such reflection may result in the mixture of the different modes or intermode coupling, which will make the RI propagation analysis extremely difficult. There exist certain types of line terminations, however, which either completely eliminate or reduce to a negligible level, any intermode coupling.

In this decoupled three phase transmission line, most of the RI analysis developed for the single-conductor line can be directly applicable in the three phase RI analysis. Thus, in this chapter only decoupled line will be considered in order to avoid unnecessary complexity in the RI analysis and to make the RI analysis more clear.

B. Transmission Line Equations

For any three phase transmission lines, the phase currents and line to ground voltages are related at any point on the line by the transmission line equations. In time-space domain, these equations can be obtained by using the same method for the single conductor line, and they are as follows:

$$- \partial V^P/\partial z = R\ I + L\ \partial I^P/\partial t \tag{5.1}$$

$$- \partial I^P/\partial z = C\ \partial V^P/\partial t + J^P \tag{5.2}$$

where

z : the axis of transmission line.

V^P : 3x1 column vector, V_i denote the line to ground voltages in phase i.

I^P : 3x1 column vector, I_i denote the phase currents in phase i.

R : 3x3 square matrix, R_{ij} denote the frequency dependent resistances between the ith conductor and jth conductor including the Carson's return.

L : 3x3 square matrix, L_{ij} denote the frequency dependent self ($i = j$) and mutual ($i \neq j$) inductances of the line including the earth effect.

C : 3x3 square matrix, C_{ij} denote the self and mutual capacitances of the line including the earth effect.

J^P : 3x1 column vector, J_i denote the corona currents injected into phase i.

In the derivation of Eqs. (5.1) and (5.2), the conductance of the line was neglected. It is worthwhile to note that in many physical three phase transmission lines, earth or ground wires are added above the phase conductors. In this connection, Eqs. (5.1) and (5.2) must be considered as the transmission line equations after taking into account earth wire effects.

Let us consider next an ensemble J_T which is obtained from the ensemble $J(z,t)$, $0 \leq z \leq L$, $-\infty < t < \infty$, with $E(J_i(x,t)^2) < \infty$ for every finite interval (t) and for i = 1,2, and 3, so that J_T vanishes everywhere outside (-T/2,T/2). Then, Eqs. (5.1) and (5.2) can be written as follows:

$$- \partial V^P(z,t)_T/\partial z = R\ I^P(z,t)_T + L\ \partial I^P(z,t)_T \tag{5.3}$$

$$- \partial I^P(z,t)_T/\partial z = C\ \partial V^P(z,t)_T/\partial t + J^P(z,t)_T\ , \tag{5.4}$$

where V_T and I_T are the voltage and current when the corona events are considered only in $-T/2 \leq t \leq T/2$. If it is assumed that each component of J_T, V_T, and I_T is absolutely integrable w.r.t. t, then there exist the Fourier transforms of V_T, J_T, and I_T componentwise. It is noted that the Fourier transforms of matrices or vectors are defined componentwise as follows:

$$F(V) = [F(V_{ij})]\ . \tag{5.5}$$

Taking the Fourier transforms on both sides of Eqs. (5.3) and (5.4), we have

$$- \partial V^{p}(z,\omega)_{T}/\partial z = Z\ I^{p}(z,\omega)_{T} \tag{5.6}$$

$$- \partial I^{p}(z,\omega)_{T}/\partial z = Y\ V^{p}(z,\omega)_{T} + J^{p}(z,\omega)_{T}, \tag{5.7}$$

where,

$$Z = R + j\omega L \tag{5.8}$$

$$Y = j\omega C \tag{5.9}$$

$$X(z,\omega) = F(X(z,t)), \text{ for } = V_{T}^{p},\ I_{T}^{p}, \text{ or } J_{T}^{p}. \tag{5.10}$$

Combining Eqs. (5.6) and (5.7),

$$\partial^{2} V^{p}(z,\omega)_{T}/\partial z^{2} - P\ V^{p}(z,\omega)_{T} = Z\ J^{p}(z,\omega)_{T}\ , \tag{5.11}$$

where

$$P = ZY\ . \tag{5.12}$$

Equation (5.11) or Eqs. (5.6) and (5.7) are the basic transmission line equations to determine the noise voltage caused by corona discharges. In the following section, the modal method will be introduced to decouple the transmission line equations.

C. Modal Analysis

For multiphase transmission line analysis, the use of symmetrical components is appropriate most of the time. Although symmetrical components are widely used in power system analysis, they are of

impractical use in this problem. At these high frequencies, the asymmetry of the line cannot be neglected. Therefore, the general eigenvalue or modal analysis is adequate for this purpose through the use of the similarity transformations. Using this technique, a lossy line consisting of n conductors has n eigenvalues or modes of propagation. Each of these modes consists of particular voltage and current composition, velocity and attenuation at a given frequency.

The main advantage of this modal method is the use of a transformation method which, when applied to the coupled systems, will decouple them. For this specific study, phase quantities are going to be transformed into modal quantities.

Let S and Q be the voltage and current transformation matrix, respectively, i.e.,

$$V^P = S\ V \tag{5.13}$$

$$I^P = Q\ I\ , \tag{5.14}$$

where V and I are the component vectors.

Denoting D^2 by the diagonal matrix whose diagonal elements are d^2/dz^2, Eq. (5.11) is written as

$$(D^2 - P)\ V_T^P = Z\ J_T^P \tag{5.15}$$

or

$$(D^2 - P)\ S\ S^{-1}\ V_T^P = Z\ Q\ Q^{-1}\ J_T^P\ . \tag{5.16}$$

Premultiplying S^{-1} on both sides of Eq. (5.16),

$$S^{-1} (D^2 - P) S S^{-1} V_T^P = S^{-1} Z Q Q^{-1} J_T^P \quad . \tag{5.17}$$

Using Eqs. (5.13) and (5.14),

$$S^{-1} (D^2 - P) S V_T = S^{-1} Z Q J_T \quad . \tag{5.18}$$

Thus,

$$(D^2 - S^{-1} P S) V_T = S^{-1} Z Q J_T \quad . \tag{5.19}$$

Let S be the model matrix of P, i.e., the columns of S are the eigenvectors of P, and let λ^2 be the diagonal matrix whose elements are the eigenvalues of P. Then, Eq. (5.19) becomes

$$(D^2 - \lambda^2) V_T = S^{-1} Z Q J_T \; . \tag{5.20}$$

If

$$S^{-1} = Q' \; , \tag{5.21}$$

$S^{-1}ZQ$ is a diagonal matrix [38]. Therefore, both sides of Eq. (5.20) yield component values which are mutually independent. This is the result needed to simplify the solution of the matrix equations.

D. Solution of Transmission Line Equations

The next step in the RI analysis of three phase transmission systems is to solve Eq. (5.20). In this section, a transmission line terminated at both ends in networks producing no or negligible coupling will be considered in order to avoid extreme difficulties in the RI

analysis. It can be shown [17] that the following terminal impedance matrix

$$Z = S\, Z^c\, Q^{-1} \tag{5.22}$$

produces no coupling. In Eq. (5.22), Z^c is the modal characteristic impedance matrix defined by [38]:

$$Z^c = \gamma^{-1}\, S^{-1}\, Z\, Q \quad . \tag{5.23}$$

From a practical point of view, it could be extremely difficult to terminate a high voltage transmission line in an impedance network defined by Eq. (5.22). A more feasible alternative is an impedance network comprising only of identical impedances between each conductor and ground [17]. In this case, there is negligible coupling for practical transmission line configurations.

Consider a short three phase transmission line of length L terminated in equal impedances between each conductor and ground for each end. If, on this line, it is assumed that only conductor 1 (phase a) is subject to corona discharge, then,

$$\begin{aligned} J_T &= Q^{-1} J^p{}_{1T} = S' J^p{}_{1T} \\ &= [S_{11} J^p{}_{1T},\ S_{12} J^p{}_{1T},\ S_{13} J^p{}_{1T}]' \end{aligned} \tag{5.24}$$

Then, the basic transmission line equation can be written as

$$(D^2 - \gamma^2)\, V_T = S^{-1}\, Z\, Q\, [S_{11} J^p{}_{1T},\ S_{12} J^p{}_{1T},\ S_{13} J^p{}_{1T}]' . \tag{5.25}$$

Define

$$G = S^{-1} Z Q \tag{5.26}$$

then, Eq. (5.25) can be reduced to

$$(D^2 - \gamma^2) V_T = [g_{11}S_{11}, g_{22}S_{12}, g_{33}S_{13}]' J^P_{1T} \tag{5.27}$$

or,

$$d^2V_{iT}/dz^2 - \gamma_i^2 V_{iT} = g_{ii}(S_{1i}J^P_{1T}), \quad i = 1,2,3. \tag{5.28}$$

It is shown that the matrix Z^c connects component currents and voltages as follows [38]:

$$\underline{V} = V^+ e^{-\gamma z} - V^- e^{\gamma z}$$

$$= Z^c (I^+ e^{-\gamma z} - I^- e^{\gamma z}) = Z^c I . \tag{5.29}$$

Because of the absence of any intermode coupling, the propagation of each mode i may be analyzed as a single conductor line having a characteristic impedance Z^c_{ii}, the propagation constant γ_i, and terminal impedances Z_A and Z_B.

Thus, comparing Eqs. (5.28) and (4.9), the component voltage due to corona discharges on conductor 1 only is

$$V^{(j)}_{il}(z,\omega)_T = - Z^c_{ii}/\Delta_i \, S_{1i} \, f^{(j)}_1(\omega)_T \{ \sum_{n=1}^{N} e^{-\gamma_i|z-z_n|} + \rho_{Ai} e^{-\gamma_i(z+z_n)} + \rho_{Bi} e^{-\gamma_i(2L-z_n-z)} + \rho_{Ai}\rho_{Bi} e^{-\gamma_i(2L-|z-z_n|)} \}, \tag{5.30}$$

where

$$\rho_{Ai} = (Z_A - Z^c_{ii})/(Z_A + Z^c_{ii})$$

$$\rho_{Bi} = (Z_B - Z^c_{ii})/(Z_B + Z^c_{ii})$$

$$\Delta_i = 2\,(1 - \rho_{Ai}\,\rho_{Bi}\,e^{-2\gamma_i L}). \tag{5.31}$$

Z_A and Z_B are the impedances between each conductor and ground at the two ends of line AB.

In the similar way, the component voltages due to corona discharges on conductors 2 and 3 (phases b and c) can be obtained. The component voltages caused by corona discharges, therefore, will be given by

$$V^{(j)}_i(z,\omega)_T = \sum_{k=1}^{3} V^{(j)}_{ik}(z,\omega)_T$$

$$= -\,Z^c_{ii}/\Delta_i \sum_{k=1}^{3} S_{ki}\, f^{(j)}_k(\omega)_T\, F_i(z,\rho_{Ai},\rho_{Bi},\gamma_i)$$

$$\text{for } i = 1,\ 2,\ 3 \tag{5.32}$$

where, $F_i(z,\rho_{Ai},\rho_{Bi},\gamma_i)$ is defined by the expression in the brace of Eq. (5.30).

E. Power Spectral Voltage of Component Voltage

The power spectral density of the ith component voltage at a given point z is evaluated as follows:

$$W_V(z,\omega)_i = \lim_{T\to\infty} 2/T\, E\{\, V^{(j)}_1(z,\omega)_T\, V^{(j)}_i\ (z,\omega)^*_T\,\}$$

$$= |Z^c_{ii}/\Delta_i|^2 \lim_{T\to\infty} 2/T\, E|\sum_{k=1}^{3} S_{ki}\, f^{(j)}_k(\omega)_T\, F_i|^2$$

$$= |Z^c_{ii}/\Delta_i|^2\, \overline{|F_i|^2} \lim_{T\to\infty} 2/T\, E|\sum_{k=1}^{3} S_{ki}\, f^{(j)}_k(\omega)_T\,|^2$$

$$= |Z^c_{ii}/\Delta_i|^2\, \overline{|F_i|^2} \lim_{T\to\infty} 2/T\, E\{\sum_{k,l=1}^{3} S_{ki}\, S^*_{li}$$

$$\times f_k^{(j)}(\omega)_T \, f^{(j)}{}_l^{*}(\omega)_T^{*})$$

$$= |Z_{ii}^c/\Delta_i|^2 \, \overline{|F_i|^2} \sum_{k,l=1}^{3} S_{ki} \, S_{li}^{*}$$

$$\times \lim_{T\to\infty} 2 \, E(f_k^{(j)}(\omega)_T \, f^{(j)}{}_l^{*}(\omega)_T^{*})/T$$

$$= |Z_{ii}^c/\Delta_i|^2 \, \overline{|F_i|^2} \sum_{k,l=1}^{3} S_{ki} \, S_{li}^{*} \, W_f(\omega)_{kl}, \tag{5.33}$$

where,

$$W_f(\omega)_{kl} = \lim_{T\to\infty} 2 \, E(f_k^{(j)}(\omega)_T \, f^{(j)}{}_l^{*}(\omega)_T^{*})/T$$

$$= 2/B \, \overline{y_k y_l} \, \overline{|u(\omega)|^2} \, . \tag{5.34}$$

$\overline{|F_i|^2}$ is the same as the expression in the outermost square bracket of Eq. (4.33), if γ, ρ_1, and ρ_2 are replaced by γ_i, ρ_{Ai}, and ρ_{Bi}, respectively.

It is noted that, in the derivation of Eq. (5.33), it was assumed that the mean number of corona events is the same in each conductor.

F. Electric Field Intensity Calculation

The analysis, so far, has led to the derivation of the component noise voltage in the power spectral form. An expression will be derived for the electric field intensity which cause radio interference to the radio placed near transmission line.

For a system of three parallel conductors, the phase voltages and the phase charges are related as [17]

$$q^P = 2\pi\varepsilon\, B^{-1}\, V^P \tag{5.35}$$

where, B is the Maxwell's coefficient of capacitance matrix.

Introducing the component voltage given by Eq. (5.13),

$$q^P = 2\pi\varepsilon\, B^{-1}\, V^P \tag{5.36}$$

where, $A = B^{-1}\, S$.

Potential function ϕ_i^P at any point P(x,y,z) due to a line charge q_i^P is given by

$$\phi_i^P = q_i^P/(4\pi\varepsilon_0)\, \ln(d_{ii}/d_{ci})$$

where,

$$d_{ii} = (x - l_i)^2 + (h_i + y)^2$$
$$d_{ci} = (x - l_i)^2 + (h_i - y)^2,$$

and l_i and h_i are the x and y coordinates of conductor i, and the x-y plane is perpendicular to the axis (z) of the line.

Thus, the total potential at P(x,y,z) is

$$\begin{aligned}
\phi^P &= \sum_{i=1}^{3} \phi_i^P \\
&= \sum_{i=1}^{3} q_i^P/(4\pi\varepsilon_0)\, \ln(d_{ii}/d_{ci}) \\
&= 1/2 \sum_{i=1}^{3}\sum_{j=1}^{3} A_{ij}\, V_j\, \ln(d_{ii}/d_{ci}) \\
&= \sum_{j=1}^{3} \left(V_j\ 1/2 \sum_{i=1}^{3} A_{ij} \ln(d_{ii}/d_{ci})\right) .
\end{aligned}$$

The electrical field intensity at P(x,y,z) is the gradient of the potential function ϕ^P. Therefore, it can be calculated as follows:

$$E(x,y,z,t) = \partial\phi^P/\partial x\ i + \partial\phi^P/\partial y\ j$$

$$= \sum_{j=1}^{3} V_j(z,t)\ \frac{1}{2} \sum_{i=1}^{3} A_{ij}/(d_{ii}d_{ci})$$

$$\times \{-8h_i y(x-l_i)\ i + 4h_i((x-l_i)^2 + h_i^2)\ j\}$$

$$= e_x\ i + e_y\ j, \tag{5.37}$$

where, i and j are the unit vector of x and y coordinates, e_x and e_y are the x and y components of E.

Eq. (5.37) connects the noise voltages on the conductors to the electric field intensities at a point P(x,y,z). It is noted that in the derivation of Eq. (5.37), the electric field vectors are assumed to lie in the plane (xy) perpendicular to the axis of the line (z).

The power spectral density of E may be defined by

$$W_E(x,y,z,\omega) = \{W_e^2(x,y,z,\omega)_x + W_e^2(x,y,z,\omega)_y\}^{\frac{1}{2}} \tag{5.38}$$

where, W_{ex} and W_{ey} are the power spectral densities of e_x and e_y, respectively. W_{ex} and W_{ey} are given by:

$$W_e(x,y,z,\omega)_x = \sum_{n=1}^{3} W_V(z,\omega)_n \left| \sum_{i=1}^{3} A_{in} 4h_i y\ (x-l_i)/(d_{ii}d_{ci}) \right|^2$$

$$W_e(x,y,z,\omega)_y = \sum_{n=1}^{3} W_V(z,\omega)_n \left| \sum_{i=1}^{3} A_{in} 2h_i\{(x-l_i)^2 + h_i^2\}/(d_{ii}d_{ci}) \right|^2.$$

The power spectral density at ground level is given by

$$W_E(x,y,z,\omega) = \sum_{n=1}^{3} W_V(z,\omega)_n \left| \sum_{i=1}^{3} 2A_{in}h_i/\{(x-l_i)^2 + h_i^2\} \right|^2.$$

The mean square value of the output field of the receiver placed near tranamission lines can be evaluated in the same way described in Section 4.E, and it can be written as follows:

$$\langle e^{(j)}(x,y,z,t)^2 \rangle = \overline{e(x,y,z,t)^2}$$

$$= |Y(j\omega')|^2 \, W_E(x,y,z,\omega+\omega') \text{ Bandwidth} \quad .$$

VI. DETERMINATION OF RANDOM PARAMETERS FROM THE EMPIRICAL RI MEASUREMENT

A. Introduction

To evaluate RI level with the stochastic RI analysis developed in the preceding chapters, random parameters such as the repetition rate, peak amplitude, and shape of corona pulses, and the mean number of corona generations per unit length along transmission line must be determined.

These parameters are random in nature, and depend on a number of deterministic and statistical factors. Thus, in order to validate the theoretical RI analysis, it appears necessary that the random parameters must be determined by experiments taking into account every possible deterministic and statistical factor. However, it would be very impractical to determine the random parameters for every possible state by experiments because some statistical factors are very hard to estimate and it is practically impossible to measure the state of the conductor surface.

Because of the need for higher transmission voltages a considerable amount of RI measurements have been made on short full-scale single- and three-phase test lines as well as on operating lines, complemented by laboratory investigation on corona discharge characteristics in the past 15 to 20 years [13,26]. Thus, it appears reasonable to utilize these considerable amounts of RI measurements,

instead of a new set of experiments, to determine analytically the random parameters generated in the stochastic RI analysis if possible.

It has been found that the most reproducible RI test data are obtained under heavy rain conditions. An empirical law to determine corona generation in the heavy rain has been established, based on the measurements on a large variety of line configurations [2].

Therefore, the new set of experiments to validate the developed stochastic RI analysis may not be needed if the random parameters can be satisfactorily determined from corona generation or other empirical data.

In this analysis, it will be attempted to determine random parameters from the generation function.

B. Generation Function

The basic relationship between corona current and the generation function was originally established by G. E. Adams [14]. However, a simpler and perhaps more intuitive approach was presented by C. H. Gary [18]. The RMS value of the injected high frequency corona current, measured at frequency ω_0 and with Δf Hz bandwidth, per unit length of conductor is given by [2,18,19]

$$I = C\,\Gamma/(2\pi\varepsilon_0) \tag{6.1}$$

where C is the capacitance per unit length between the conductor and the ground.

Gary's work extended to multiphase transmission lines. The equation proves to be valid, put in general matrix form:

$$[I] = [C]\,[\Gamma]/(2\pi\varepsilon_0)\ ,\ \mu A/m^{\frac{1}{2}}\ . \qquad (6.2)$$

It is, therefore, the generation function which must be considered as the really specific measure of the cause of interference. Γ is expressed in μA per $m^{\frac{1}{2}}$.

It should be noted that the magnitude that can be measured is the current I and not the generation function. In a general case, Γ represents an intermediary parameter in the calculation of the RI and has to be derived from experimental measurements of corona currents and the capacitance of the system.

As was previously stated, the most reproducible test data are obtained from heavy rain. Besides, heavy rain RI data have a practical significance, since generally RI levels are highest when the rain is heaviest [2]. An empirical law, based on the results of a large number of cage and line tests, has been established in [2] as follows:

$$\Gamma_{HR} = 85 - 580/g + 38 \log d/3.8 \qquad (6.3)$$

where,

Γ_{HR} : the heavy rain generation function in dB above $\mu A/m^{\frac{1}{2}}$.

g : the maximum gradient in kv_{rms}/cm .

d : the diameter of conductor in cm .

It should be noted that the heavy rain generation function in Eq. (6.3) is the quasi-peak value measured at 1.0 MHz and with 5 kHz bandwidth.

A joint IEEE/CIGRE Survey [13] has compared the average fair weather RI level with the heavy rain RI level for operating lines ranging from 220 kv to 765 kv. From these data and the limited fair weather data, an average value of 22 dB difference in generation between heavy rain and average fair weather is suggested [2,13].

C. Determination of Random Parameters From Generation Functions

The spectral density $W_J(\omega)$ of the injected corona current due to single corona discharge has been derived in section 3.C, and is given by

$$W_J(\omega) = 2/B\ E(y^2)\ E(|u(\omega)|^2) \quad . \tag{3.11}$$

Since the mean number of corona events per unit length is λ, the spectral density per unit length $\phi(\omega)$ will be given by

$$\phi(\omega) = \lambda\ W_J(\omega) \quad . \tag{6.4}$$

If the injected corona current is measured with RMS detector having Δf bandwidth, the mean square value of corona current will be

$$E\{I(t)^2\} = \phi(\omega)\ \Delta f \quad . \tag{6.5}$$

If it is assumed that the current signal of the detector is ergodic, the time average of any member of output ensemble I(t) can be obtained as follows:

$$\langle I^{(j)}(x,y,z,t)\rangle = (\overline{I(t)^2})^{\frac{1}{2}} \quad . \tag{6.6}$$

Therefore, the average injected corona can be given by

$$\langle I^{(j)}(x,y,z,t)\rangle = (\phi(\omega)\ \Delta f)^{\frac{1}{2}} \quad . \tag{6.7}$$

From the preceding section, the RMS value of the injected corona current, measured at frequency ω_0 and with Δf Hz bandwidth, per unit length of conductor is given by

$$I = C\ \Gamma/(2\pi\varepsilon_0) \quad . \tag{6.1}$$

Equating Eqs. (6.7) and (6.1), random parameter $E(y^2)$ can be obtained, and is given by

$$E(y^2) = (C\ \Gamma/(2\pi\varepsilon_0))^2\ B/(2\ \Delta f\ \overline{|u(\omega)|^2}\ \lambda) \tag{6.8}$$

where, $B = 1/60$, and Δf is the bandwidth of the detector.

In order to make the analysis more clear, consider matched line, in which the power spectral density of noise voltage is given by Eq. (4.36), i.e.,

$$W_V(x,\omega) = \frac{|Z_0|^2}{2B}\ \lambda\ \overline{y^2}\ \overline{|u(\omega)|^2}\ \left[\frac{1}{2\alpha}\left(2 - e^{-2\alpha x} - e^{-2\alpha(L-x)}\right)\right.$$
$$\left. + \frac{\lambda}{|\gamma|^2}\left|2 - e^{-\gamma x} - e^{-\gamma(L-x)}\right|^2\right].$$

Substitution of Eq. (6.8) into the above equation yields

$$W_V(x,\omega) = \left(\frac{C\ \Gamma}{2\pi\varepsilon_0}\right)^2 \frac{|Z_0|^2}{4\Delta f}\left[\frac{1}{2\alpha}\left(2 - e^{-2\alpha x} - e^{-2\alpha(L-x)}\right)\right.$$
$$\left. + \frac{\lambda}{|\gamma|^2}\left|2 - e^{-\gamma x} - e^{-\gamma(L-x)}\right|^2\right]. \tag{6.9}$$

As L goes to infinity, Eq. (6.9) becomes

$$W_V(x,\omega) = \left(\frac{C\Gamma}{2\pi\varepsilon_0}\right)^2 \frac{|Z_0|^2}{4\Delta f} \left(\frac{1}{\alpha} + \frac{4\lambda}{|\delta|^2}\right)^{\frac{1}{2}}.$$

Therefore, the RMS interference voltage will be

$$V(x,\omega) = \frac{C\Gamma}{4\pi\varepsilon_0} Z_0 \left(\frac{1}{\alpha} + \frac{4\lambda}{|\delta|^2}\right)^{\frac{1}{2}}.$$

In the RI analysis using a generation function, the RMS interference voltage is given by (see page 164 of [2])

$$V(x,\omega) = \frac{C\Gamma}{4\pi\varepsilon_0 \alpha} Z_0 \quad .$$

From the above analysis, it is shown that the interference voltage depends on the number of corona events in the stochastic RI analysis, but does not in the generation function RI analysis.

The detailed analysis on $E|u(\omega)|^2$ will be followed in the next section.

D. Determination of the Mean Square Spectrum of Corona Pulse

The shape of the positive pulse in the high voltage transmission lines can be represented by the following double exponential form [35,36]:

$$i(t) = A\left(e^{-at} - e^{-bt}\right) \quad . \tag{6.10}$$

A little simpler expression, which is the special case of Eq. (6.10), was developed empirically by Perel'man and Chernobrodov [37], and is given by

$$i(t) = A\, a\, t\, e^{(1-at)}. \qquad (6.11)$$

A statistical study was made of the parameters of streamer pulses on twisted conductors 17 to 33 mm in diameter in [39]. Investigated were the shapes of the streamer pulses, the high frequency current generated by one source of corona, and the variation of the h.f. noise current as a function of the pulse of the supply voltage. It was confirmed in [39] that the corona pulse shape was well approximated by equation (6.11).

It was found that the build-time of pulses increased with increasing diameter of the conductor. The following relationship was obtained between the coefficient a and the conductor diameter (in the investigated range of diameters from 17 to 33 mm):

$$a = 10^9/(2.5d + 28) \quad , 1/\text{sec} \qquad (6.12)$$

where, d is the conductor diameter in mm.

The impulse amplitude, the variation of the maximum field strength on the surface of the conductor in the interval from 25 to 34 kv/cm and the presence of an adjacent conductor at a distance of 0.1 to 0.15 m from the corona conductor had no important effect on the shape and width of corona pulses [39].

Equation (6.11) will be used for the evaluation of $E|u(\omega)|^2$ in this section for simplicity. Since u(t) has unit peak value, u(t) is given by

$$u(t) = a\, t\, e^{(1-at)}. \qquad (6.13)$$

Taking the Fourier transforms on the both sides of Eq. (6.13), we have

$$|u(\omega)| = a\, e/(a^2 + \omega^2) \quad . \tag{6.14}$$

At this point, random variable a is assumed to be uniformly distributed so that the density function of a is given by

$$f_1(a) = \begin{cases} 1/(q - p) & \text{for } p \le a \le q \\ 0 & \text{otherwise.} \end{cases} \tag{6.15}$$

The expectation of $|u(\omega)|^2$ can be easily evaluated and the result is given by:

$$\overline{|u(\omega)|^2} = \frac{e^2}{2\omega(q-p)}\left|\tan^{-1}\left(\frac{q}{\omega}\right) - \tan^{-1}\left(\frac{p}{\omega}\right) - \frac{\omega(q-p)(\omega^2-pq)}{(q^2+\omega^2)(p^2+\omega^2)}\right|. \tag{6.16}$$

E. Summary and Conclusions

Most parameters generated in the stochastic RI analysis such as the repetition rate, peak amplitude, and the shape of corona pulses, and the mean number of corona events are shown to be determined from the existing RI data. Among these random parameters, the repetition rate and the shape of corona pulses are assumed to be deterministic. The peak amplitude of corona pulses is shown to depend on the generation function, the mean number of corona events, and the mean square spectrum of basic corona pulse with unit peak amplitude. The mean square spectrum of basic pulse is determined from the deterministic pulse shape.

From the analysis in Section 6.C, the following may be concluded:

1. In the generation function RI analysis, interference voltage is independent of the number of corona events per unit length.
2. In the stochastic RI analysis, interference voltage is dependent of the number of corona events.
3. The RI value obtained by the stochastic method will be close to the RI value obtained by the generation function method if λ is close to zero.
4. From Eq. (6.8), as λ goes to zero, however, $E(y^2)$ goes to infinity, which is not possible in practice. Therefore, one way to determine λ is to know the mean value of peak amplitude of corona pulse, of which theoretical [35] and experimental [36,37,40,41] data exist, and use Eq. (6.8).

VII. NUMERICAL CALCULATIONS AND DISCUSSIONS

A. Introduction

In order to demonstrate practical applications of newly developed stochastic RI analysis, the radio interference levels represented by the electric field intensity at the output of the i-f stage of the radio receiver will be calculated for a high voltage three phase transmission line.

Line impedances are derived taking into account the conductor geometry, conductor internal impedances, and earth return path. Since the method to obtain line impedances is presented well in [42], only the results are shown in the Fortran program.

A computer program has been developed to calculate RI levels for comparative studies, and is shown in Appendix II.

B. Base Case Line Characteristics

A single-circuit horizontal line shown in Figure 3 is considered in this chapter. The maximum system voltage is 362 kv. The basic geometry is chosen as average values presently used for EHV transmission lines [2]. The average conductor height is used for the purpose of corona performance calculations and represents the height of a perfectly horizontal line which yields the same performance as an actual line. The average height is equal to the mid-span height plus one third of the sag.

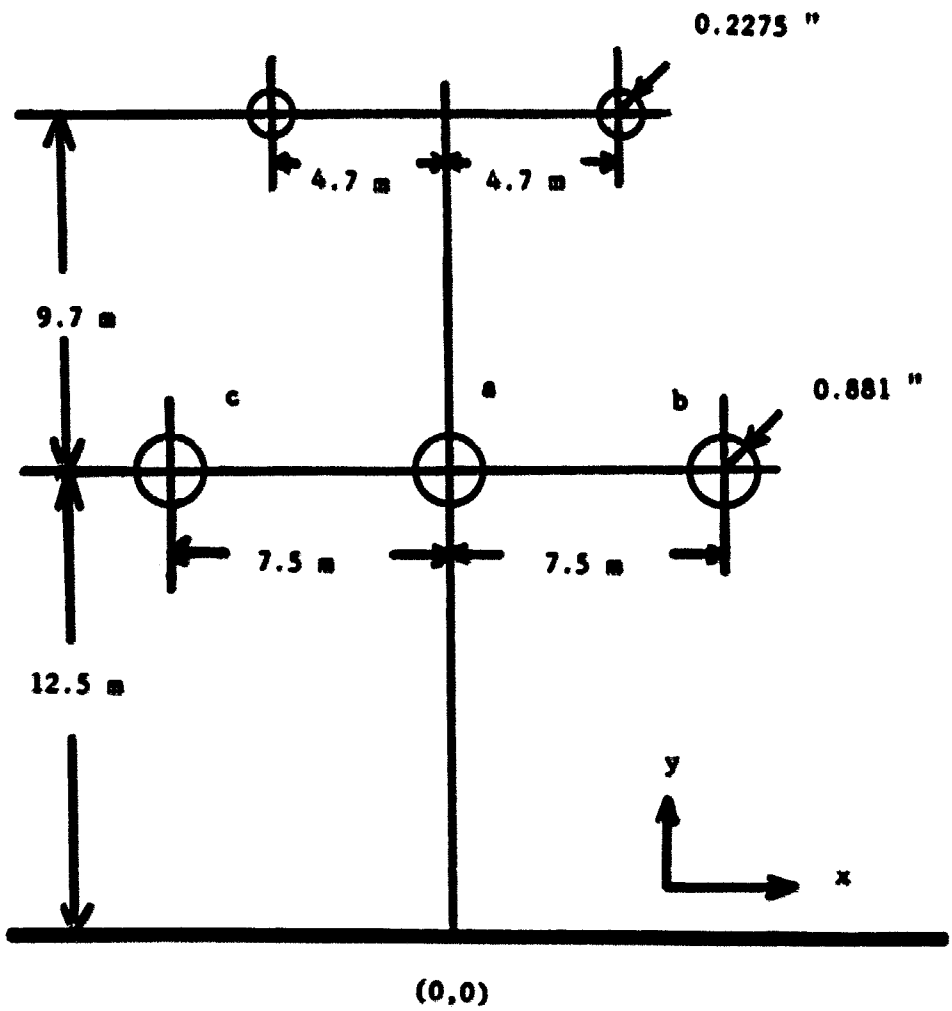

FIGURE 3. Single-Circuit Horizontal Line Configuration, 345 kv

The following constants are assumed in the calculations:

Conductor	84 / 19 Al / St Bluebird
Shield wire	7/16" St
Diameter of conductor	1.762 in
Diameter of shield wire	0.455 in
Impedance of shield wire	4.97 + j1.58 at 60 Hz
Conductor resistivity	3.21×10^{-8} Ω.m
Shield wire resistivity	20×10^{-8} Ω.m
Earth resistivity	100 Ω.m
Relative permeability of shield wire	1000
Relative permeability of conductor	1

C. Random Parameters

Since the most reproducible RI test data are obtained under heavy rain, the generation function represented by Eq. (6.3) is used to obtain random parameters.

The mean square peak-amplitude $\overline{y^2}$ is given by Eq. (6.8), i.e.,

$$\overline{y^2} = (Cf/2\pi\varepsilon_0)^2 B/(2\,\Delta f\,\overline{|u(\omega)|^2}\,\lambda)\ . \qquad (6.8)$$

Since

$$\overline{y^2} = \overline{(y - \bar{y})^2} + (\bar{y})^2 = var(y) + (\bar{y})^2\ , \qquad (7.1)$$

$\bar{y}$ can be written by

$$y = C\Gamma/(2\pi\varepsilon_0)\sqrt{B/(2\,\Delta f\,\overline{|u(\omega)|^2}\,\lambda\,(1+pc^2))}, \tag{7.2}$$

where, $var(y) = (\bar{y}\ pc)^2$. (7.3)

It should be noted that $\langle I^{(j)}\rangle$ represented by Eq. (6.7) is an RMS value. It is an American (ANSI) Standard [43,44] to use a quasi-peak detector for the measurement of radio interference field from overhead power lines. Generation functions are also usually represented by quasi-peak value. Thus, $\langle I^{(j)}\rangle$ must be converted to a quasi-peak value. It is assumed that a quasi-peak value is the same as an RMS value times $\sqrt{2}$ because peak value is close to quasi-peak value [11,12]. Then, when the generation function is expressed in the quasi-peak value, the peak amplitude of the pulse is given by

$$y = C\Gamma/(2\pi\varepsilon_0)\sqrt{B/(4\Delta f\,\overline{|u(\omega)|^2}\lambda\,(1+pc^2)}. \tag{7.4}$$

The bandwidth of radio noise meter is assumed to be 5 KHz. The inverse of build-time (a) is assumed to have a uniform distribution denoted by Eq. (6.15). $\overline{|u(\omega)|^2}$ is then given by Eq. (6.16).

λ can be approximately determined if the approximated peak amplitude of corona current pulse is known. The amplitudes of positive streamers are assumed to be in the range from 50 to 200 milliamperes.

Unknown parameters pc, p, q are assumed as follows:

$pc = .75$

$p = .5\ \bar{a}$

$q = 2\ \bar{a}$

where, $\bar{a}$ is given by Eq. (6.12).

D. Calculated Results

The radio interference fields were calculated for various cases to compare the effects of different factors on the RI levels. These factors are:

1. Terminating impedances of the line;
2. Mean number of corona events along the line;
3. Frequency (0.1 - 10 MHz);
4. Line length; and
5. Design parameters such as conductor diameter, system voltage, conductor height, and the phase spacings.

1. Effect of the terminating impedances of the line

Table 1 shows the radio interference levels for different line terminations. Four terminations are considered for two different line lengths.

For a relatively long line, there is no significant difference in the RI level for different terminations. This fact is reasonable because the reflective waves from terminations are attenuated to negligible values. However, the RI field for the line of length 10 m open-circuited at one end and terminated with a coupled capacitor 4000 pF at the other end is considerably different from the RI fields for the other cases.

Therefore, it is suggested that a care be given in the analysis of RI field data obtained in the short test line and in the extension of those data to the actual long line.

TABLE 1. The Effect of Line Terminations on the RI Field

Z_A and Z_B are the termination impedances of line AB from each conductor and ground. L denotes the total length of line. RI field is the quasi-peak value calculated at 1MHz and 5KHz bandwidth. The mean number of corona events per meter is assumed to be 1. Terminal impedance -j39.79 represents a coupled capacitor 4000 pF.

Terminal Impedances		RI Field (dB above μv/m)	
$Z_A(\Omega)$	$Z_B(\Omega)$	L = 10 m	L = 1600 m
10^{10}	10^{10}	82.860	82.860
10^{10}	-j39.79	69.290	83.162
0.0	0.0	82.285	81.028
-j39.79	-j39.79	82.285	82.530
matched	matched	82.285	82.530

2. Effect of the mean number of corona events

To determine the approximated value of λ and the effect of λ on the RI field, the RI fields for different values of λ were calculated for the constant generation function given by Eq. (6.3). λ is the random parameter making the stochastic RI analysis distinct from other RI analyses. It is noted that in most of cases, corona generations are assumed to be uniform along the line.

Figure 4 and Tables 2 and 3 show the corona currents of center and outer phases. The RI fields were calculated for the lateral distance of 15 m from the outer conductor.

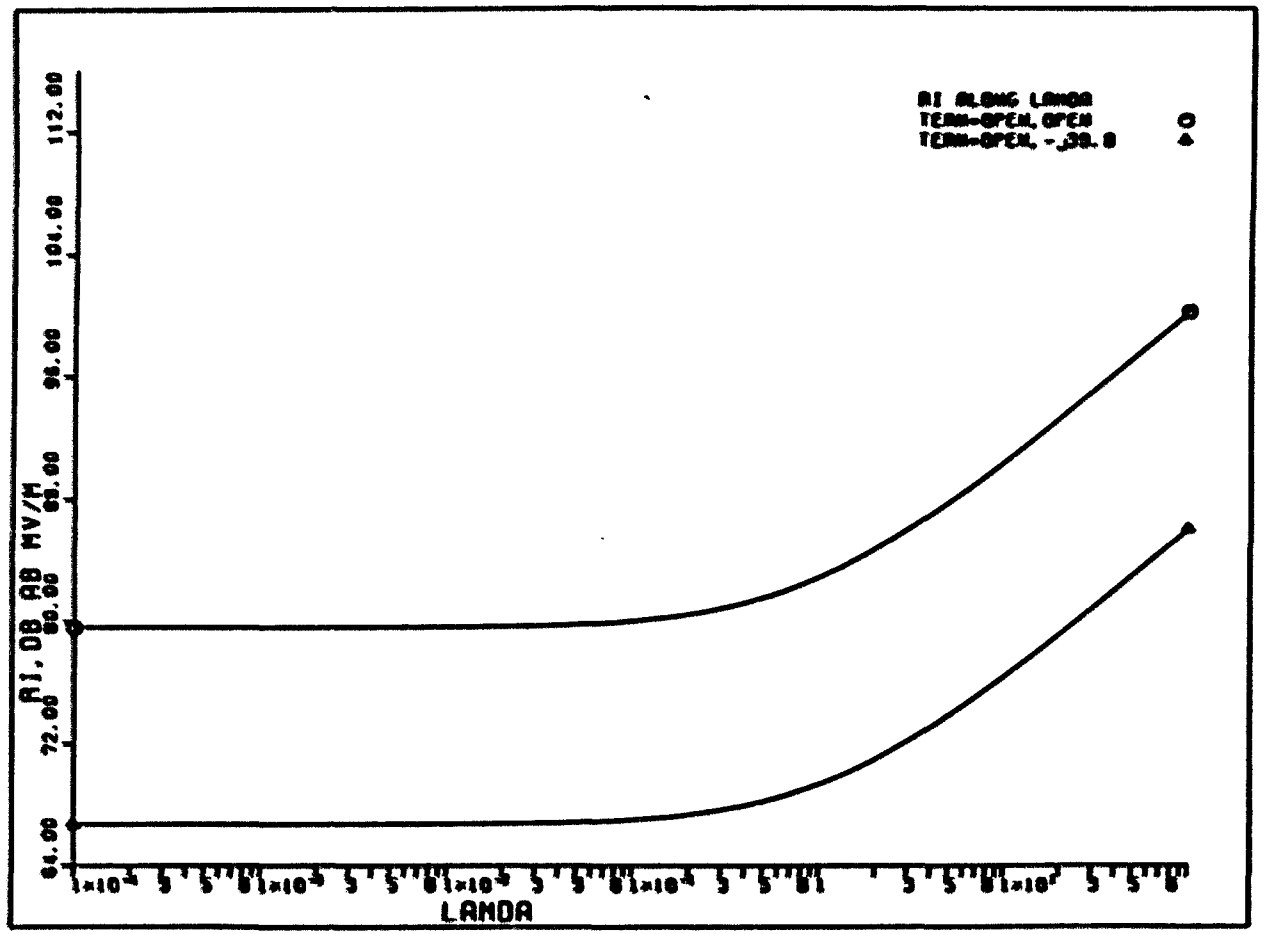

FIGURE 4. The Effect of λ on the RI Field

TABLE 2. The Effect of λ on the RI field and Corona Current, Case 1

λ denotes the mean number of corona events along the line per meter. The line is open circuited at one end and terminated with a coupled capacitor 4000 pF from each conductor to ground at the other end (case 1). The RI field is the quasi-peak value calculated at 1 MHz with 5 KHz bandwidth. The total length of line is 10 m.

Lamda	Current of Center phase	Current of Outer phase		RI Field
0.100D-03	0.187D 02	0.138D 02	0.138D 02	0.795D 02
0.158D-03	0.148D 02	0.110D 02	0.110D 02	0.795D 02
0.251D-03	0.118D 02	0.874D 01	0.874D 01	0.795D 02
0.398D-03	0.940D 01	0.694D 01	0.694D 01	0.795D 02
0.630D-03	0.746D 01	0.551D 01	0.551D 01	0.795D 02
0.100D-02	0.593D 01	0.438D 01	0.438D 01	0.795D 02
0.158D-02	0.471D 01	0.348D 01	0.348D 01	0.795D 02
0.251D-02	0.374D 01	0.276D 01	0.276D 01	0.795D 02
0.398D-02	0.297D 01	0.219D 01	0.219D 01	0.795D 02
0.630D-02	0.236D 01	0.174D 01	0.174D 01	0.795D 02
0.100D-01	0.187D 01	0.138D 01	0.138D 01	0.796D 02
0.158D-01	0.148D 01	0.110D 01	0.110D 01	0.796D 02
0.251D-01	0.118D 01	0.874D 00	0.874D 00	0.796D 02
0.398D-01	0.940D 00	0.694D 00	0.694D 00	0.797D 02
0.630D-01	0.746D 00	0.551D 00	0.551D 00	0.798D 02
0.100D 00	0.593D 00	0.438D 00	0.438D 00	0.800D 02
0.158D 00	0.471D 00	0.348D 00	0.348D 00	0.802D 02
0.251D 00	0.374D 00	0.276D 00	0.276D 00	0.806D 02
0.398D 00	0.297D 00	0.219D 00	0.219D 00	0.811D 02
0.630D 00	0.236D 00	0.174D 00	0.174D 00	0.819D 02
0.100D 01	0.187D 00	0.138D 00	0.138D 00	0.828D 02
0.158D 01	0.148D 00	0.110D 00	0.110D 00	0.840D 02
0.251D 01	0.118D 00	0.874D-01	0.874D-01	0.854D 02
0.398D 01	0.940D-01	0.694D-01	0.694D-01	0.869D 02
0.630D 01	0.746D-01	0.551D-01	0.551D-01	0.886D 02
0.100D 02	0.593D-01	0.438D-01	0.438D-01	0.904D 02
0.158D 02	0.471D-01	0.348D-01	0.348D-01	0.923D 02
0.251D 02	0.374D-01	0.276D-01	0.276D-01	0.942D 02
0.398D 02	0.297D-01	0.219D-01	0.219D-01	0.962D 02
0.630D 02	0.236D-01	0.174D-01	0.174D-01	0.981D 02
0.100D 03	0.187D-01	0.138D-01	0.138D-01	0.100D 03

TABLE 3. The Effect of λ on the RI field and Corona Current, Case 2

λ denotes the mean number of corona events along the line per meter.
The line is open circuited at both ends (case 2).
The RI field is the quasi-peak value calculated at 1 MHz with 5 KHz bandwidth. The total length of line is 10 m.

Lamda	Current of Center Phase	Current of Outer Phase		RI Field
0.100D-03	0.187D 02	0.138D 02	0.138D 02	0.666D 02
0.158D-03	0.148D 02	0.110D 02	0.110D 02	0.666D 02
0.251D-03	0.118D 02	0.874D 01	0.874D 01	0.666D 02
0.398D-03	0.940D 01	0.694D 01	0.694D 01	0.666D 02
0.630D-03	0.746D 01	0.551D 01	0.551D 01	0.666D 02
0.100D-02	0.593D 01	0.438D 01	0.438D 01	0.666D 02
0.158D-02	0.471D 01	0.348D 01	0.348D 01	0.666D 02
0.251D-02	0.374D 01	0.276D 01	0.276D 01	0.666D 02
0.398D-02	0.297D 01	0.219D 01	0.219D 01	0.666D 02
0.630D-02	0.236D 01	0.174D 01	0.174D 01	0.666D 02
0.100D-01	0.187D 01	0.138D 01	0.138D 01	0.666D 02
0.158D-01	0.148D 01	0.110D 01	0.110D 01	0.666D 02
0.251D-01	0.118D 01	0.874D 00	0.874D 00	0.667D 02
0.398D-01	0.940D 00	0.694D 00	0.694D 00	0.667D 02
0.630D-01	0.746D 00	0.551D 00	0.551D 00	0.668D 02
0.100D 00	0.593D 00	0.438D 00	0.438D 00	0.669D 02
0.158D 00	0.471D 00	0.348D 00	0.348D 00	0.671D 02
0.251D 00	0.374D 00	0.276D 00	0.276D 00	0.674D 02
0.398D 00	0.297D 00	0.219D 00	0.219D 00	0.678D 02
0.630D 00	0.236D 00	0.174D 00	0.174D 00	0.684D 02
0.100D 01	0.187D 00	0.138D 00	0.138D 00	0.692D 02
0.158D 01	0.148D 00	0.110D 00	0.110D 00	0.703D 02
0.251D 01	0.118D 00	0.874D-01	0.874D-01	0.715D 02
0.398D 01	0.940D-01	0.694D-01	0.694D-01	0.730D 02
0.630D 01	0.746D-01	0.551D-01	0.551D-01	0.746D 02
0.100D 02	0.593D-01	0.438D-01	0.438D-01	0.763D 02
0.158D 02	0.471D-01	0.348D-01	0.348D-01	0.782D 02
0.251D 02	0.374D-01	0.276D-01	0.276D-01	0.800D 02
0.398D 02	0.297D-01	0.219D-01	0.219D-01	0.820D 02
0.630D 02	0.236D-01	0.174D-01	0.174D-01	0.839D 02
0.100D 03	0.187D-01	0.138D-01	0.138D-01	0.859D 02

For reasonable ranges of pulse amplitude from 50 to 200 milliamperes, λ ranges from about 1 to 16. The RI fields for λ less than 1 show a nearly constant value of about 79.5 dB above μv/m, which is close to some of the measured or calculated RI fields by various methods tabulated in Table 4 (for detailed methods and empirical formulas, see [2]). However, it should be noted that the RI fields calculated by the stochastic model are based on the RI data established in the Project UHV.

TABLE 4. The RI Fields by Different Methods during Foul-Weather

The RI Fields are the quasi-peak value measured at the lateral distance of 15 m from the outer conductor at 1 MHz with 5 KHz bandwidth.

RI Analysis Method	RI Field (dB above μv/m)
Project UHV Base case (USA)	78.5
400-kv-FG (Germany)	78.3
Ontario Hydro (Canada)	75.3
ENEL (Italy)	71.7
EGU (Czechoslovakia)	63.2

From Figure 4, it is observed that the RI values for λ greater than 1 are significantly different from those obtained by the conventional RI analysis methods. Therefore, once again, it is shown that the uniform distribution of corona generation is unpractical.

Thus, it must be emphasized that the measured RI fields will pretty much depend on the number of corona events along the line during foul-weather conditions. However, there may be not much difference between the stochastic and conventional methods during fair-weather conditions because the number of corona events is much smaller during fair-weather than during foul-weather.

3. RI frequency spectrum

The frequency spectrums were calculated over the range from 0.1 to 10 MHz at the center of the open ended line at both ends. In order to see the effects of line length and the number of corona events on the RI spectrum, the RI fields were calculated for three cases of line length, and for two values of λ at each frequency from 0.1 to 10 MHz. Calculated RI fields are shown in Figures 5 and 6, and Tables 5 and 6.

From equation (4.33), which is the formula to obtain the power spectral density of noise voltage, it can be easily noticed that the shape of RI spectrum fields is the function of line length, observation position, propagation constant, the mean number of corona events, and the shape of basic corona current pulse. The shape of corona current pulse decides the general trends of RI spectrum along frequency. The RI field, for example, decreases as 20 $\log(1/f^2)$ with frequency of greater than about 2 MHz [13,24,26,35,36,37]. It is observed that the RI field decreases about 28 dB with frequency increases from 0.1 to 1 MHz, and 44 dB with frequency increases from 1 to 10 MHz. The 44 dB decrease with frequency increases from 1 to 10 MHz agrees with most published results.

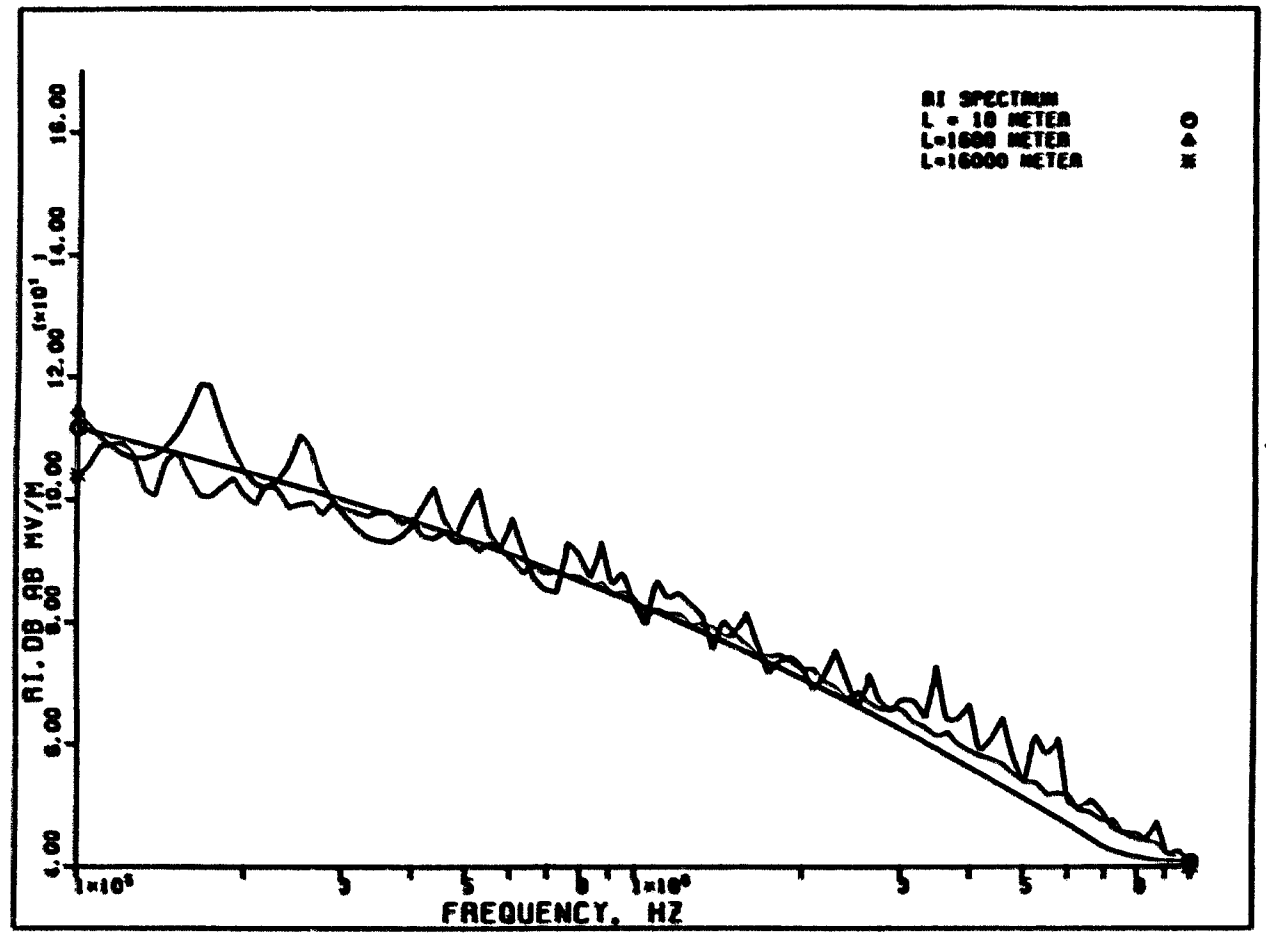

FIGURE 5. RI Field Spectrum for Different Line Length, $\lambda = 1$

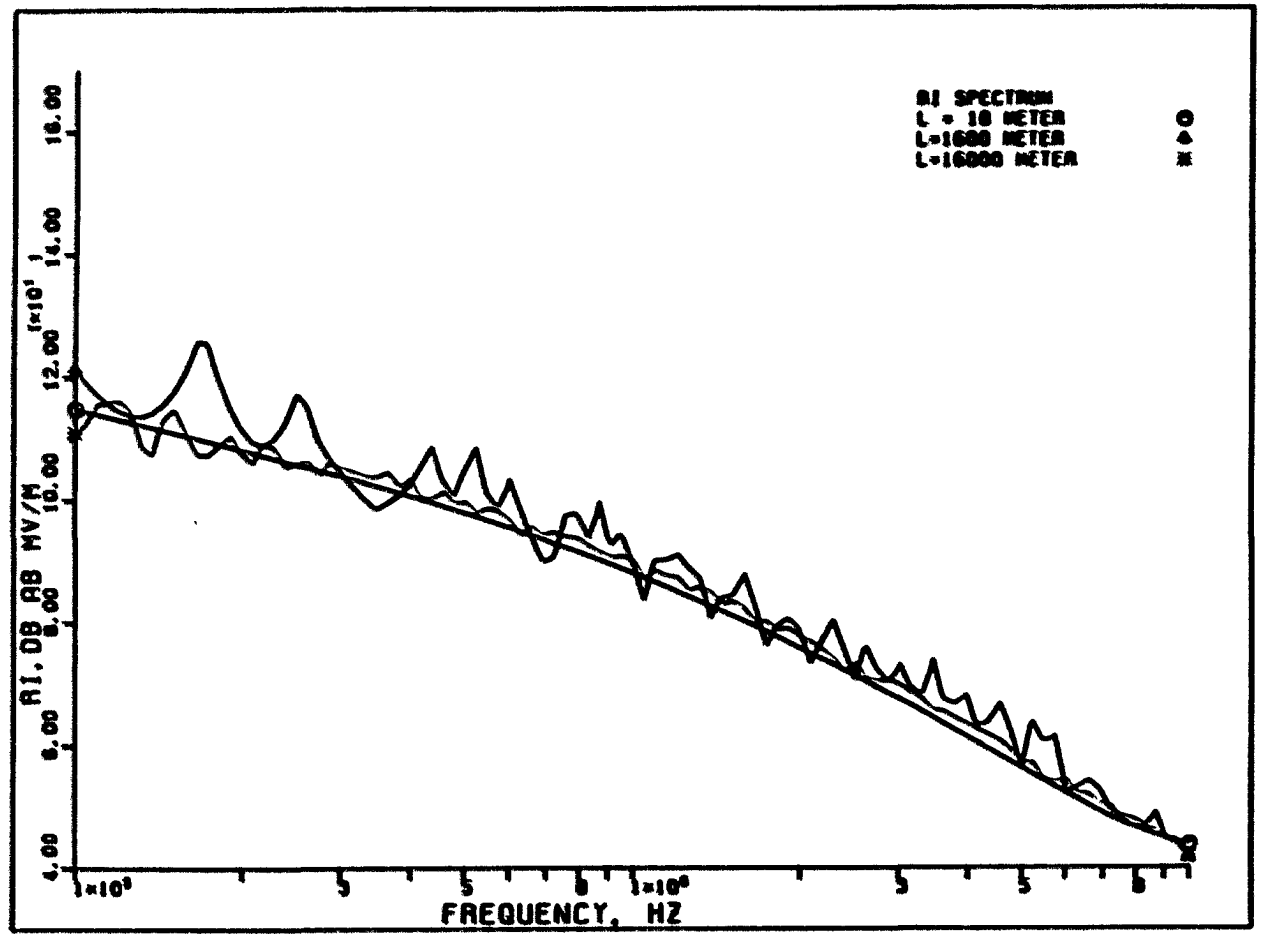

FIGURE 6. RI Field Spectrum for Different Line Length, $\lambda = 5$

TABLE 5. RI Field Spectrum for Different Line Length, λ = 1

The line is open-circuited at both ends. L denotes total line length. The RI field is the quasi-peak value calculated at the lateral distance of 15 m from the outer phase conductor with 5KHz bandwidth.

Frequency (MHz)	L = 10 m	L = 1600 m	L = 16000 m
0.10000D 06	0.11163D 03	0.11414D 03	0.10376D 03
0.10471D 06	0.11116D 03	0.11191D 03	0.10544D 03
0.10965D 06	0.11068D 03	0.11002D 03	0.10849D 03
0.11482D 06	0.11021D 03	0.10844D 03	0.10885D 03
0.12023D 06	0.10973D 03	0.10724D 03	0.10897D 03
0.12589D 06	0.10925D 03	0.10654D 03	0.10694D 03
0.13183D 06	0.10877D 03	0.10648D 03	0.10154D 03
0.13804D 06	0.10829D 03	0.10714D 03	0.10062D 03
0.14454D 06	0.10781D 03	0.10853D 03	0.10616D 03
0.15136D 06	0.10732D 03	0.11073D 03	0.10730D 03
0.15849D 06	0.10683D 03	0.11398D 03	0.10356D 03
0.16596D 06	0.10634D 03	0.11841D 03	0.10041D 03
0.17378D 06	0.10585D 03	0.11777D 03	0.10026D 03
0.18197D 06	0.10535D 03	0.11205D 03	0.10177D 03
0.19055D 06	0.10485D 03	0.10759D 03	0.10322D 03
0.19953D 06	0.10435D 03	0.10428D 03	0.10043D 03
0.20893D 06	0.10384D 03	0.10222D 03	0.98975D 02
0.21878D 06	0.10333D 03	0.10174D 03	0.10193D 03
0.22909D 06	0.10282D 03	0.10289D 03	0.10124D 03
0.23988D 06	0.10230D 03	0.10552D 03	0.98315D 02
0.25119D 06	0.10177D 03	0.11015D 03	0.98900D 02
0.26303D 06	0.10124D 03	0.10767D 03	0.99176D 02
0.27542D 06	0.10071D 03	0.10219D 03	0.97156D 02
0.28840D 06	0.10017D 03	0.99313D 02	0.98944D 02
0.30200D 06	0.99618D 02	0.96976D 02	0.97958D 02
0.31623D 06	0.99065D 02	0.94955D 02	0.97511D 02
0.33113D 06	0.98506D 02	0.93476D 02	0.96796D 02
0.34674D 06	0.97940D 02	0.92920D 02	0.97530D 02
0.36308D 06	0.97368D 02	0.92603D 02	0.97578D 02
0.38019D 06	0.96788D 02	0.93569D 02	0.95632D 02
0.39811D 06	0.96203D 02	0.95318D 02	0.96607D 02
0.41687D 06	0.95613D 02	0.98616D 02	0.93532D 02
0.43652D 06	0.95015D 02	0.10155D 03	0.93243D 02
0.45709D 06	0.94410D 02	0.96058D 02	0.94456D 02
0.47863D 06	0.93798D 02	0.93583D 02	0.92595D 02
0.50119D 06	0.93178D 02	0.97843D 02	0.92760D 02
0.52481D 06	0.92549D 02	0.10129D 03	0.91106D 02

TABLE 5 (continued)

Frequency (MHz)	L = 10 m	L = 1600 m	L = 16000 m
0.54954D 06	0.91913D 02	0.93803D 02	0.92466D 02
0.57544D 06	0.91269D 02	0.91963D 02	0.91441D 02
0.60256D 06	0.90616D 02	0.96618D 02	0.89682D 02
0.63096D 06	0.89954D 02	0.91362D 02	0.87615D 02
0.66069D 06	0.89285D 02	0.86746D 02	0.88781D 02
0.69183D 06	0.88606D 02	0.84989D 02	0.87534D 02
0.72444D 06	0.87919D 02	0.84555D 02	0.87908D 02
0.75858D 06	0.87223D 02	0.92484D 02	0.87205D 02
0.79433D 06	0.86519D 02	0.90607D 02	0.87046D 02
0.83176D 06	0.85805D 02	0.86772D 02	0.85666D 02
0.87096D 06	0.85082D 02	0.92585D 02	0.85980D 02
0.91201D 06	0.84351D 02	0.85864D 02	0.83999D 02
0.95499D 06	0.83610D 02	0.87354D 02	0.84428D 02
0.10000D 07	0.82860D 02	0.82530D 02	0.83415D 02
0.10471D 07	0.82101D 02	0.79312D 02	0.80556D 02
0.10965D 07	0.81333D 02	0.86328D 02	0.81813D 02
0.11482D 07	0.80555D 02	0.83576D 02	0.81006D 02
0.12023D 07	0.79768D 02	0.84277D 02	0.80926D 02
0.12589D 07	0.78971D 02	0.82491D 02	0.79053D 02
0.13183D 07	0.78165D 02	0.80835D 02	0.79230D 02
0.13804D 07	0.77349D 02	0.75239D 02	0.78742D 02
0.14454D 07	0.76524D 02	0.79811D 02	0.77126D 02
0.15136D 07	0.75688D 02	0.78182D 02	0.77591D 02
0.15849D 07	0.74844D 02	0.81139D 02	0.75977D 02
0.16596D 07	0.73989D 02	0.76097D 02	0.74237D 02
0.17378D 07	0.73125D 02	0.71364D 02	0.74053D 02
0.18197D 07	0.72252D 02	0.73248D 02	0.74389D 02
0.19055D 07	0.71369D 02	0.73981D 02	0.73132D 02
0.19953D 07	0.70477D 02	0.72205D 02	0.71942D 02
0.20893D 07	0.69576D 02	0.68668D 02	0.72092D 02
0.21878D 07	0.68665D 02	0.70898D 02	0.69919D 02
0.22909D 07	0.67746D 02	0.75055D 02	0.68853D 02
0.23988D 07	0.66819D 02	0.70259D 02	0.67015D 02
0.25119D 07	0.65883D 02	0.65718D 02	0.68333D 02
0.26303D 07	0.64939D 02	0.71136D 02	0.66413D 02
0.27542D 07	0.63988D 02	0.66553D 02	0.65283D 02
0.28840D 07	0.63029D 02	0.65236D 02	0.65656D 02
0.30200D 07	0.62063D 02	0.67015D 02	0.65133D 02
0.31623D 07	0.61091D 02	0.66656D 02	0.63280D 02
0.33113D 07	0.60112D 02	0.64016D 02	0.62442D 02
0.34674D 07	0.59127D 02	0.72511D 02	0.61036D 02
0.36308D 07	0.58136D 02	0.63745D 02	0.61840D 02

TABLE 5 (continued)

Frequency (MHz)	L = 10 m	L = 1600 m	L = 16000 m
0.38019D 07	0.57139D 02	0.64023D 02	0.59742D 02
0.39811D 07	0.56138D 02	0.66217D 02	0.58690D 02
0.41687D 07	0.55127D 02	0.58643D 02	0.57845D 02
0.43652D 07	0.54112D 02	0.60816D 02	0.57304D 02
0.45709D 07	0.53091D 02	0.64041D 02	0.56590D 02
0.47863D 07	0.52062D 02	0.57441D 02	0.54942D 02
0.50119D 07	0.51025D 02	0.53531D 02	0.53775D 02
0.52481D 07	0.49978D 02	0.61102D 02	0.53623D 02
0.54954D 07	0.48919D 02	0.56251D 02	0.51569D 02
0.57544D 07	0.47845D 02	0.60736D 02	0.51832D 02
0.60256D 07	0.46753D 02	0.50370D 02	0.51455D 02
0.63096D 07	0.45637D 02	0.49459D 02	0.49002D 02
0.66069D 07	0.44488D 02	0.50815D 02	0.48584D 02
0.69183D 07	0.43358D 02	0.48794D 02	0.47315D 02
0.72444D 07	0.42494D 02	0.46090D 02	0.47560D 02
0.75858D 07	0.41975D 02	0.45338D 02	0.45269D 02
0.79433D 07	0.41533D 02	0.45214D 02	0.44298D 02
0.83176D 07	0.41173D 02	0.44339D 02	0.44055D 02
0.87096D 07	0.40901D 02	0.47154D 02	0.43536D 02
0.91201D 07	0.40727D 02	0.41726D 02	0.41898D 02
0.95499D 07	0.40663D 02	0.42341D 02	0.40926D 02
0.10000D 08	0.40732D 02	0.40182D 02	0.39736D 02

TABLE 6. RI Field Spectrum for Different Line Length, λ = 5

The line is open-circuited at both ends. L denotes total line length. The RI field is the quasi-peak value calculated at the lateral distance of 15 m from the outer phase conductor with 5KHz bandwidth.

Frequency (MHz)	L = 10 m	L = 1600 m	L = 16000 m
0.10000D 06	0.11477D 03	0.12111D 03	0.11067D 03
0.10471D 06	0.11433D 03	0.11889D 03	0.11239D 03
0.10965D 06	0.11389D 03	0.11699D 03	0.11543D 03
0.11482D 06	0.11345D 03	0.11541D 03	0.11582D 03
0.12023D 06	0.11300D 03	0.11421D 03	0.11594D 03
0.12589D 06	0.11256D 03	0.11351D 03	0.11389D 03
0.13183D 06	0.11211D 03	0.11345D 03	0.10844D 03
0.13804D 06	0.11167D 03	0.11411D 03	0.10749D 03
0.14454D 06	0.11122D 03	0.11551D 03	0.11307D 03
0.15136D 06	0.11077D 03	0.11771D 03	0.11426D 03
0.15849D 06	0.11032D 03	0.12096D 03	0.11049D 03
0.16596D 06	0.10986D 03	0.12539D 03	0.10730D 03
0.17378D 06	0.10941D 03	0.12475D 03	0.10715D 03
0.18197D 06	0.10895D 03	0.11902D 03	0.10869D 03
0.19055D 06	0.10848D 03	0.11456D 03	0.11016D 03
0.19953D 06	0.10802D 03	0.11125D 03	0.10733D 03
0.20893D 06	0.10755D 03	0.10918D 03	0.10565D 03
0.21878D 06	0.10708D 03	0.10870D 03	0.10885D 03
0.22909D 06	0.10660D 03	0.10983D 03	0.10806D 03
0.23988D 06	0.10612D 03	0.11244D 03	0.10516D 03
0.25119D 06	0.10563D 03	0.11694D 03	0.10579D 03
0.26303D 06	0.10514D 03	0.11453D 03	0.10594D 03
0.27542D 06	0.10465D 03	0.10909D 03	0.10400D 03
0.28840D 06	0.10415D 03	0.10624D 03	0.10581D 03
0.30200D 06	0.10364D 03	0.10391D 03	0.10484D 03
0.31623D 06	0.10313D 03	0.10182D 03	0.10431D 03
0.33113D 06	0.10261D 03	0.99899D 02	0.10355D 03
0.34674D 06	0.10209D 03	0.98257D 02	0.10352D 03
0.36308D 06	0.10156D 03	0.99235D 02	0.10429D 03
0.38019D 06	0.10102D 03	0.10045D 03	0.10201D 03
0.39811D 06	0.10047D 03	0.10220D 03	0.10322D 03
0.41687D 06	0.99923D 02	0.10520D 03	0.10021D 03
0.43652D 06	0.99365D 02	0.10835D 03	0.99977D 02
0.45709D 06	0.98799D 02	0.10294D 03	0.10109D 03
0.47863D 06	0.98225D 02	0.10048D 03	0.99308D 02
0.50119D 06	0.97643D 02	0.10474D 03	0.99510D 02
0.52481D 06	0.97053D 02	0.10821D 03	0.97475D 02

TABLE 6 (continued)

Frequency (MHz)	L = 10 m	L = 1600 m	L = 16000 m
0.54954D 06	0.96454D 02	0.10071D 03	0.98348D 02
0.57544D 06	0.95846D 02	0.98730D 02	0.97822D 02
0.60256D 06	0.95229D 02	0.10310D 03	0.96313D 02
0.63096D 06	0.94604D 02	0.98136D 02	0.94022D 02
0.66069D 06	0.93969D 02	0.93395D 02	0.95339D 02
0.69183D 06	0.93324D 02	0.89746D 02	0.94004D 02
0.72444D 06	0.92670D 02	0.90961D 02	0.94518D 02
0.75858D 06	0.92007D 02	0.97182D 02	0.93789D 02
0.79433D 06	0.91334D 02	0.97270D 02	0.93499D 02
0.83176D 06	0.90651D 02	0.93535D 02	0.92233D 02
0.87096D 06	0.89957D 02	0.99404D 02	0.91198D 02
0.91201D 06	0.89254D 02	0.92520D 02	0.90395D 02
0.95499D 06	0.88541D 02	0.93831D 02	0.90517D 02
0.10000D 07	0.87817D 02	0.89068D 02	0.89814D 02
0.10471D 07	0.87083D 02	0.83434D 02	0.86628D 02
0.10965D 07	0.86339D 02	0.89924D 02	0.88218D 02
0.11482D 07	0.85585D 02	0.90012D 02	0.87355D 02
0.12023D 07	0.84817D 02	0.90868D 02	0.87079D 02
0.12589D 07	0.84040D 02	0.86697D 02	0.84963D 02
0.13183D 07	0.83253D 02	0.87080D 02	0.85440D 02
0.13804D 07	0.82454D 02	0.80431D 02	0.84631D 02
0.14454D 07	0.81644D 02	0.83868D 02	0.82688D 02
0.15136D 07	0.80823D 02	0.84421D 02	0.83126D 02
0.15849D 07	0.79990D 02	0.87665D 02	0.81996D 02
0.16596D 07	0.79147D 02	0.82228D 02	0.79569D 02
0.17378D 07	0.78292D 02	0.76024D 02	0.79900D 02
0.18197D 07	0.77426D 02	0.79227D 02	0.78596D 02
0.19055D 07	0.76549D 02	0.80307D 02	0.78699D 02
0.19953D 07	0.75662D 02	0.78271D 02	0.77573D 02
0.20893D 07	0.74763D 02	0.73115D 02	0.76626D 02
0.21878D 07	0.73854D 02	0.76732D 02	0.75381D 02
0.22909D 07	0.72935D 02	0.80093D 02	0.73840D 02
0.23988D 07	0.72005D 02	0.75259D 02	0.71758D 02
0.25119D 07	0.71067D 02	0.70386D 02	0.73199D 02
0.26303D 07	0.70119D 02	0.75753D 02	0.70534D 02
0.27542D 07	0.69162D 02	0.72012D 02	0.70129D 02
0.28840D 07	0.68197D 02	0.70088D 02	0.70446D 02
0.30200D 07	0.67224D 02	0.72854D 02	0.69449D 02
0.31623D 07	0.66244D 02	0.69030D 02	0.68224D 02
0.33113D 07	0.65258D 02	0.68075D 02	0.67185D 02
0.34674D 07	0.64265D 02	0.73641D 02	0.65342D 02
0.36308D 07	0.63267D 02	0.67128D 02	0.65115D 02

TABLE 6 (continued)

Frequency (MHz)	L = 10 m	L = 1600 m	L = 16000 m
0.38019D 07	0.62265D 02	0.66565D 02	0.64121D 02
0.39811D 07	0.61258D 02	0.67842D 02	0.63206D 02
0.41687D 07	0.60248D 02	0.62934D 02	0.62235D 02
0.43652D 07	0.59234D 02	0.63646D 02	0.61384D 02
0.45709D 07	0.58219D 02	0.66490D 02	0.60450D 02
0.47863D 07	0.57201D 02	0.61971D 02	0.59002D 02
0.50119D 07	0.56182D 02	0.56144D 02	0.57038D 02
0.52481D 07	0.55162D 02	0.63484D 02	0.57062D 02
0.54954D 07	0.54142D 02	0.60498D 02	0.54348D 02
0.57544D 07	0.53121D 02	0.61326D 02	0.53880D 02
0.60256D 07	0.52100D 02	0.52030D 02	0.54306D 02
0.63096D 07	0.51078D 02	0.53082D 02	0.51944D 02
0.66069D 07	0.50055D 02	0.54127D 02	0.51799D 02
0.69183D 07	0.49047D 02	0.52486D 02	0.50307D 02
0.72444D 07	0.48124D 02	0.49138D 02	0.49933D 02
0.75858D 07	0.47310D 02	0.48260D 02	0.47512D 02
0.79433D 07	0.46543D 02	0.47769D 02	0.46484D 02
0.83176D 07	0.45831D 02	0.46660D 02	0.46310D 02
0.87096D 07	0.45185D 02	0.48958D 02	0.45838D 02
0.91201D 07	0.44618D 02	0.44650D 02	0.44458D 02
0.95499D 07	0.44151D 02	0.44181D 02	0.43359D 02
0.10000D 08	0.43807D 02	0.41497D 02	0.41552D 02

The 28 dB decrease appears a little higher than the experimental data which is about 20 dB. This is caused by the lack of exact statistical data for the build-up time of basic corona pulse. It should be noted that Eq. (6.12) is the formula of build-up time for the diameter ranges from 17 to 33 mm.

Line length, measurement position, propagation constants, and λ determine the fluctuations of RI fields with frequencies around the geometric mean RI values which is determined from the basic shape of corona pulse. The frequency maximums occur at the frequencies at which $\Gamma(\lambda;x,L,w,\gamma,\rho_1,\rho_2)$ represented by Eqs. (6.33) and (6.34) has a maximum value. The calculated frequency maximums at the center of line of length 1600 m occur at .115, .166, .251, .437, .603, .759, and .871 MHz in the frequency ranges from .1 to 1 MHz. An interesting observation can be made if it is noticed that the frequency maximums are close to the frequencies at which one of cos βL, cos $2\beta L$, sin βL, and sin $2\beta L$ is maximum assuming a velocity of propagation equal to the speed of light. This result agrees well with the observations found by tests or experiments [2,3,36,37,45,46,47].

The mean number of corona events does not appear to affect the shape of frequency spectrum even though the RI levels increase as it increases. The measurement position is important in the shape of spectrum since the frequency maximums shift with it.

The difference between the maximum and minimum RI levels at a given frequency can be observed to be as much as 17 dB from Tables 5 and

6. This fact may explain the fact [26] that the conventional RI analyses do not entirely explain the differences between the measured noise fields of different lines, nor the substantial fluctuations in the RI level. It was found [23] that even in dry weather the RI level can fluctuate over 12 dB.

From this analysis, therefore, it can be suggested that the RI analysis in the operating line must be based on the detailed analytical method taking into account the line length, terminations of the line, the mean number of corona events, and measuring position.

4. Lateral RI field profile

The RI field strength along lateral distance from an open ended transmission line is shown in the Figure 7. Lateral distance is taken from center conductor along a horizontal axis in a plane perpendicular to the line at mid-span.

Figure 8 shows typical lateral attenuation curves for high voltage lines investigated by a joint CIGRE and IEEE task force [23]. A careful comparison between the curve in Fig. 7 and 330-400 kv (HORIZ) attenuation curve in Fig. 8 shows no significant difference.

5. Axial RI field profile

Figure 9 shows the RI field strength along axial distance from an open ended line of length 1 mile. Axial distance is taken along the axis of the line at 15 m laterally away from the outer phase conductor. Since there is no axial RI profile reported in published literature,

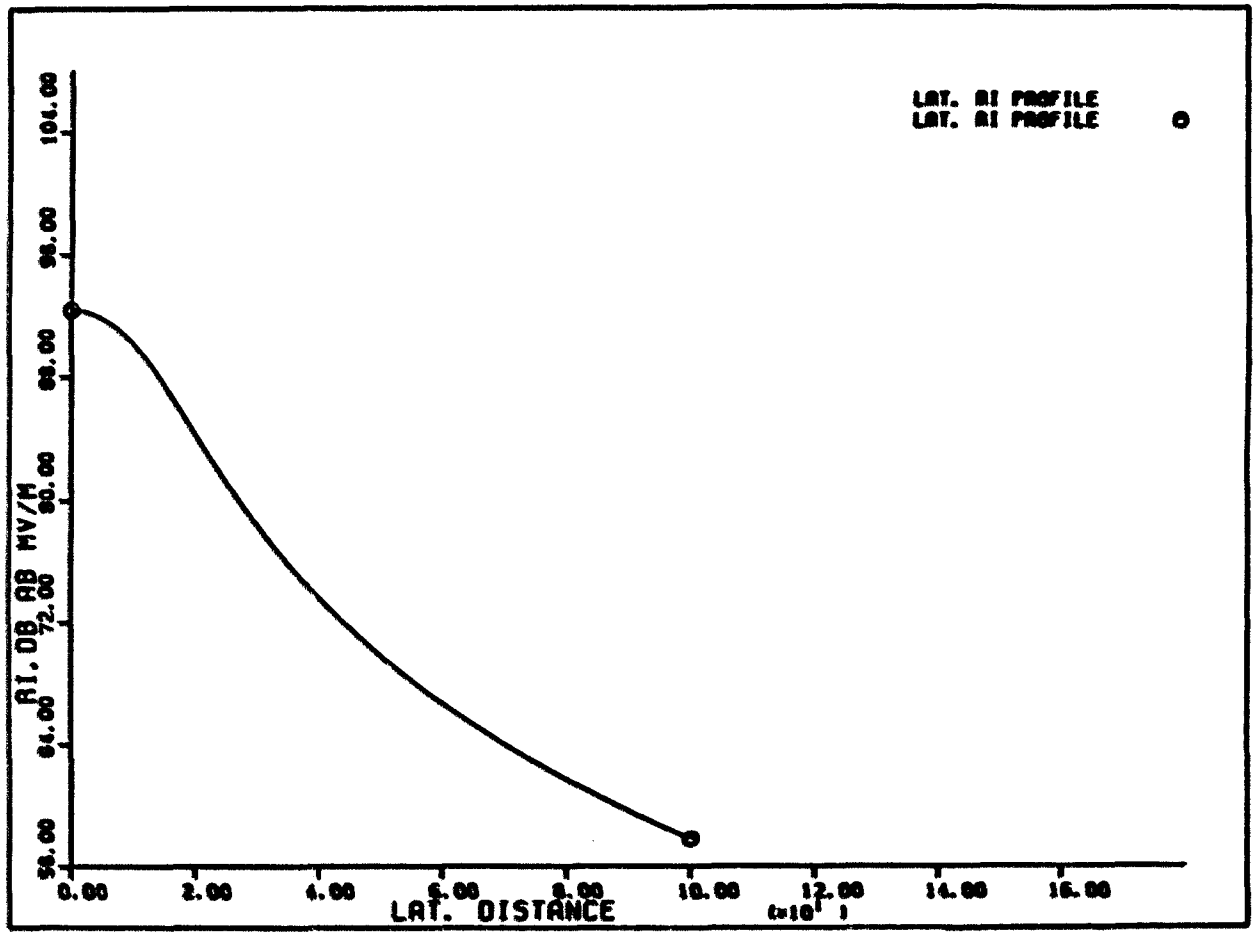

FIGURE 7. Lateral RI Field Profile

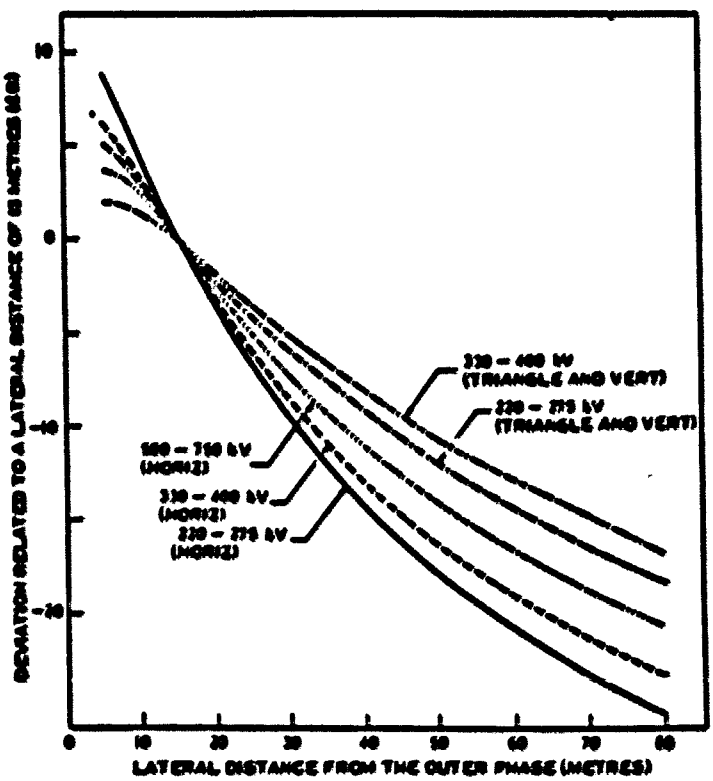

FIGURE 8. Typical Lateral Profile Attenuation Curves [26]

this calculated axial RI profile is believed to be useful in the RI analysis.

From Figure 9, it is found that the difference between the maximum and minimum RI fields is as much as 3.94 dB. It can be easily imagined that the axial locations where the maximums and minimums occur depend on the terminations of the line.

The numerical result in this section, therefore, suggests the need of a axial RI profile to find the maximum RI field.

6. Design parameters

In the preliminary stages of the line design one is perhaps interested, not so much in an accurate determination of the RI level of a proposed design, but more in obtaining a rough idea of weather or not the RI level is within reasonable limits. Or perhaps one is interested in obtaining a quick indication of how a small decrease in conductor size, or increase in phase spacing, or change in conductor height, etc., will affect the RI level. This section gives such design curves, enabling one to obtain, with an acceptable degree of accuracy, the RI level of any line whose geometry is reasonably close to base case geometry shown in Fig. 3.

The RI levels depending on the design parameters such as diameter, voltage, conductor height, and phase spacing are given in Figures 10 - 13. In these figures, RI refers to a measuring location 15 m from an outside phase and are given for a typical ground resistivity of 100 Ω.m and for a measuring frequency of 1 MHz and meter bandwidth of 5 KHz.

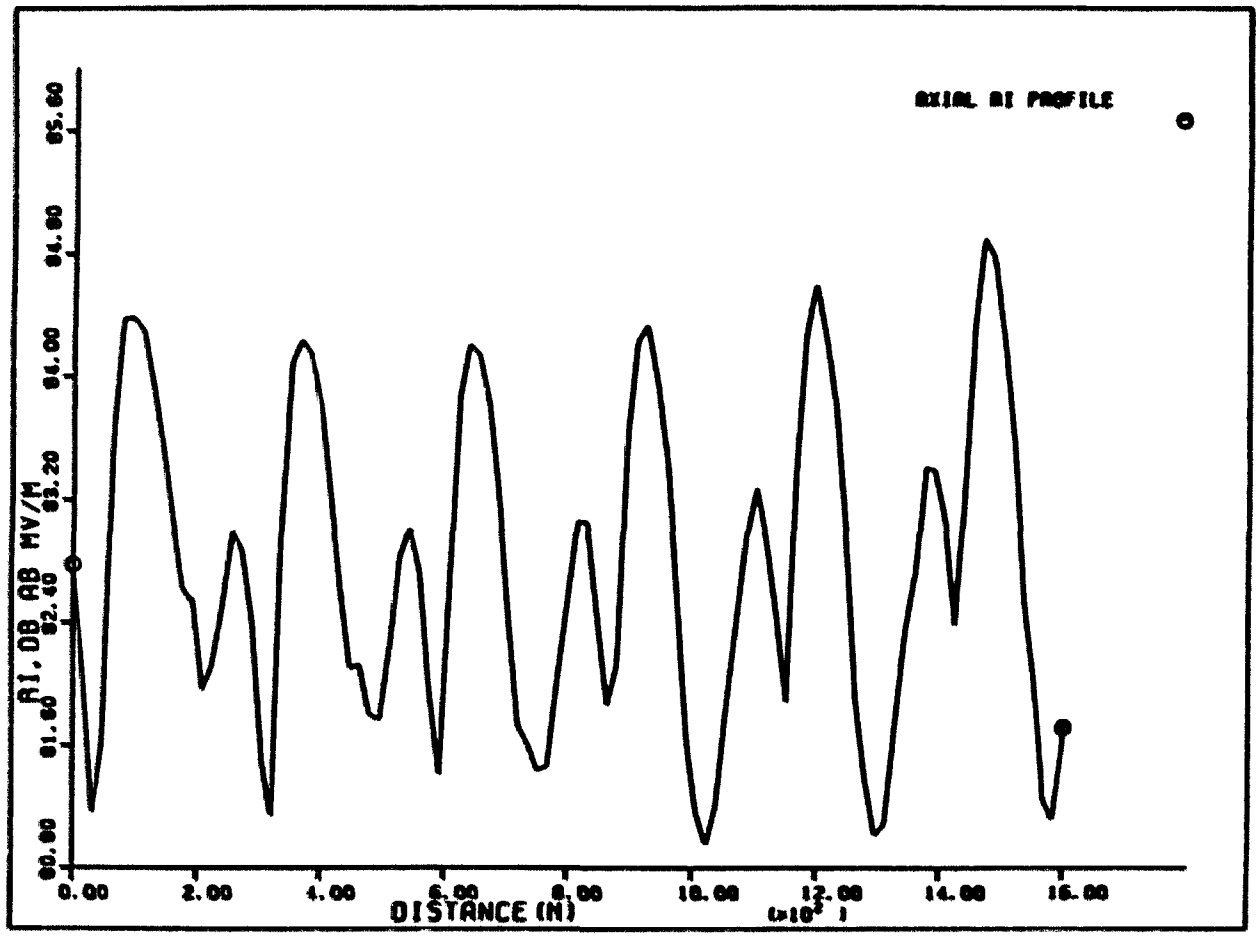

FIGURE 9. Axial RI Field Profile

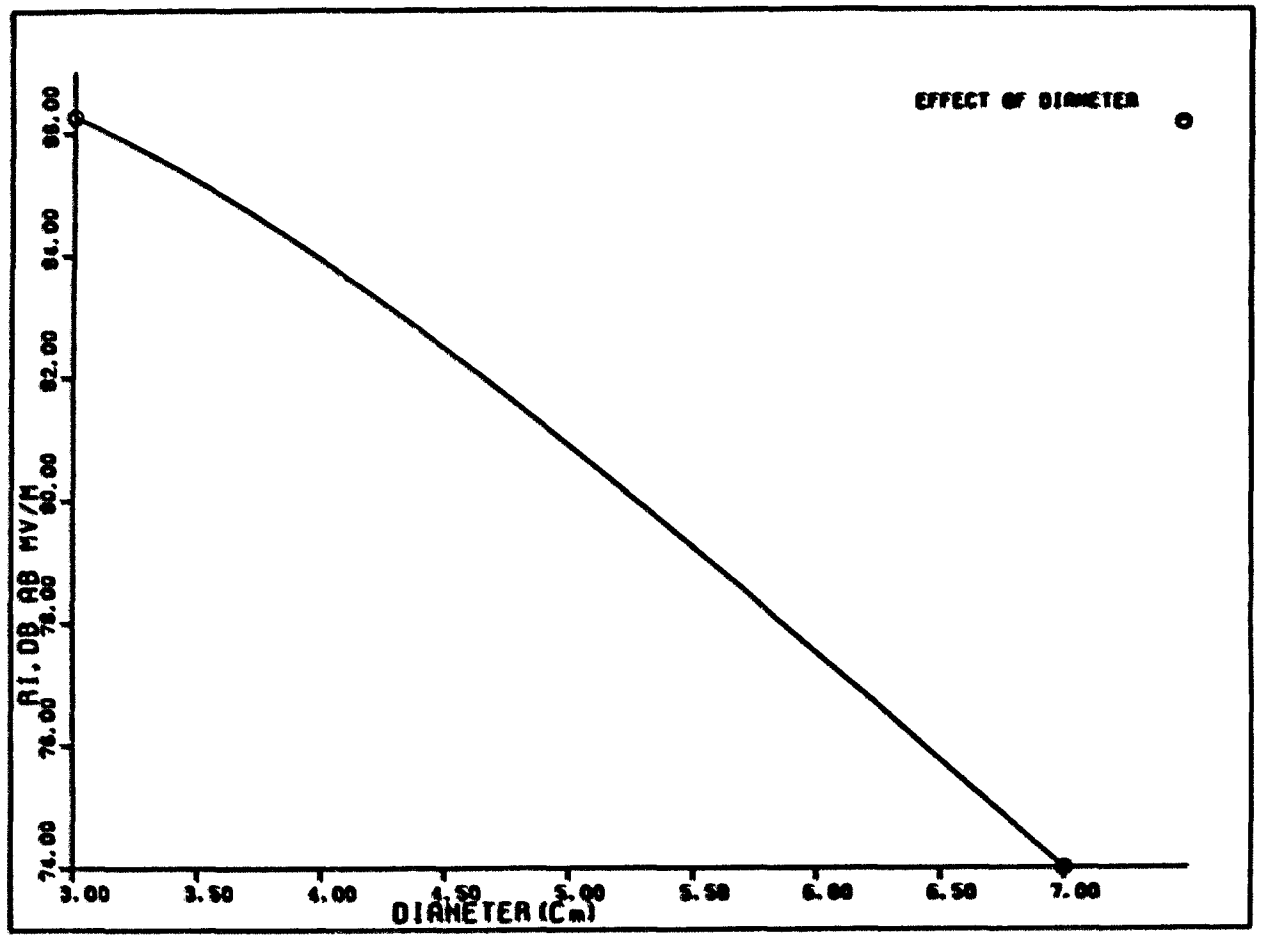

FIGURE 10. Effect of Variation of Conductor Diameter

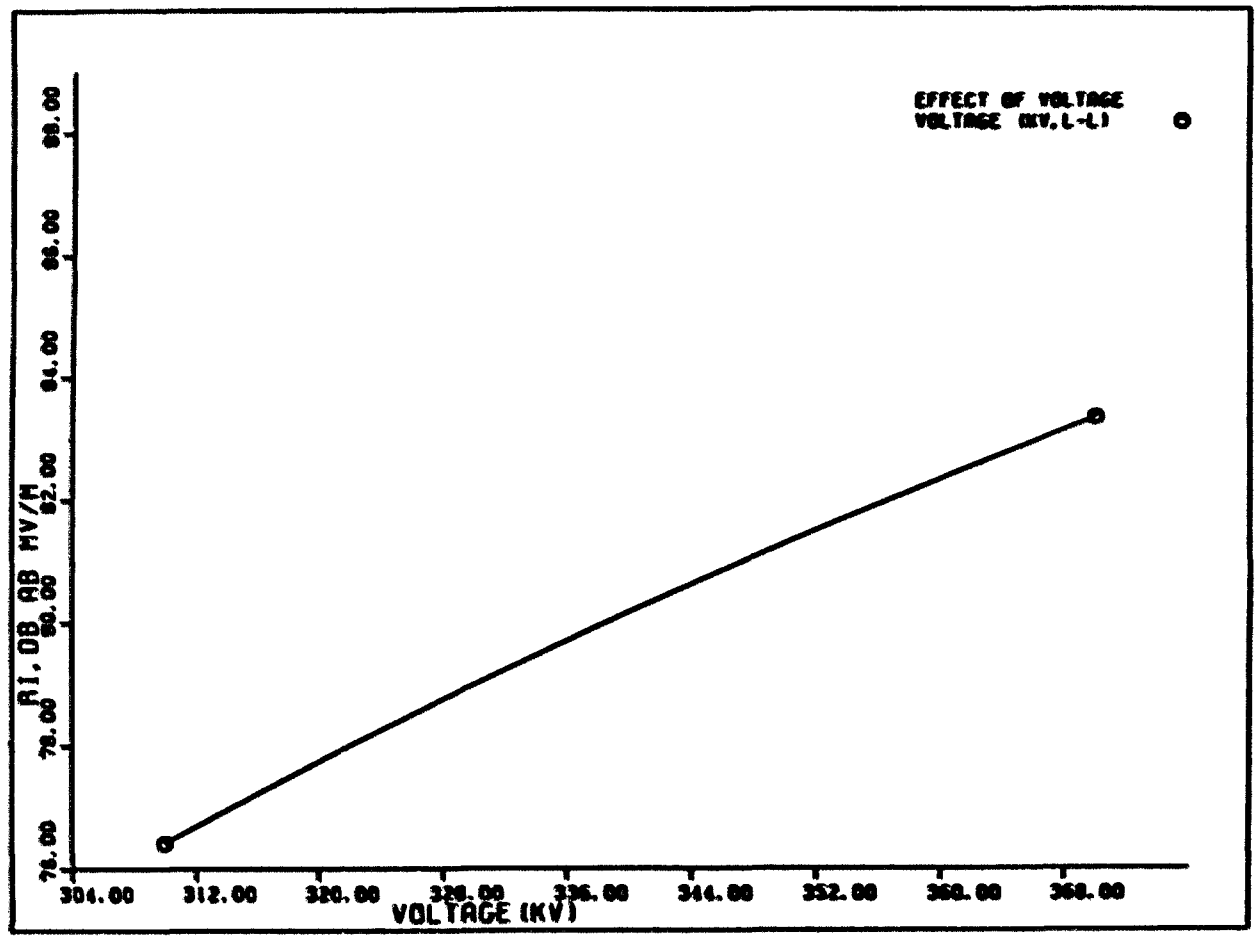

FIGURE 11. Effect of Variation of Voltage

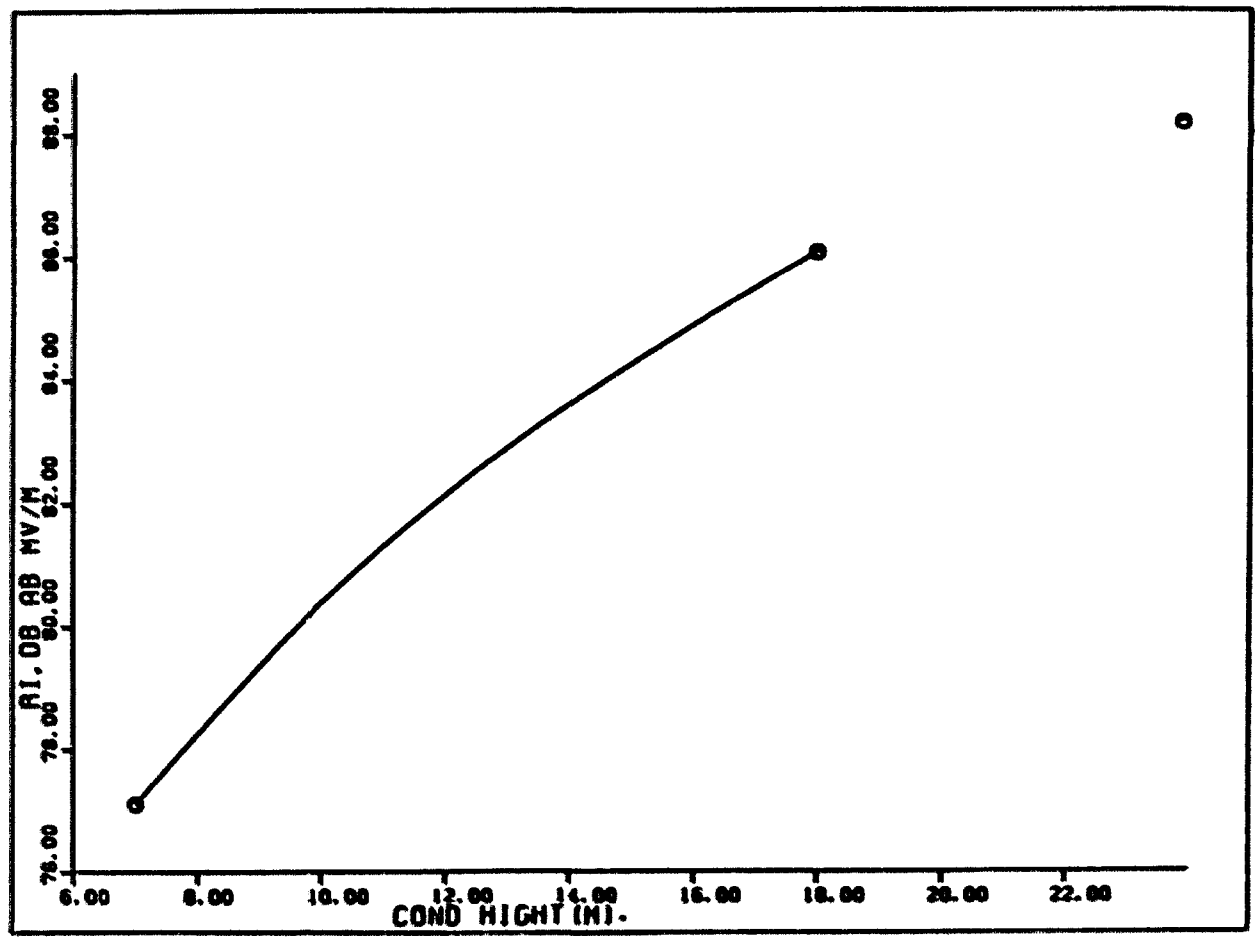

FIGURE 12. Effect of Variation of Conductor Height

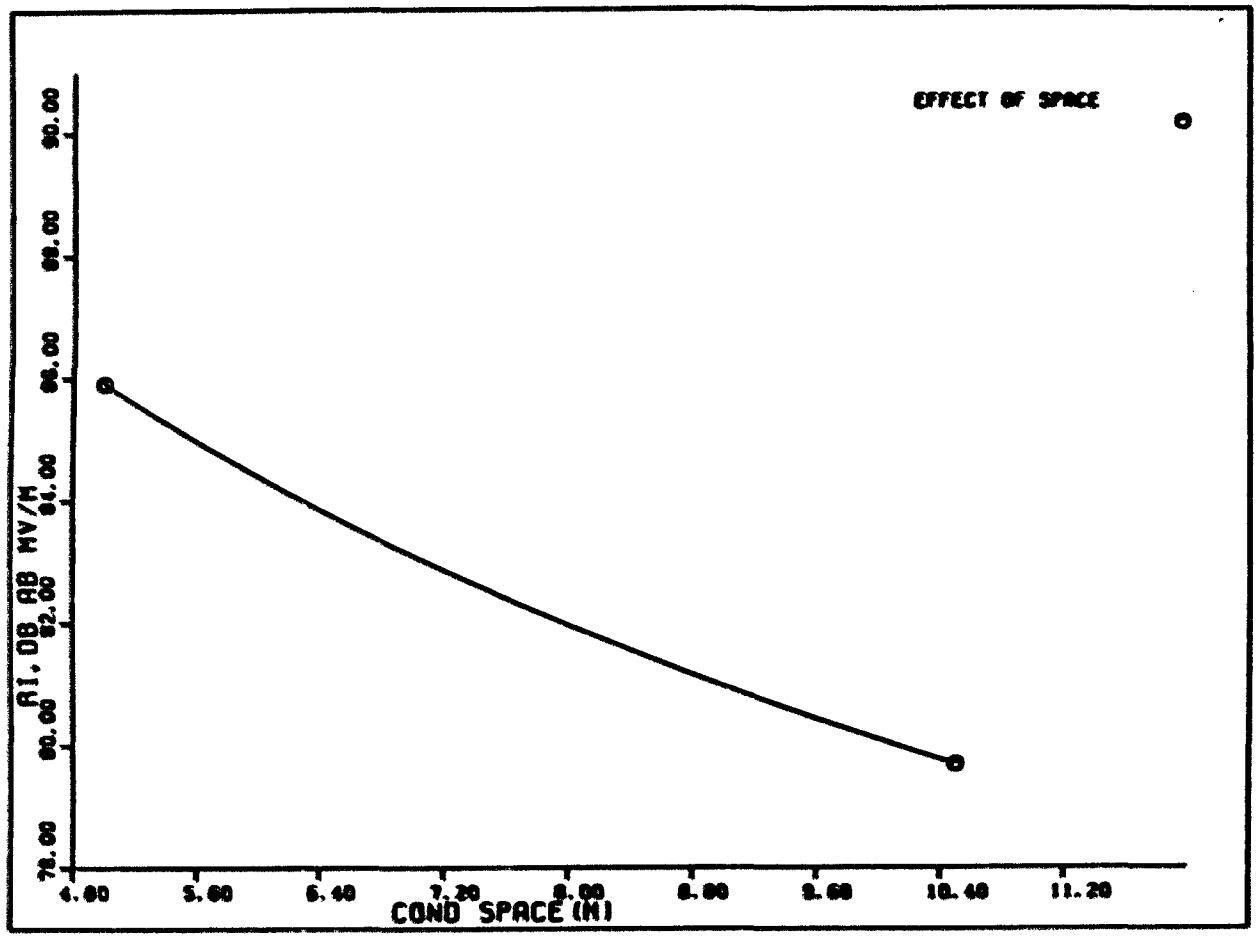

FIGURE 13. Effect of Variation of Phase Spacing

The curves presented in Figures 10 - 13 refer to specific conductor diameters, voltages, conductor heights, and phase spacings. Adjustment of the RI levels determined from the curves is necessary if any of the parameters differ from those of the base case.

VIII. CONCLUSIONS

A comprehensive and rigorous analysis has been presented in this dissertation of a stochastic model to predict radio interference caused by corona on high voltage transmission systems. The analysis presented makes the following principal contributions:

1. A stochastic model of the corona current injected into the high voltage power transmission line has been proposed. It is found that the proposed corona current is a stationary process under certain assumptions. Injected corona current is represented by the power spectral density.
2. A rigorous analysis is developed for the derivation of a stochastic transmission line equation. The solution of a developed stochastic transmission line equation with the influence of line terminations is obtained from rigorous and comprehensive analyses.
3. The power spectral density of interference voltage caused by corona is obtained by a rigorous stochastic analysis.
4. The radio interference field strength at the radio receiver located near the line is developed by using the Wiener-Khintchine theorem.
5. It is shown that the single conductor stochastic RI analysis can be easily extended to the three phase RI analysis.

6. Most random parameters are shown to be found from existing RI data obtained by test or experiment.
7. Numerical analysis has shown many important results which the existing RI analyses couldn't figure out analytically. The following are such examples:
   1). The RI level varies as much as 13 dB depending on the line terminations.
   2). The number of corona events along the line significantly affects the RI level if it is greater than the order of 1, which is assumed to be the number of corona events during foul-weather conditions.
   3). The frequency spectrums are found to vary depending on the line length, line terminations, mean number of corona events along the line, measuring position, and the shape of streamer. It was shown that the RI level fluctuates as much as 17 dB at a given frequency, which was not entirely explained by the conventional RI analysis.
   4). The RI level is shown to vary as much as 4 dB axially. It is suggested that the axial RI profile is needed to find the maximum RI level.

IX. BIBLIOGRAPHY

1. A Report to the Federal Power Commission on The Transmission of Electric Power. The Transmission Technical Advisory Committee for the National Power Survey, n.p.:February 1971.

2. Transmission Line Reference Book 345 kv and above. Electrical Power Research Institute: Palo Alto, CA, 1975.

3. Annestrand, S. A.; Parks, G. A. "Bonneville Power Administration's Prototype 1100/1200 kv Transmission Line Project." IEEE Transactions, PAS-96 (March/April 1977):357-366.

4. Mahmoud, A. A. "High Voltage Engineering." Unpublished Classroom notes, Department of Electrical Engineering, Iowa State University, 1979.

5. Townsend, J. S. Electricity in Gases. Oxford: Clarendon Press, 1915.

6. Peek, F. W. Jr. Dielectric Phenomena in High-Voltage Engineering. 3rd ed. New York: McGraw-Hill, 1929.

7. Loeb, L. B. Electrical Coronas - Their Physical Mechanisms. Berkeley: University of California Press, 1965.

8. Giao, T. N.; Gordan J. B. "Modes of Corona Discharges in Air." IEEE Transactions, PAS-86 (May 1968):1207-1215.

9. Nasser, E. Fundamentals of Gaseous Ionization and Plasma Electronics. New York: John Wiley and Sons, 1971.

10. Sigmond, R. S.; Goldman, M. "Corona Discharge in Physics and Application." in Electrical Breakdown and Discharges in Gases, Part B. New York: Plenum Press, 1983:1-64.

11. Nigol, O. "Analysis of Radio Noise from High-Voltage Lines I - Meter Response to Corona Pulses." IEEE Transactions, PAS-83 (May 1964):524-533.

12. Nigol, O. "Analysis of Radio Noise from High-Voltage Lines II - Propagation Theory." IEEE Transactions, PAS-83 (May 1964):533-541.

13. IEEE Committee Report. "Comparison of Radio Noise Prediction Methods with CIGRE/IEEE Survey Results." IEEE Transactions, PAS-92 (May/June 1973):1029-1042.

14. Adams, G. E. "The Calculation of the Radio Interference Level of Transmission Lines Caused by Corona Discharges." AIEE Transactions, Pt. III, Power Apparatus and Systems 75 (February 1956):411-419.

15. Adams, G. E. "An Analysis of the Radio Interference Characteristics of Bundled Conductors." AIEE Transactions, Pt. III, Power Apparatus and Systems 75 (February 1956):1569-1584.

16. Adams, G. E.; Liao, T. W.; Poland, M. G.; Trebby, F. J. "Radio Noise Propagation and Attenuation Tests on the Bonneville Power Administration McNary-Ross 345 kv Lines." AIEE Transactions, Pt. III, PAS-78 (1959):380-388.

17. Wedepohl, L. M.; Saha, J. N. "Radio-Interference Fields in Multiconductor Overhead Transmission Lines." Proc. IEE 116 (November 1969):1875-1884.

18. Gary, C. H. "The Theory of the Excitation Functions: a Demonstration of Its Physical Meaning." IEEE Transactions, PAS-91 (January/February 1972):305-310.

19. Dallaire, R. D.; Maruvada, P. S. "Analysis of Radio-Interference from Short Multiconductor Lines." IEEE Transactions, PAS-100 (April 1981):2100-2108.

20. Reichman,J.; Leslie, J. R. "A Summary of Radio Interference Studies to EHV Lines." IEEE Transactions, PAS-83 (March 1964):223-228.

21. Pakala, W. E.; Taylor, E. R. Jr. "A Method for Analysis of Radio Noise on High-Voltage Transmission Lines." IEEE Transactions, PAS-87 (February 1968):334-345.

22. Paris, L.; Storzini, M. "RI Problems in HV-Line Design." IEEE Transactions, PAS-87 (April 1968):940-946.

23. Cortina, R.; Serravalli, W.; Storzini, M. "Radio Interference Long Term Recording on an Operating 420-kv Line." IEEE Transactions, PAS-89 (May/June 1970):881-892.

24. Sawada, Y. "Calculating Methods of Radio Noise Level and its Application to Design of AC Power Transmission Line." IEEE Transactions, PAS-89 (May/June 1970):844-853.

25. Perry, D. E.; Chartier, V. L.; Reiner, G. L. "BPA 1100 kv Transmission System Development Corona and Electric Field Studies." IEEE Transactions, PAS-98 (September/October 1979):1728-1738.

26. IEEE Committee Report. "CIGRE/IEEE Survey on Extra High Voltage Transmission Line Radio Noise." IEEE Transactions, PAS-92 (May/June 1973):1019-1028.

27. Soliman, E. D. "Calculating the Corona Pulse Characteristics and its Radio Interference." IEEE Transactions, PAS-90 (January/February 1971):165-179.

28. Newell, H. H., Warburton, F. W. "Variation in Radio and TV Interference from Transmission Lines." AIEE Transactions, PAS-75 (June 1956):420/426.

29. Liao, T., Hoglund, N. A. "Fair Weather RI, Part I : Artificial and Natural Sources." IEEE Transactions, PAS-89 (May/June):837-844.

30. Newell, H. H.; Liao, T.; Warbuton, F. W. "Corona and RI Caused by Particles on or Near EHV Conductors : I - Fair Weather." IEEE Transactions, PAS-86 (November 1967):1375-1383.

31. Middleton, D. An Introduction to Statistical Communication Theory. New York: McGraw-Hill Book Co., 1960.

32. Thomas, J. B. Statistical Communication Theory. New York: John Wiley and Sons, 1969.

33. Melsa, J. L.; Sage, A. P. An Introduction to Probability and Stochastic Processes. Englewood Cliffs: Prentice-Hall, Inc., 1973.

34. Lin, Y. K. Probability Theory of Structural Dynamics. New York: McGraw-Hill Book Co.,1967.

35. El-Debeiky, S.; Khalifa, M. "Calculating the Corona Pulse Characteristics and Radio Interference." IEEE Transactions, PAS-90 (January/February):165-179.

36. Rakoshdas, B. "Pulses ad Radio-Interference Voltage of Direct Voltage Corona." IEEE Transactions, PAS-83 (May 1964):483-491.

37. Perel'man, L. S.; Chernobrodov, M. I. Elekrichestvo, No.4, (1966):62-66. English Translation Published as Study of Corona and the Radio Interference of a Conductor in actual Conditions. Electric Technology U.S.S.R. 2/3 (1966):218-229.

38. Wedepohl, L. M. "Application of Matrix Methods to the Solution of Travelling-Wave Phenomena in Polyphase Systems." Proc. IEE 110 (December 1963):2200-2212.

39. Rokhinson, P. Z. Elekrichestvo, No.2 (1976):75-78. English Translation Published as Statistical Study of Positive Corona Impulses on Conductors of Different Diameter. Electric Technology U.S.S.R. 1 (1976):83-92.

40. Denholm, A. S. "The Pulses and Radio Interference Voltage of Power Frequency Corona." AIEE Transactions, Pt. III, PAS-79 (October 1960):698-707.

41. Vuhuu, Q.; Comsa, R. P. "Influence of Gap Length on Wire-Plane Corona." IEEE Transactions, PAS-88 (October 1969):1462-1475.

42. Galloway, R. H.; Shorrocks, W. B.; Wedepohl, L. M. "Calculation of Electrical Parameters for Short and Long Polyphase Transmission Lines." PROC. IEE, 111 (December 1964):2051-2059.

43. ANSI (American National Standards Institute, 1430 Broadway, New York, N. Y.). "Specifications for Radio Noise and Field Strength Meters .015 to 30 Megacycles/seconds." Spec. C 63.2-1963, Reaffirmed in 1964.

44. ANSI. "IEEE Standard Procedures for the Measurement of Radio Noise from Overhead Power Lines." ANSI/IEEE, Std. 430-1976, 1976.

45. Schrooder, T. W.; England, G. L.; O'Neil, J. E.; Pakala, W. E. " 345-kv Wood Pole Test Line - Radio Interference and Leakage Current Investigations." IEEE Transactions, PAS-83 (March 1964):228-236.

46. Maruvada, P. S.; Giao, T.; Dallaire, D.; Rivest, N. "Corona Performance of a Conductor for Bipolar HVDC Transmission at +/- 750 kv." IEEE Transactions, PAS-96 (November/December 1977):1872-1880.

47. Maruvada, P. S.; Giao, T.; Dallaire, D.; Rivest, N. "Corona Studies for Bipolar HVDC Transmission at Voltages between +/- 600 kv and +/- 1200 kv Part I: Long Term Bipolar Line Studies." IEEE Transactions, PAS-100 (March 1981):1453-1460.

48. Chow, Y.S.; Teicher, H. Probability Theory. New York: Springer Verlag, 1978.

49. Soong, T. T. Random Differential Equations in Science and Engineering. New York: Academic Press, 1973.

50. Wong, E. Stochastic Processes in Information and Dynamical Systems. New York: McGraw-Hill Book Co., 1971.

51. Gihman, I. I.; Skorhod, A. V. The Theory of Stochastic Process I. New York: Springer Verlag, 1974

52. Medhi, J. Stochastic Processes. New Delhi: Wiley Eastern Limited, 1982.

X. ACKNOWLEDGMENT

It is with great pleasure and gratitude that the author wishes to express his thanks to all who have contributed directly or indirectly to this research. This research could not have been carried out without the special encouragement and guidance of Professors Aly A. Mahmoud and Robert E. Post. The author is therefore most grateful to his co-major professors, Dr. A. A. Mahmoud and Dr. R. E. Post, for their continuous advice and supervision throughout this research.

Thanks are given to all my teachers, including the author's committee members Drs. R. J. Lambert, K. C. Kruempel, and A. L. Day.

Thanks are also given to Dr. Wolfgang Kliemann for his valuable discussion and advice in many stochastic problems.

The author wishes to thank Mr. Mahmood Mirheydar for his friendship and assistance in the computer programming.

Acknowledgment must be made to the Iowa Test and Evaluation Facility and the Power Affiliate Research Program for their financial support throughout this research.

Special gratitude must be given to the author's parents and father-in-law and mother-in-law for their understanding, encouragement, and financial support during the author's stay in the United States.

Gratitudes are also given to Mr. Daiseung Shin for his encouragement and to the author's best friend Mr. Hwajung Youn for his friendship.

Finally, the author wishes to express his heartfelt gratitude to his wife for her understanding, patience, and encouragement throughout this research. Further thanks go to the author's daughters A-young, Ami whose smile and health kept the author in peace and comfort through the dark days.

XI. APPENDIX I. STATISTICAL PRELIMINARIES

The mathematical theory of probability and the basic concepts of random variables and stochastic process form the basis of the development in this study. In this appendix, some basic definitions and results in probability theory, random variables, and stochastic process which are needed in the Chapters 2, 3, 4, and 5 are reviewed.

A. Elements of Probability Theory

1. Events and probability

The basic notions of probability theory are experiment, event and probability of events. When formalizing the notions of probability theory the first assumption is that the results of collection of experiments under investigation in a given situation are represented by a certain set Ω called space. Every meaningful event corresponds to a certain set A of Ω in such a manner that the probabilistic operations on events correspond to set-theoretical operations on the corresponding subsets of Ω.

Moreover the points $w \in \Omega$ correspond to atoms - namely, every event is a sum of points while each point w cannot be represented as a sum of other events. It is noted that only arbitrary subset of Ω is called an event. However, one must select out of Ω a suitable class of events from both a practical as well as a purely mathematical point of view.

Given a space Ω, a Borel field, or a σ-algebra B of subsets of Ω is a class of subsets A_j , j= 1,2,... , having following properties [48,49]:

1. $\Omega \in B$
2. If $A_1 \in B$, then $A_1' \in B$
3. If $A_j \in B$, j=1,2,... , then $U_1^{\infty} A_j \in B$.

A Borel field is thus a class of sets, including the empty set ϕ and the space Ω, which is closed under all countable unions and intersections of its sets.

The space Ω along with the σ-algebra of sets B defined on it is called measurable space (Ω, B) and the subsets of Ω belonging to B are called B-measurable sets or simply measurable sets.

A triple (Ω, B, P) consisting of a space of elementary events Ω, a selected σ-algebra of events B in Ω, and a measure P on B such that $P(\Omega) = 1$ is called a probability space and the measure P is called the probability [48,49,50,51].

Probability spaces are the initial objects of Probability theory. This, however, does not contradict the fact that when solving many specific problems the probability space is not given explicitly.

Given a random experiment E, a finite number P(A) is assigned to every event A in the σ-field B. The number P(A) is a function of set A and is assumed to be defined for all sets in B. It is assumed to have the following properties:

1. $P(A) \geq 0$.
2. $P(\Omega) = 1$.

3. For a countable collection of mutually disjoint $A_1, A_2, \ldots,$ in B

$$P\left(\bigcup_j A_j\right) = \sum_j P(A_j).$$

2. Random variables

The concept of a random variable corresponds to the description of a stochastic experiment which measure a certain numerical quantity X. It is assumed that for any pair of numbers a and b ($a < b$) the event A(a,b) expressing that $X \in (a,b)$ is an observable event.

The point function X(w) is called a random variable (r.v.) if (1) it is a finite real-valued function defined on a sample space Ω of a random experiment for which a probability is defined on the σ-algebra B of events and (2) for every real number x, the set $\{w: X(w) \leq x\}$ is an event in B, i.e., X is measurable on B [51].

The relation $X = X(w)$ takes every element w in Ω unto a point x on the real line $R = (-\infty, +\infty)$. There are many occasions to consider a sequence of r.v.'s X_j, $j=1,2,\ldots,n$. In these cases, it is assumed that they are defined on the same probability space. The r.v.'s $X_1, X_2, \ldots, X_n$ will then map every element w of Ω in the probability space unto a point of the n-dimensional Euclidean space. It is noted here that an analysis involving n r.v.'s is equivalent to considering a random vector having the r.v.'s as components.

Let X be a random variable with value in the measurable space (Ω, B). The function $F_X(x)$ defined by [31,49]

$$F_X(x) = P(w: X(w) \leq x) = P(X \leq x)$$

is called the distribution function of X.

A random variable X is called a continuous r.v. if its associated distribution function is continuous and differentiable almost everywhere. It is a discrete r.v. when the distribution function assumes the form of a staircase with a finite or countably infinite jumps.

For a continuous r.v. X, the derivative

$$f_X(x) = dF_X(x)/dx$$

in this case exists and is called the density function of the r.v. X [31]. On the other hand, the density function of a discrete r.v. does not exist in the ordinary sense. However, it can be constructed with the aid of Dirac delta function. Consider the case where a r.v. X takes on only discrete values $x_1, x_2, \ldots, x_n$. A definition of its density function is [31]

$$f_X(x) = \sum_{j=1}^{n} P_j \, \delta(x - x_j)$$

where $\delta(x)$ is the Dirac delta function and

$$P_j = P(X = x_j).$$

Let X_j ,j= 1,2,...,n, be random variables with values in the measurable space (R^n, B^n). The function

$$F_{X_1X_2\ldots X_n}(x_1,x_2,\ldots,x_n) = P\{(X_1 \leq x_1) \bullet \bullet \bullet (X_n \leq x_n)\}$$

is called the joint distribution function of a sequence of a n r.v.'s (X^n) [31].

The corresponding joint density function is defined by [31]

$$f_{X_1X_2..X_n}(x_1,x_2,\ldots,x_n) = \partial^n F_{X_1\ldots X_n}(x_1,x_2,\ldots,x_n)/\partial x_1\partial x_2\ldots\partial x_n$$

if the indicated partial derivative exists.

3. Expectation of random variable

Let f(x) be the density function of a random variable X, which may exhibit either continuous or singular properties, or both. Consider now some real function g(x) of the original random variable, integrable over $(-\infty, \infty)$ with respect to f(x). Define [31]

$$\overline{g(X)} = E(g(x)) = \int_{-\infty}^{\infty} g(x)\, f(x)\, dx \qquad (A.1)$$

as the mean value, or expectation of g(X) with respect to the density function f(x). Here, E is the expectation operator, defined according to Eq.(A.1). Note that, for purely discrete distributions, this becomes

$$\overline{g(x)} = E(g(x)) = \int_{-\infty}^{\infty} g(x) \sum_{k=1}^{n} p_k\, \delta(x - x_k)\, dx$$

$$= \sum_{k=1}^{n} g(x_k)\, p_k \,.$$

The n th moment of X, a_n, is defined by

$$a_n = E(X_n) = \int_{-\infty}^{\infty} x^n\, f(x)\, dx$$

if $\int_{-\infty}^{\infty} |x|^n\, f(x)\, dx$ is finite. Moments of particular interest are $E(X)$, $E(X^2)$, the mean and mean-square values of X, while

$$E\{(X - EX)^2\} = E(X^2) - (EX)^2 = \sigma_X^2$$

is called the covariance of X and σ its standard deviation.

4. Independence

Let (Ω, B, P) be a fixed probability space. Two events A and B is called independent if $P(A \cdot B) = P(A)\,P(B)$.

Random variables X_i $(i \in I)$ are independent [51] if for any n and any $i_k \in I$, $k=1,2,\ldots,n$, the joint distribution function of the variables $X_{i1}, X_{i2}, \ldots, X_{in}$ is equal to the product of the distribution functions of the variables X_{ik}:

$$P(X_{i1} < a_1, \ldots, X_{in} < a_n) = \prod_{k=1}^{n} P(X_{ik} < a_k).$$

If, therefore, X and Y are independent,

$$f(x,y) = f(x)\,f(y).$$

B. Stochastic Processes

1. Definition and preliminary considerations

Random variables or random vectors are adequate for describing results of random experiments which assume scalar or vector values in a given trial. In many physical trials, however, the outcomes of random experiment are represented by functions X(t) depending upon a parameter. These outcomes are then described by a random function X(t), where t is the parameter assuming values in a reference set T. Random function,

random process, and stochastic process will be used synonymously in the subsequent discussions. Each realization of a given random experiment is called a sample function or a member function. This description suggests that a stochastic process (s.p) X(t), t ε T, is a family of sample functions of the variable t, all defined on the same underlying probability space (Ω, B, P).

Let (Ω, B, P) be a given probability space. If the realization of an experiment is described by means of a function f(t) of a definite argument t, t ε T, it is said that a <u>random function</u> is defined on (Ω, B, P) [49].

Thus, a random function is the mapping: $w \rightarrow f(t) = f(t,w)$, $w \in \Omega$. Additionally, it is required that the function f(x,w) for a fixed x will be a random variable. A stochastic process defined in this way is specified by the probability of the realizations of various sample functions. This generally requires advanced mathematics in measure theory. In order to circumvent this difficulty, another definition of a stochastic process will be given, which will be more fruitful in this study.

At a fixed t, a s.p. X(t), t ε T, is a random variable. Hence, another characterization of a s.p. is to regard it as a family of random variables, say $X(t_1)$, $X(t_2)$,..., depending upon a parameter. The totality of all the random variables define the s.p. X(t).

If to every finite set $(t_1,t_2,..,t_n)$ of t ε T, there corresponds a set of r.v.'s $X_1 = X(t_1)$, $X_2 = X(t_2)$,...,$X_n = X(t_n)$, having a well-defined joint probability distribution function

$$F_{X_1 \ldots X_n}(x_1,t_1;x_2,t_2;\ldots;x_n,t_n)$$

$$= P((X_1 \leq x_1) \cdot (X_2 \leq x_2) \cdot \cdot \cdot (X_n \leq x_n)) \quad , n=1,2,\ldots$$

then this family of joint distribution functions defines a s.p. X(t), t ε T [49].

In the theory of stochastic processes, a commonly used notion for the joint distribution function given above is

$$F_n(x_1,t_1;\ldots;x_n,t_n) = F_{X_1 \ldots X_n}(x_1,t_1;\ldots;x_n,t_n) \ ,$$

and it is called the n th distribution function of the s.p. X(t). Its associated joint density function, assuming it exists,

$$f_n(x_1,t_1;\ldots;x_n,t_n) = \partial^n F(x_1,t_1;\ldots;x_n,t_n)/\partial x_1 \ldots \partial x_n$$

is the n th density function of X(t).

A complex s.p. Z(t) can be represented by

$$Z(t) = X(t) + jY(t)$$

where X(t) and Y(t) are real s.p.'s. It is clear that Z(t) is completely characterized by a two-dimensional vector stochastic process.

2. Moments of stochastic processes

As in the case of random variables, some of the most important properties of a s.p. are characterized by its moments. In the sequel, the existence of density function shall be assumed.

In terms of its first density function $f_1(x,t)$, the n th moment of a s.p. X(t) at a given t ε T, $\alpha_n(t)$, is defined by [31,49]

$$\alpha_n(t) = E(X^n(t)) = \int_{-\infty}^{\infty} x^n f_1(x,t)\, dx.$$

The first moment is the mean of the s.p. X(t) at t. The n th central moment of X(t) at a given point x is

$$\mu_n(t) = E([X(t) - EX(t)]) = \int_{-\infty}^{\infty} (x - x)^n f_1(x,t)\, dx.$$

Of practical importance is $\mu_2(t)$, the covariance of X(t) at t.

The moments of X(t) defined in terms of its second density function $f_2(x_1,t_1;x_2,t_2)$ are, in effect, joint moments of two random variables. The joint moment $\alpha_{nm}(t_1,t_2)$ of X(t) at t_1 and t_2 is defined by [31,49]

$$\alpha_{nm}(t_1,t_2) = E(X^n(t_1)\, X^m(t_2))$$

$$= \int_{-\infty}^{\infty} \int_{-\infty}^{\infty} x_1^n x_2^m f_2(x_1,t_1;x_2,t_2)\, dx_1 dx_2.$$

$\alpha_{11}(t_1,t_2)$ is called the <u>autovariance function</u> of the s.p. X(t) and is denoted by $\Gamma_{XX}(t_1,t_2)$. $\Gamma_{XY}(t_1,t_2) = E(X(t_1)\, Y(t_2))$ is called the cross-variance function where the random variables involved belong two different stochastic processes. Similarly, the autocovariance function of X(t) is given by

$$K_{XX}(t_1,t_2) = E[\{X(t_1) - m(t_1)\}\{X(t_2) - m(t_2)\}]$$

where, $m(t_i) = EX(t_i)$, for i = 1,2.

3. Stationary and wide-sense stationary processes

A s.p. $X(t)$, $t \in T$, is said to be stationary or strictly stationary [52] if its collection of probability distribution stays invariant under an arbitrary translation of the time parameters, that is, for each n and arbitrary τ,

$$F_n(x_1,t_1;\ldots;x_n,t_n) = F_n(x_1,t_1 + \tau;\ldots;x_n,t_n + \tau),$$

where $t_j + \tau \in T$, $j = 1,2,3,..,n$. For practical purposes, a wider class of stationary stochastic processes is of interest.

A s.p. $X(t)$, $t \in T$, is called a wide-sense stationary process [49,52] if

1. $|EX(t)| =$ constant.
2. $EX^2(t) < \infty$, $E(X(t_1)\, X(t_2)) =$ function of $(t_2 - t_1)$.

4. Ergodicity

Ergodicity deals with the specific questions of relating statistical or ensemble averages of a stationary stochastic process to time averages of its individual sample functions.

Let $x^{(j)}(t)$ be a sample function of a stationary s.p. $X(t)$, $t \in T$. The time average of a given function of $x^{(j)}(t)$, $g[x^{(j)}(t)]$, denoted by $< g[x^{(j)}(t)] >$, is defined by [31]

$$< g[x^{(j)}(t)] > = \lim_{T\to\infty} 1/2T \int_{-T}^{T} g[x^{(j)}(t + \tau)]\, d\tau$$

if the limit exists.

A stationary process X(t), t ε T, is said to be ergodic relative to G if, for every $g[x^{(j)}(t)]$, G being an appropriate domain of g[ ],

$$< g[x^{(j)}(t)] > = E\{g[X(T)]\} \qquad \text{with probability one.}$$

5. Independent-increment processes

Consider a s.p. X(t), t ≥ 0. The random variable $X(t_2) - X(t_1)$, $0 \leq t_1 \leq t_2$, is denoted by $X(t_1,t_2)$ and is called an increment of X(t). If for all $t_1 < t_2 < \ldots < t_n$ the increment $X(t_1,t_2),\ldots,X(t_{n-1},t_n)$ are mutually independent, the s.p. X(t) is called an independent-increment stochastic process. In practice, this definition is used only in the case of continuous parameter stochastic process.

An important example of an independent-increment process is the Poisson process. Short effects, thermal noise, and a large class of impulse noises are examples of physical situations modeled mathematically by the Poisson process.

A stochastic process N(t), having following properties is called a Poisson process [52]:

1. N(t) is independent of the number of occurrences in an interval (0,t).
2. $p_n(t)$ or P{N(t) = n} depends only on the length t of the interval and is independent of where this interval is situated, i.e., $p_n(t)$ gives the probability of occurrences in the interval $(t_1, t + t_1)$ for every t_1.

3. In an interval of infinitesimal length h, the probability of exactly one occurrence is $\lambda h + o(h)$ and that of more than one occurrence is of $o(h)$. $o(h)$ is used as a symbol to denote a function of h which tends to 0 more rapidly than h.

Two important results on the Poisson process are presented without proofs (see pp 98 - 100 of [52], pp 123 - 124 of [34] for detailed proofs).

If $N(t)$, $t \geq 0$ is a Poisson process, then

$$p_n(t) = e^{-\lambda t} \frac{(\lambda t)^n}{n!} \quad , n=0,1,2,\ldots .$$

The mean and variance can be computed easily and given by

$$E(N(t)) = \lambda t \ , \quad var(N(t)) = \lambda t \ .$$

Let $N(t)$, $0 \leq t \leq T$, be a Poisson process. If t_i, $i = 1,2,\ldots,N$, are the occurrence time, the joint probability density function of t_1, $t_2,\ldots,t_N$, and N is given by

$$f(t_1,t_2,\ldots,t_N,N) = f_N(N)\ f_1(t_1) \ \ldots \ f_1(t_N)$$

where,

$$f_N(N) = e^{-EN}\ (EN)^N/N! \quad , N = 0,1,2,\ldots$$

$$f_1(t_i) = 1/T \quad \text{for } 0 \leq t_i \leq T \ , \ i = 1,2,3,\ldots \ .$$

XII. APPENDIX II. FORTRAN PROGRAM FOR R.I. FIELD CALCULATION

```
C MAIN PROGRAM
C
C     ****************************************************************
C     *              RADIO INTERFERENCE COMPUTATION                  *
C     *     BASED ON STOCHASTIC MODELING OF CORONA DISCHARGE          *
C     *        ON HIGH VOLTAGE POWER TRANSMISSION SYSTEMS            *
C     ****************************************************************
C
C
C     ----------------------------------------------------------------
C          ABSTRACT
C
C        THIS PROGRAM IS TO COMPUTE RADIO INTERFERENCE FIELD CAUSED
C     BY CORONA DISCHARGES ON THE HIGH VOLTAGE POWER TRANSMISSION
C     LINES. LINE CONFIGURATIONS CONSIDERED HERE ARE SINGLE CIRCUIT
C     -THREE PHASE LINES WITH GROUND WIRES,BUT ONE CONDUCTOR PER
C     PHASE.
C        THE  BASIC SCHEME TO COMPUTE R.I. FIELD CAN BE SUMMARIZED AS
C    FOLLOWS:
C
C      (1) READ INPUT DATA SUCH AS:
C                    EARTH RESISTIVITY (RHO)
C                    PULSE PERIOD (WIDTH)
C                    BANDWIDTH OF RECEIVER (BAND)
C                    LINE LENGTH (TL)
C                    PROPORTIONAL FACTOR (PC)
C                    TERMINATION IMPEDANCES (TZA, TZB)
C                    LINE TO LINE VOLTAGE (VOLT)
C                    CONDUCTOR HIGHT (H)
C                    X-COORDINATE OF CONDUCTOR (XL)
C                    RESISTIVITY OF CONDUCTOR (RES)
C                    RELATIVE PERMEABILITY OF CONDUCTOR (RELP)
C                    RADIUS OF CONDUCTOR (RAD)
C
C     (2) COMPUTE MEAN AMPLITUDE OF CORONA PULSE (AMP). TO DO THIS
C         FOLLWING PARAMETERS MUST BE COMPUTED :
C                    GENERATION FUNCTION (GENF)
C                    SPECTRAL DENSITY OF EACH PULSE (WSP)
C                    MAXIMUM GRADIENT OF EACH PHASE (GRAD)
C
C     (3) COMPUTE LINE PARAMETERS (Z AND Y).
C
C     (4) COMPUTE MODAL PROPAGATION CONSTANT (GAM) , TRANSFORMATION
C         MATRICES (S FOR VOLTAGE, Q FOR CURRENT),AND CHARACTERISTIC
C         IMPEDANCES (ZC)
C
C     (5) COMPUTE RADIO INTERFERENCE VOLTAGE.
```

```
C
C     (6) COMPUTE RADIO INTERFERENCE FIELD.
C     ------------------------------------------------------------
C
      COMPLEX*16 Z(3,3),Y(3,3),S(3,3),Q(3,3),GAM(3,3)
      COMPLEX*16 VO(3),ZP(5,5),GAMMA(3),AMAT(3,3)
      COMPLEX*16 ZC(3,3),TZA,TZB,RHA(3),RHB(3)
      REAL*8 DLA(5,5),BBI(3,3),ALPH(3),RAD(5),VAR(3),AMP(3)
      REAL*8 XL(5),RFV(3),XLA(800),GRAD(3),F(200),RFI1(1000)
      REAL*8 H(5),RES(5),RELP(5),X,DLB(3,3),GAMF(3)
      REAL*8 RFI2(1000),RAMD,RHO,WA,WB,XM,WIDTH,WSP,W,WK(60)
      REAL*8 TL,BAND,KSI,FL,RFI,VOLT,PC,GENF(3),WF
      REAL*8 TZAR,TZAI,TZBR,TZBI
      INTEGER K,N1,N,NB
C
C
C     N: TOTAL NUMBER OF PHASE CONDUCTORS AND GROUND WIRES
C     K: NUMBER OF PHASE CONDUCTORS
C     N1: NUMBER OF ITERATION FOR R.I. SPECTRUM.
      N=5
      K=3
      NB=2*(N*N+N)
      N1=101
C
C     INPUT DATA AND WRITE OUT THESE DATA.
C
      READ(12,*) TZAR,TZAI,TZBR,TZBI
      READ(12,*) RHO,WIDTH,BAND,TL,PC,VOLT
      READ(12,*)(H(I),XL(I),RES(I),RELP(I),RAD(I),I=1,N)
      WRITE(6,200)
      WRITE(6,202) TZAR,TZAI,TZBR,TZBI
      WRITE(6,205)
      WRITE(6,210) RHO,WIDTH,BAND,TL,VOLT,PC
      WRITE(6,215)
      WRITE(6,220)(H(I),XL(I),RES(I),RELP(I),RAD(I),I=1,N)
C
      TZA=DCMPLX(TZAR,TZAI)
      TZB=DCMPLX(TZBR,TZBI)
C
C     COMPUTE LINE TO GROUND VOLTAGE(VO) AND INVERSE OF PEAK TIME OF
C     CURRENT PULSE (KSI).
C
      VOLT=VOLT/DSQRT(3.D0)
      VO(1)=VOLT*(1.0D0,0.0D0)
      VO(2)=VOLT*(-.5D0,-0.8660254D0)
      VO(3)=VOLT*(-0.5D0,0.8660254D0)
      KSI=1.0D09/(2555.6*RAD(1)*2.+27.778)
      WA=KSI/2.
      WB=KSI*2.
C
```

```
C       COMPUTE MAXWELL'S COEFFICIENT (DLA). REDUCE DLA BY KRON
C       REDUCTION,AND FIND ITS INVERSE(BBI).
C
        CALL POTEN(N,H,XL,RAD,DLA)
        CALL KRONR(N,K,DLA,DLB)
        CALL INVR(DLB,BBI)
C
C       SET FREQUENCY(W) AND MEAN NUMBER OF CORONA(RAMD).
C
        W=6.283185D06
        RAMD=10.
C
C       COMPUTE GRADIENT OF CONDUCTOR .
C
        CALL GRADSB(N,K,BBI,VO,RAD,GRAD)
        DO 40 I=1,K
40      GENF(I)=10.**((85-580./GRAD(I)+38.*DLOG10(RAD(I)*200.DO/3.8DO))
        1         /20.)/1.0D06
C
C       COMPUTE SPECTRAL DENSITY OF PULSE(WSP) AND PULSE AMPLITUDE(AMP).
C
        CALL WSPSB(W,WA,WB,WSP)
        CALL PULAMP(K,RAMD,BAND,WIDTH,GENF,GRAD,WSP,PC,BBI,AMP,VAR)
C
C       THIS DO LOOP COMPUTES SPECTRUM OF R.I.(VARIATION OF R.I. ALONG
C       FREQUENCY) FROM .1MHZ TO 10 MHZ.
C
        DO 500 L=1,N1
        F(L)=10.**(.02*DFLOAT(L)+4.98)
        FL=F(L)
        W=F(L)*6.283185
C
C       COMPUTE LINE PARAMETERS, Z AND Y (SUBPROGRAM IMPED).
C
C       COMPUTE PROPAGATION CONSTANT, CHARACTERISTIC IMPEDENCE,
C       TRANSFORMATION MATRICES, AMAT(=2.*PI*EPSILON*Y*S) ,ATTENUATION
C       CONSTANT (SUBPROGRAM TRANS).
C
C       COMPUTE REFLECTION COEFFICIENT (SUBPROGRAM REFL)
C
C       COMPUTE PROPAGATION FACTORS (SUBPROGRAM GAMF)
C
C       COMPUTE RADIO INTERFERENCE VOLTAGE (SUBPROGRAM RIV)
C
        CALL WSPSB(W,WA,WB,WSP)
        CALL IMPED(N,K,FL,RES,RELP,DLA,RAD,RHO,H,XL,BBI,ZP,Z,Y)
        CALL TRANS(K,NB,WK,FL,Z,Y,S,Q,ZC,ALPH,GAMMA,GAM,AMAT)
        XM=TL/2.
        CALL REFL(K,TZA,TZB,TL,ZC,GAM,RHA,RHB)
        CALL GAMSB(K,ALPH,GAM,RAMD,RHA,RHB,TL,XM,ZC,GAMF)
```

```
      CALL RIV(K,AMP,VAR,WSP,WIDTH,S,GAMF,ZC,RFV)
C
C     COMPUTE R.I. PROFILE ALONG LATERAL DISTANCE AT 1 MHZ
C
      IF(DABS(F(L)-1.0D06).GT.100.) GO TO 150
      X=-1.0D0
      DO 60 I=1,101
      X=X+1.0D0
      XLA(I)=X
C
C     COMPUTE RADIO INTERFERENCE FIELD RFI (SUBPROGRAM FIELD)
C
      CALL FIELD(K,N,AMAT,X,H,XL,BAND,RFV,RFI)
60    RFI1(I)=RFI
C
C     WRITE OUT R.I.( DB ABOVE MICROVOLT PER METER ).
C
      PRINT,' '
      PRINT,'          ═══════════════════════════════════════ '
      PRINT,'           R.I. AT 1 MHZ ALONG LAT. DIST.(DB ABV MV/M)'
      PRINT,'          ═══════════════════════════════════════ '
      WRITE(6,320)(XLA(I),RFI1(I),I=1,101)
C
C     COMPUTE R.I. FOR VARIOUS FREQUENCY AT 15 METERS FROM OUTER
C     CONDUCTOR.
C
150   X=XL(2)+15.D0
      CALL FIELD(K,N,AMAT,X,H,XL,BAND,RFV,RFI)
      RFI2(L)=RFI
500   CONTINUE
C
C     WRITE OUT R.I. SPECTRUM.
C
      WRITE(6,320)(F(I),RFI2(I),I=1,N1)
C
C
200   FORMAT('1',9X,'TERMINATION A',14X,'TERMINATIONB')
202   FORMAT(/,4D14.5)
205   FORMAT(//,3X,'RHO',7X,'WIDTH',6X,'BAND',7X,'TL',7X,'VOLT',7X,
     1        'PC')
210   FORMAT(//,F10.2,F10.4,4F10.2)
215   FORMAT(//,3X,'HIGHT',4X,'XL',10X,7X,'RELP',
     1        7X,'RELPER',4X,'RADIUS')
220   FORMAT(/,2F10.2,D12.4,F10.1,D12.4)
320   FORMAT(/,3X,2D15.5)
      STOP
      END
C
C
C
```

```
C      SUBROUTINE TO MULTIPLY(K1,K2)*(K2,K3)
C
       SUBROUTINE MULT(K1,K2,K3,MAT1,MAT2,B)
       COMPLEX*16 MAT1(3,3),MAT2(3,3),B(3,3),SUM
       INTEGER L
       DO 200 I=1,K1
       DO 200 L=1,K3
       SUM=(0.D0,0.D0)
       DO 150 J=1,K2
  150 SUM=SUM+MAT1(I,J)*MAT2(J,L)
       B(I,L)=SUM
  200 CONTINUE
       RETURN
       END
C
C
C      SUBROUTINE TO INVERT (3,3) COMPLEX MATRIX.
C
       SUBROUTINE INVC(U,MAT)
       COMPLEX*16 U(3,3),V(3,3),MAT(3,3),DTR
       DTR=U(1,1)*U(2,2)*U(3,3)+U(1,2)*U(2,3)*U(3,1)+U(1,3)*U(2,1)*U(3,2)
      *-U(1,3)*U(2,2)*U(3,1)-U(2,3)*U(3,2)*U(1,1)-U(1,2)*U(2,1)*U(3,3)
       V(1,1)=U(2,2)*U(3,3)-U(2,3)*U(3,2)
       V(1,2)=U(1,3)*U(3,2)-U(1,2)*U(3,3)
       V(1,3)=U(1,2)*U(2,3)-U(1,3)*U(2,2)
       V(2,2)=U(1,1)*U(3,3)-U(1,3)*U(3,1)
       V(2,3)=U(1,3)*U(2,1)-U(1,1)*U(2,3)
       V(3,3)=U(1,1)*U(2,2)-U(1,2)*U(2,1)
       V(2,1)=U(2,3)*U(3,1)-U(2,1)*U(3,3)
       V(3,1)=U(2,1)*U(3,2)-U(2,2)*U(3,1)
       V(3,2)=U(1,2)*U(3,1)-U(1,1)*U(3,2)
       DO 10 J=1,3
       DO 10 I=1,3
10     MAT(I,J)=V(I,J)/DTR
       RETURN
       END
C
C
C     SUBROUTINE TO INVERT (3,3) REAL MATRIX.
C
       SUBROUTINE INVR(U,MAT)
       REAL*8 U(3,3),V(3,3),MAT(3,3),DTR
       DTR=U(1,1)*U(2,2)*U(3,3)+U(1,2)*U(2,3)*U(3,1)+U(1,3)*U(2,1)*U(3,2)
      *-U(1,3)*U(2,2)*U(3,1)-U(2,3)*U(3,2)*U(1,1)-U(1,2)*U(2,1)*U(3,3)
       V(1,1)=U(2,2)*U(3,3)-U(2,3)*U(3,2)
       V(1,2)=U(1,3)*U(3,2)-U(1,2)*U(3,3)
       V(1,3)=U(1,2)*U(2,3)-U(1,3)*U(2,2)
       V(2,2)=U(1,1)*U(3,3)-U(1,3)*U(3,1)
       V(2,3)=U(1,3)*U(2,1)-U(1,1)*U(2,3)
       V(3,3)=U(1,1)*U(2,2)-U(1,2)*U(2,1)
```

```
      V(2,1)=U(2,3)*U(3,1)-U(2,1)*U(3,3)
      V(3,1)=U(2,1)*U(3,2)-U(2,2)*U(3,1)
      V(3,2)=U(1,2)*U(3,1)-U(1,1)*U(3,2)
      DO 10 J=1,3
      DO 10 I=1,3
10    MAT(I,J)=V(I,J)/DTR
      RETURN
      END
C
C
C     SUBROUTINE TO COMPUTE DLA (=2.*PI*EPSILON*POTENTIAL COEFF. ).
C     PARAMETERS ARE D (DISTANCE FROM I TH COND. TO IMAGE OF J TH
C     COND.), SD (DISTANCE FROM I TH COND. TO J TH COND.).
C
      SUBROUTINE POTEN(N,H,XL,RAD,DLA)
      REAL*8 H(N),XL(N),RAD(N),DLA(N,N),D,SD
      DO 100 I=1,N
      DO 100 J=1,I
      D=DSQRT((H(I)+H(J))**2+(XL(I)-XL(J))**2)
      SD=DSQRT((H(J)-H(I))**2+(XL(J)-XL(I))**2)
      IF(I.EQ.J) SD=RAD(I)
      DLA(I,J)=DLOG(D/SD)
      DLA(J,I)=DLA(I,J)
100   CONTINUE
      RETURN
      END
C
C
C     SUBROUTINE TO REDUCE COMPLEX MATRIX Y(N,N) TO X(K,K) BY KRON
C     REDUCTION.
C
      SUBROUTINE KRONC(N,K,Y,X)
      COMPLEX*16 Y(N,N),X(K,K)
      INTEGER END
      END=N
10    END=END-1
      DO 20 I=1,END
      DO 20 J=1,END
      M=END+1
20    Y(I,J)=Y(I,J)-Y(I,M)*Y(M,J)/Y(M,M)
      IF(END.GT.K) GO TO 10
      DO 30 I=1,K
      DO 30 J=1,K
 30   X(I,J)=Y(I,J)
      RETURN
      END
C
C
C     SUBROUTINE TO REDUCE REAL MATRIX Y(N,N) TO X(K,K) BY KRON
C     REDUCTION.
```

```
C
      SUBROUTINE KRONR(N,K,Y,X)
      REAL*8 Y(N,N),X(K,K)
      INTEGER END
      END=N
10    END=END-1
      DO 20 I=1,END
      DO 20 J=1,END
      M=END+1
20    Y(I,J)=Y(I,J)-Y(I,M)*Y(M,J)/Y(M,M)
      IF(END.GT.K) GO TO 10
      DO 30 I=1,K
      DO 30 J=1,K
 30   X(I,J)=Y(I,J)
      RETURN
      END
C
C
C     SUBROUTINE TO COMPUTE SPECTRAL DENSITY OF CORONA PULSE.
C     PARAMETERS ARE WA(=KSI/2) AND WB(=KSI*2).
C
      SUBROUTINE WSPSB(W,WA,WB,WSP)
      REAL*8 W,WA,WB,WSP
      WSP=3.694528*(DATAN(WB/W)-DATAN(WA/W)-W*(WB-WA)*(W**2-WA*WB)/
     *(W**2+WB**2)/(W**2+WA**2))/W/(WB-WA)
      RETURN
      END
C
C
C     SUBROUTINE TO COMPUTE BOTH MEAN AND VARIANCE OF CORONA
C     CURRENT PULSE.
C
      SUBROUTINE PULAMP(K,RAMD,BAND,WIDTH,GENF,GRAD,WSP,PC,BBI,AMP,VAR)
      REAL*8 RAMD,AMP(K),VAR(K),GENF(K),BBI(K,K),BAND,WIDTH
      REAL*8 WSP,PC,SUM,GRAD(K)
      DO 20 I=1,K
      SUM=0.0
      DO 10 J=1,K
10    SUM=SUM+BBI(I,J)*GENF(J)
      AMP(I)=DSQRT(WIDTH/(4.*BAND*RAMD*WSP*(1.+PC**2)))*SUM
20    VAR(I)=(AMP(I)*PC)**2
      RETURN
      END
C
C
C     SUBROUTINE TO COMPUTE MAXIMUM GRADIENT OF CONDUCTOR.
C
      SUBROUTINE GRADSB(N,K,BBI,VO,RAD,GRAD)
      COMPLEX*16 VO(K),SUM
      REAL*8 RAD(N),GRAD(K),BBI(K,K)
```

```
      DO 20 I=1,K
      SUM=(0.0,0.0)
      DO 10 J=1,K
10    SUM=SUM+BBI(I,J)*VO(J)
20    GRAD(I)=CDABS(SUM/RAD(I)/100.DO)
      RETURN
      END
C
C
C     SUBROUTINE TO COMPUTE LINE PARAMETERS, Z AND Y.
C     PARAMETERS ARE:
C                  XG ; REACTANCE BY GEOMETRY OF CONDUCTOR.
C                  RC ; INTERNAL RESISTANCE OF CONDUCTOR.
C                  RE ; RESISTANCE CONTRIBUTED BY GROUND.
C                  XE ; REACTANCE CONTRIBUTED BY GROUND.
C                  R AND SETA ; PARAMETERS
C
      SUBROUTINE IMPED(N,K,FL,RES,RELP,DLA,RAD,RHO,H,XL,BBI,ZP,Z,Y)
      COMPLEX*16 Z(K,K),Y(K,K),ZP(N,N)
      REAL*8 DLA(N,N),FL,RES(N),RELP(N),RAD(N)
      REAL*8 RHO,H(N),XL(N)
      REAL*8 BBI(K,K),XG,RC,SETA,R,RE,XE
      DO 20 I=1,N
      DO 20 J=1,I
      XG=1.256637D-6*FL*DLA(I,J)
      IF(I.EQ.J) XG=1.256637D-06*FL*(DLA(I,I)+1.2497442)
      RC=6.324555D-4*DSQRT(RES(I)*RELP(I)*FL)/RAD(I)
      IF(I.NE.J) RC=0.0DO
      R=2.809926D-3*DSQRT(FL/RHO)*DSQRT((H(I)+H(J))**2+(XL(I)
     1      -XL(J))**2)
      SETA=DARCOS((H(I)+H(J))/DSQRT((H(I)+H(J))**2+(XL(I)
     1           -XL(J))**2))
      IF(I.EQ.J) SETA=0.0DO
      RE=2.513274D-6*(DCOS(SETA)/(DSQRT(2.DO)*R)
     *           -DCOS(2.DO*SETA)/(R**2)+DCOS(3.*SETA)/(DSQRT(2.DO)*
     *           R**3)+3.*DCOS(5.*SETA)/(DSQRT(2.DO)*R**5))*FL
      XE=2.513274D-6*(DCOS(SETA)/(DSQRT(2.DO)*R)
     *          -DCOS(3.*SETA)/(DSQRT(2.DO)*R**3)+
     *          3.*DCOS(5.*SETA)/(DSQRT(2.DO)*R**5))*FL
      ZP(I,J)=DCMPLX(RC+RE,XG+RC+XE)
      ZP(J,I)=ZP(I,J)
20    CONTINUE
      CALL KRONC(N,K,ZP,Z)
      DO 30 I=1,K
      DO 30 J=1,K
30    Y(I,J)=DCMPLX(0.0DO,3.495419D-10*FL*BBI(I,J))
      RETURN
      END
C
C
```

```
C     SUBROUTINE TRANS COMPUTES CHARACTERISTIC IMPEDANCE, ATTENUATION
C     CONSTANT, PROPAGATION CONSTANT, AMAT.
C
      SUBROUTINE TRANS(K,NB,WK,FL,Z,Y,S,Q,ZC,ALPH,GAMMA,GAM,AMAT)
      COMPLEX*16 Z(K,K),Y(K,K),S(K,K),Q(K,K),GAM(K,K),AMAT(K,K)
      COMPLEX*16 GAMMA(K),ZC(K,K)
      REAL*8 ALPH(K),WK(NB),FL
      INTEGER IER
      CALL MULT(K,K,K,Z,Y,AMAT)
C
C     SUBROUTINE EIGCC IS I.M.S.L. LIB TO COMPUTE EIGENVALUES (GAMMA)
C     , MODAL MATRIX (WHOSE COLUMNS ARE EIGENVECTORS, S) OF (K,K)
C     COMPLEX MATRIX AMAT. WK(NB) IS THE WORK SPACE.
C
      CALL EIGCC (AMAT,3,3,2,GAMMA,S,3,WK,IER)
      CALL INVC(S,AMAT)
      DO 60 I=1,3
      DO 60 J=1,3
      GAM(I,J)=(0.D0,0.D0)
      Q(J,I)=AMAT(I,J)
      IF(I .EQ. J) GAM(I,I)=1./CDSQRT(GAMMA(I))
   60 CONTINUE
C
      CALL MULT(K,K,K,GAM,AMAT,ZC)
      CALL MULT(K,K,K,ZC,Z,GAM)
      CALL MULT(K,K,K,GAM,Q,ZC)
C
C
C     COMPUTE (AMAT)=-j(2*PI*OMEGA*EPSILON)*(Y)*(S)
C
      CALL MULT(K,K,K,Y,S,AMAT)
      DO 70 I=1,K
      DO 70 J=1,K
   70 AMAT(I,J)=DCMPLX(0.D0,-2.86088D09/FL)*AMAT(I,J)
      DO 90 I=1,K
      DO 90 J=1,K
      GAM(I,J)=(0.D0,0.D0)
      GAM(I,I)=CDSQRT(GAMMA(I))
90    ALPH(I)=DREALF(GAM(I,I))
      RETURN
      END
C
      FUNCTION DREALF(A)
      COMPLEX*16 A
      DREALF=CDABS((A+DCONJG(A))/2.D0)
      RETURN
      END
C
C
C     SUBROUTINE TO COMPUTE RADIO INTERFERENCE VOLTAGE.
```

```
C
      SUBROUTINE RIV(K,AMP,VAR,WSP,WIDTH,S,GAMF,ZC,RFV)
      COMPLEX*16 S(K,K),ZC(K,K),SUM1,SUM
      REAL*8 AMP(K),VAR(K),WSP,WIDTH,GAMF(K),RFV(K),WF,AMPV
      DO 10 M=1,K
      SUM1=(0.D0,0.D0)
      DO 20 I=1,K
      AMPV=AMP(I)**2+VAR(I)
      SUM=(0.D0,0.D0)
      DO 30 J=1,K
      WF=2.*WSP*AMP(I)*AMP(J)/WIDTH
      IF(I.EQ.J) WF=2.*WSP*AMPV/WIDTH
30    SUM=SUM+DCONJG(S(J,M))*WF
20    SUM1=SUM1+SUM*S(I,M)
10    RFV(M)=DREALF(SUM1)*GAMF(M)*CDABS(ZC(M,M))**2
      RETURN
      END
C
C
C
C     SUBROUTINE TO COMPUTE RADIO INTERFERENCE FIELD.
C
      SUBROUTINE FIELD(K,N,AMAT,X,H,XL,BAND,RFV,RFI)
      REAL*8 X,H(N),XL(N),RFI,SUM3,RFV(K),BAND
      COMPLEX*16 AMAT(K,K),SUM1
      SUM3=0.0D0
      DO 10 I=1,K
      SUM1=(0.D0,0.D0)
      DO 20 J=1,K
20    SUM1=SUM1+AMAT(J,I)*2.0*H(J)/((X-XL(J))**2+H(J)**2)
10    SUM3=SUM3+RFV(I)*CDABS(SUM1)**2
      RFI=10.*DLOG10(SUM3*1.D12*BAND)
      RETURN
      END
C
C
C
C     SUBROUTINE REFL COMPUTE REFLECTION COEFFICIENTS.
C
      SUBROUTINE REFL (K,TZA,TZB,TL,ZC,GAM,RHA,RHB)
      COMPLEX*16 TZA,TZB,RHA(K),RHB(K),ZC(K,K),GAM(K,K)
      REAL*8 TL
      DO 10 I=1,K
      RHA(I)=(TZA-ZC(I,I))/(TZA+ZC(I,I))
10    RHB(I)=(TZB-ZC(I,I))/(TZB+ZC(I,I))
      RETURN
      END
C
C
C
```

```
C     SUBROUTINE GAMSB COMPUTES PROPAGATION FACTOR WHICH IS CAUSED
C     BY PROPAGATION OF INJECTED CORONA CURRENTS AND THEIR IMAGES
C     DISTRIBUTED STOCHASTICALLY ALONG TRANSMISSION LINE.
C
      SUBROUTINE GAMSB(K,ALPH,GAM,RAMD,RHA,RHB,TL,XM,ZC,GAMF)
      COMPLEX*16 RHA(K),RHB(K),ZC(K,K),U,R,E,G,CG,P,Q,GAM3,GAM5
      COMPLEX*16 GAM(K,K)
      REAL*8 ALPH(K),RAMD,TL,XM,GAMF(K),A,B,L,X,S,T,GAM1,GAM2,GAM4,D
      DO 10 I=1,K
      A=ALPH(I)
      B=RAMD
      P=RHA(I)
      Q=RHB(I)
      L=TL
      X=XM
      S=CDABS(P)**2
      T=CDABS(Q)**2
      U=DCONJG(P)
      R=DCONJG(Q)
      E=(GAM(I,I)-DCONJG(GAM(I,I)))/2.D0
      G=GAM(I,I)
      CG=DCONJG(G)
      GAM1=B*(2.-DEXP(-2.D0*A*X)*(1-S)-DEXP(-2.D0*A*(L-X))*(1-T)-
     1    DEXP(-2.D0*A*(L+X))*S*(1-T)-T*(1-S)*DEXP(-2.D0*A*(2.D0
     2    *L-X))-S*T*DEXP(-4.D0*A*L))/(2.*A)
      GAM2=B*DREALF(P*(DEXP(-2.D0*A*L)-CDEXP(-2.D0*(A*L+E*X)))+
     1    Q*(CDEXP(-2.D0*G*(L-X))-(1-S)*CDEXP(-2.D0*(G*L-E*X))
     2    -S*T*CDEXP(-2.D0*(G*L+CG*X)))+T*P*(CDEXP(-2.D0*(A*L
     3    +2.D0*E*X))-CDEXP(-2.D0*(2.D0*A*L-CG*X))))/(A)
      GAM3=P*(DEXP(-2.D0*A*X)-CDEXP(-2.*G*X))+Q*(DEXP(-2.D0*A*
     2     (L-X))-CDEXP(-2.D0*G*(L-X)))+P*Q*(CDEXP(-2.D0*(G*L-E*X))+
     2     CDEXP(-2.D0*(A*L+E*X))-2.*CDEXP(-2.*G*L))+U*Q*(CDEXP(
     3     -2.D0*(A*L-E*X))-CDEXP(-2.D0*(G*L-E*X)))+Q*S*(DEXP(
     4     -2.D0*A*(L+X))-CDEXP(-2.D0*(CG*X+G*L)))+P*T*(DEXP(-2.D0*
     5     A*(2.D0*L-X))-CDEXP(-2.D0*(2.D0*A*L-CG*X)))
      GAM3=(GAM3+DCONJG(GAM3))/(0.D0,2.D0)*B/CDABS(E)
      GAM4=B**2/CDABS(G)**2*(CDABS(2.D0-CDEXP(-1.D0*G*X)-CDEXP(-1.D0
     1    *G*(L-X)))**2+S*CDABS(CDEXP(-1.D0*G*X)-CDEXP(-1.D0*G*(X+L))
     2    )**2+T*CDABS(CDEXP(-1.D0*G*(2.D0*L-X))-CDEXP(-1.D0*G*(L-X)
     3    ))**2+S*T*CDABS(CDEXP(-1.D0*G*(2.D0*L-X))+CDEXP(-1.D0*G*
     4    (L+X))-2.*DEXP(-2.D0*A*L))**2)
      GAM5=(2.-CDEXP(-1.D0*CG*X)-CDEXP(
     1    CG*(L-X)))*(P*CDEXP(-1.D0*G*X)-P*(1-Q)*CDEXP(-1.D0*G*(L+X)
     2    )-Q*(1-P)*CDEXP(-1.D0*G*(2.D0*L-X))+Q*CDEXP(-1.D0*G*(L-X))-
     3    2.*P*Q*CDEXP(-2.D0*G*L))+U*Q*(CDEXP(-1.*CG*X)-CDEXP(-1.*CG*
     4    (X+L)))*(CDEXP(-1.*G*(L-X))-(1-U)*CDEXP(-1.*G*(2.*L-X))+
     5    U*CDEXP(-1.*G*(L+X))-2.*U*CDEXP(-2.*G*L))
      GAM5=GAM5+P*T*DEXP(-4.D0*A*L)*(CDEXP(G*X)+CDEXP(G*(L-X))-2.)
     1          *(CDEXP(CG*(X+L))-CDEXP(CG*X))
      GAM5=2.*B**2/CDABS(G)**2*DREALF(GAM5)
```

```
        D=CDABS(2.D0*(1.D0-P*Q*CDEXP(-2.D0*G*L)))**2
        GAMF(I)=(GAM1+GAM2+CDABS(GAM3)+GAM4+CDABS(GAM5))/D
10      CONTINUE
        RETURN
        END
$ENTRY
```